



Measurement of the CP properties of Higgs boson interactions with τ -leptons with the ATLAS detector

The ATLAS Collaboration

A study of the charge conjugation and parity (CP) properties of the interaction between the Higgs boson and τ -leptons is presented. The study is based on a measurement of CP -sensitive angular observables defined by the visible decay products of τ -leptons produced in Higgs boson decays. The analysis uses 139 fb^{-1} of proton–proton collision data recorded at a centre-of-mass energy of $\sqrt{s} = 13 \text{ TeV}$ with the ATLAS detector at the Large Hadron Collider. Contributions from CP -violating interactions between the Higgs boson and τ -leptons are described by a single mixing angle parameter ϕ_τ in the generalised Yukawa interaction. Without constraining the $H \rightarrow \tau\tau$ signal strength to its expected value under the Standard Model hypothesis, the mixing angle ϕ_τ is measured to be $9^\circ \pm 16^\circ$, with an expected value of $0^\circ \pm 28^\circ$ at the 68% confidence level. The pure CP -odd hypothesis is disfavoured at a level of 3.4 standard deviations. The results are compatible with the predictions for the Higgs boson in the Standard Model.

1 Introduction

A detailed analysis of Higgs boson (H) decays into τ -lepton pairs observed at the LHC [1–3] allows a direct probe of the charge conjugation and parity (CP) properties of the Yukawa coupling of the Higgs boson to the τ -lepton. The Standard Model (SM) of particle physics predicts the Higgs boson to be a CP -even (scalar) particle. The presence of a CP -odd (pseudoscalar) admixture has not yet been excluded, and any observed CP -odd contribution to the $H\tau\tau$ coupling properties would be a sign of physics beyond the SM.

Studies of the CP properties of Higgs boson interactions with gauge bosons performed by the ATLAS and CMS experiments [4–9] have shown no deviation from the SM predictions. However, these measurements probe the bosonic couplings in which CP -odd contributions enter only via higher-order operators that are suppressed by powers of $1/\Lambda^2$ [10], where Λ is the scale of the new physics in an effective field theory. In contrast, a CP -odd contribution to Yukawa couplings can be present at tree level. Recently, measurements of the CP properties of the interaction between the Higgs boson and top quarks were performed by the ATLAS [11] and CMS [12] Collaborations, and excluded a pure CP -odd structure for the top-quark Yukawa coupling at 3.9σ and 3.2σ , respectively.

This paper presents a measurement of the CP properties of the Higgs boson interaction with τ -leptons. The measurement is based on CP -sensitive angular observables defined using the visible τ -lepton decay products. Ideas about how to probe a CP -odd and CP -even admixture in the τ -lepton Yukawa coupling in $H \rightarrow \tau\tau$ decay were initially developed in the context of e^+e^- colliders [13–17]. Originally, hadronic decays of the τ -leptons into $\pi^\pm\nu$ and $\rho^\pm\nu$ were used, and observables sensitive to the transverse spin correlations between the τ -lepton decay products were constructed. These methods, extended to $\ell^\pm (= e^\pm, \mu^\pm)\nu\nu$ and $a_1^\pm\nu$ decays and re-evaluated in the context of pp collisions at the LHC [18–23], are adopted in this analysis. Recently, a similar study was also performed by the CMS Collaboration [24].

The general effective Yukawa interaction between the Higgs boson and τ -leptons can be parameterised as in Refs. [21, 23]:

$$\mathcal{L}_{H\tau\tau} = -\frac{m_\tau}{v}\kappa_\tau(\cos\phi_\tau\bar{\tau}\tau + \sin\phi_\tau\bar{\tau}i\gamma_5\tau)H,$$

where $v = 246$ GeV is the vacuum expectation value of the Higgs field, κ_τ is the reduced Yukawa coupling strength, and ϕ_τ (where $\phi_\tau \in [-90^\circ, 90^\circ]$) is the CP -mixing angle that parameterises the relative contributions of the CP -even and CP -odd components to the $H\tau\tau$ coupling. The SM CP -even hypothesis is realised for $\phi_\tau = 0^\circ$, while the pure CP -odd scenario corresponds to $\phi_\tau = \pm 90^\circ$. Other values of ϕ_τ represent admixtures of the two components and would indicate a CP -violating scenario.

The CP -mixing angle ϕ_τ is encoded in the correlations between the transverse spin components of the τ -leptons in the $H \rightarrow \tau\tau$ decays, which are then reflected in the directions of the τ -lepton decay products. The signed acoplanarity angle φ_{CP}^* between the τ decay planes (described in Section 3 and illustrated in Figure 1) is sensitive to the transverse spin correlations impacted by the CP -mixing angle of the Yukawa coupling. Such correlations are usually calculated by contracting the polarimeter vectors of the decayed τ -leptons¹ and the spin density matrix of the τ -lepton-pair spin state, $R_{i,j}$, which depends on the τ -lepton pair-production process [26–28]. In the case of Higgs boson decays, the spin density matrix $R_{i,j}$ has only transverse components with respect to the τ -lepton direction, and these are first-order trigonometric

¹ A polarimeter vector is calculated from the matrix element of the τ -lepton decay process and is usually expressed in terms of the momenta of the decay products. Its direction gives the most probable direction of the τ polarization vector, while its magnitude determines the efficiency of a given decay as a polarimeter [25].

Table 1: Notation for the dominant leptonic and hadronic τ -lepton decay modes used and their branching fractions. The symbol ‘ ℓ^\pm ’ stands for e^\pm or μ^\pm , and ‘ h^\pm ’ includes π^\pm and K^\pm . The parentheses show the hadronic decays involving π^\pm and their corresponding branching fractions.

Notation	Decay mode	Branching fraction
ℓ	$\ell^\pm \bar{\nu} \nu$	35.2%
1p0n	$h^\pm \nu (\pi^\pm \nu)$	11.5% (10.8%)
1p1n	$h^\pm \pi^0 \nu (\pi^\pm \pi^0 \nu)$	25.9% (25.5%)
1pXn	$h^\pm \geq 2\pi^0 \nu (\pi^\pm 2\pi^0 \nu)$	10.8% (9.3%)
3p0n	$3h^\pm \nu (3\pi^\pm \nu)$	9.8% (9.0%)

polynomials in the $2\phi_\tau$ angle. Per-event sensitivity to CP -mixing depends on the τ -lepton-pair decay modes and on the way in which the polarimeter vectors and decay planes are reconstructed from observable quantities. The φ_{CP}^* angle is directly related to ϕ_τ in the $H \rightarrow \tau\tau$ differential decay rate and the relation has the form of a first-order trigonometric polynomial in $\cos(\varphi_{CP}^* - 2\phi_\tau)$ at leading order [14, 21, 22]:

$$d\Gamma_{H \rightarrow \tau^+ \tau^-} \approx 1 - b(E_+)b(E_-) \frac{\pi^2}{16} \cos(\varphi_{CP}^* - 2\phi_\tau),$$

where E_\pm are the energies of the charged decay particles in their respective τ -lepton rest frames, and $b(E_\pm)$ are the spectral functions [29] describing the spin analysing power of a given decay mode. Different methods [15–23] have been developed in an attempt to approximately reconstruct τ -lepton decay planes. The φ_{CP}^* variable used in this analysis is constructed with various methods depending on the τ -lepton decay modes, largely following the strategy presented in Ref. [23].

The analysis is performed using 139 fb^{-1} of $\sqrt{s} = 13 \text{ TeV}$ proton–proton (pp) collision data recorded from 2015 to 2018 with the ATLAS detector. Two τ -lepton-pair decay channels are considered in the analysis: the first with one leptonically (τ_{lep}) and one hadronically decaying τ -lepton (τ_{had}), referred to as the $\tau_{\text{lep}}\tau_{\text{had}}$ channel, and the second with two hadronically decaying τ -leptons, referred to as the $\tau_{\text{had}}\tau_{\text{had}}$ channel. The leptonic decay $\tau^\pm \rightarrow \ell^\pm \nu \nu$ includes decays to either an electron or a muon. In the case of hadronic decay, the dominant τ_{had} decay modes are considered: single-pion decay $\pi^\pm \nu$, two-pion decay $\pi^\pm \pi^0 \nu$ with an intermediate ρ^\pm , and three-pion decay $\pi^\pm 2\pi^0 \nu$ and $3\pi^\pm \nu$ with an intermediate a_1^\pm . A small fraction of events with τ decays to K^\pm mesons is also included in the analysis. The τ -lepton decay modes used in the analysis are summarised in Table 1 with their branching fractions [30] and the notation used throughout this paper. The τ_{had} decay modes are labelled by YpXn in accord with the number of charged (Y) and neutral (X) pions among the decay products. The τ -lepton-pair decay modes considered in this analysis account for 68% of all possible τ pair decays.

This paper is structured as follows. In Section 2 the ATLAS detector is briefly described. The methodology and observables used in the analysis are discussed in Section 3. Section 4 gives a summary of the data and simulated event samples. Section 5 describes the object reconstruction and event selection, and defines the signal and control regions. Section 6 details the experimental and theoretical systematic uncertainties. The fit model and statistical analysis strategy are explained in Section 7. Section 8 presents the measurement results. Section 9 concludes the paper.

2 ATLAS detector

The ATLAS detector [31] at the LHC covers nearly the entire solid angle around the collision point.² It consists of an inner tracking detector surrounded by a thin superconducting solenoid, electromagnetic and hadron calorimeters, and a muon spectrometer incorporating three large superconducting air-core toroidal magnets.

The inner-detector system (ID) is immersed in a 2 T axial magnetic field and provides charged-particle tracking in the range $|\eta| < 2.5$. The high-granularity silicon pixel detector covers the vertex region and typically provides four measurements per track, the first hit normally being in the insertable B-layer [32, 33] installed before Run 2. It is followed by the silicon microstrip tracker, which usually provides eight measurements per track. These silicon detectors are complemented by the transition radiation tracker (TRT), which enables radially extended track reconstruction up to $|\eta| = 2.0$. The TRT also provides electron identification information based on the fraction of hits (typically 30 in total) above a higher energy-deposit threshold corresponding to transition radiation.

The calorimeter system covers the pseudorapidity range $|\eta| < 4.9$. Within the region $|\eta| < 3.2$, electromagnetic calorimetry is provided by barrel and endcap high-granularity lead/liquid-argon (LAr) calorimeters, with an additional thin LAr presampler covering $|\eta| < 1.8$ to correct for energy loss in material upstream of the calorimeters. Hadron calorimetry is provided by the steel/scintillator-tile calorimeter, segmented into three barrel structures within $|\eta| < 1.7$, and two copper/LAr hadron endcap calorimeters. The solid angle coverage is completed with forward copper/LAr and tungsten/LAr calorimeter modules optimised for electromagnetic and hadronic energy measurements respectively.

The muon spectrometer comprises separate trigger and high-precision tracking chambers measuring the deflection of muons in a magnetic field generated by the superconducting air-core toroidal magnets. The field integral of the toroids ranges between 2.0 and 6.0 T m across most of the detector. Three sets of precision chambers cover the region $|\eta| < 2.7$ with multiple layers of monitored drift tubes, complemented by cathode-strip chambers in the forward region, where the background is highest. The muon trigger system covers the range $|\eta| < 2.4$ with resistive-plate chambers in the barrel and thin-gap chambers in the endcap regions.

Interesting events are selected by the first-level trigger system implemented in custom hardware, followed by selections made by algorithms implemented in software in the high-level trigger [34]. The first-level trigger accepts events from the 40 MHz bunch crossings at a rate below 100 kHz, which the high-level trigger reduces in order to record events to disk at about 1 kHz.

An extensive software suite [35] is used in data simulation, in the reconstruction and analysis of real and simulated data, in detector operations, and in the trigger and data acquisition systems of the experiment.

² ATLAS uses a right-handed coordinate system with its origin at the nominal interaction point in the centre of the detector and the z -axis along the beam pipe. The x -axis points from the interaction point to the centre of the LHC ring, and the y -axis points upwards. Cylindrical coordinates (r, ϕ) are used in the transverse plane, ϕ being the azimuthal angle around the z -axis. The pseudorapidity is defined in terms of the polar angle θ as $\eta = -\ln \tan(\theta/2)$. Angular distance is measured in units of $\Delta R \equiv \sqrt{(\Delta\eta)^2 + (\Delta\phi)^2}$.

3 Analysis strategy

A CP -sensitive observable φ_{CP}^* is built with different methods depending on the τ -lepton decay modes. In general, φ_{CP}^* is the signed acoplanarity angle between the τ -lepton decay planes. Each τ decay plane is constructed from the spatial momentum vector of a charged decay particle and either its impact parameter (impact parameter method) or the spatial momentum vectors of other visible τ -lepton decay particles (ρ -decay plane and a_1 methods). All vectors are boosted to the zero-momentum frame (ZMF) of the visible τ -lepton-pair decay particles. Figures 1(a)–1(c) illustrate the methods used to construct the φ_{CP}^* observable in $H \rightarrow \tau^+\tau^- \rightarrow \pi^+\pi^- + 2\nu$, $H \rightarrow \tau^+\tau^- \rightarrow \pi^+\pi^0\nu\pi^-\pi^0\nu$ and $H \rightarrow \tau^+\tau^- \rightarrow \pi^+\pi^0\nu\pi^-\nu$ decays, respectively. The visible τ -lepton-pair ZMF (indicated by *) is used to approximate the Higgs boson rest frame, which is not accessible due to the presence of undetected neutrinos in the τ -lepton decays.

Figure 2 shows the normalised distribution of φ_{CP}^* for simulated $H \rightarrow \tau^+\tau^- \rightarrow \pi^+\pi^- + 2\nu$ events at the generator level. The distribution peaks at $\varphi_{CP}^* = 180^\circ$ for a CP -even (e.g. SM) Higgs boson, whereas for the case of a pure CP -odd Higgs boson, the distribution peaks at $\varphi_{CP}^* = 0^\circ$ and 360° . The phase difference between the φ_{CP}^* distributions for two different mixing scenarios is twice their ϕ_τ difference.

The τ -lepton-pair decay combinations used in the analysis and the respective methods for constructing the φ_{CP}^* observable are summarised in Table 2. The corresponding fraction of events relative to the total from all possible di- τ decay combinations is calculated from the single- τ -lepton decay mode branching fractions in Table 1. Other decay combinations are not considered in this analysis because their respective φ_{CP}^* observables perform relatively poorly in discriminating between different CP scenarios.

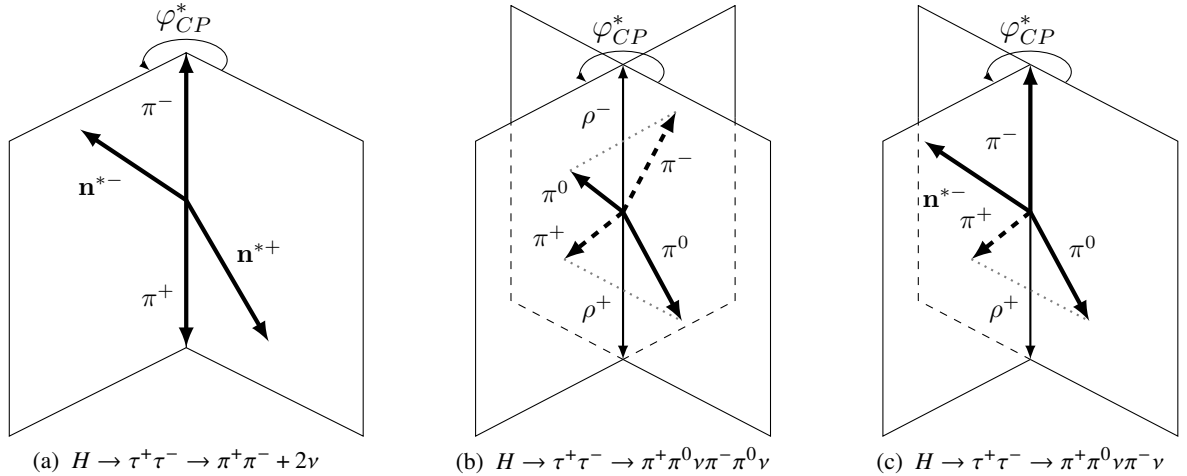


Figure 1: Illustration of the τ -lepton decay planes for constructing the φ_{CP}^* observable in (a) $H \rightarrow \tau^+\tau^- \rightarrow \pi^+\pi^- + 2\nu$ decay using the impact parameter method, (b) $H \rightarrow \tau^+\tau^- \rightarrow \pi^+\pi^0\nu\pi^-\pi^0\nu$ using the ρ -decay plane method, and (c) $H \rightarrow \tau^+\tau^- \rightarrow \pi^+\pi^0\nu\pi^-\nu$ using the combined impact parameter and ρ -decay plane method. The decay planes are spanned by the spatial momentum vector of the charged decay particle of the τ -lepton (π^\pm) and either its impact parameter $\mathbf{n}^{*\pm}$ or the spatial momentum vector of the neutral decay particle of the τ -lepton (π^0).

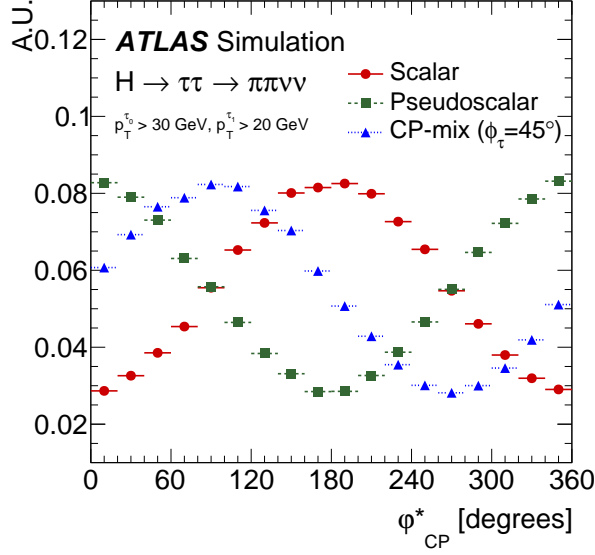


Figure 2: Normalised φ_{CP}^* distributions in simulated $H \rightarrow \tau^+\tau^- \rightarrow \pi^+\pi^- + 2\nu$ events at the generator level for different CP hypotheses. The predictions for a pure CP -even SM Higgs boson (scalar, red circle), a pure CP -odd hypothesis (pseudoscalar, green square), and CP -mix hypothesis ($\phi_\tau = 45^\circ$, blue triangle) are shown. The transverse momentum of the simulated τ leptons is required to be larger than 30 GeV (20 GeV) for the leading (sub-leading) τ lepton during the event generation.

Table 2: Decay mode combinations of the τ -lepton pair and the corresponding methods to construct the φ_{CP}^* observable used in this analysis. The fraction of events for each decay mode combination relative to the total from all di- τ decay combinations (last column) is calculated using the τ -lepton decay mode branching fractions in Table 1.

Decay channel	Decay mode combination	Method	Fraction in all τ -lepton-pair decays
$\tau_{lep}\tau_{had}$	$\ell-1p0n$	IP	8.1%
	$\ell-1p1n$	IP- ρ	18.3%
	$\ell-1pXn$	IP- ρ	7.6%
	$\ell-3p0n$	IP- a_1	6.9%
$\tau_{had}\tau_{had}$	$1p0n-1p0n$	IP	1.3%
	$1p0n-1p1n$	IP- ρ	6.0%
	$1p1n-1p1n$	ρ	6.7%
	$1p0n-1pXn$	IP- ρ	2.5%
	$1p1n-1pXn$	ρ	5.6%
	$1p1n-3p0n$	$\rho-a_1$	5.1%

3.1 Impact parameter (IP) method

The IP method is applied to τ -lepton decays with only one charged particle in the final state, specifically the direct hadronic decay $\tau^\pm \rightarrow \pi^\pm\nu$ or leptonic decays $\tau^\pm \rightarrow \ell^\pm\nu\nu$. This refers to the $1p0n-1p0n$ and $\ell-1p0n$ decay mode combinations. In this case, the τ -lepton decay plane is formed from the spatial momentum vector \mathbf{q}^\pm of the charged particle (π^\pm, ℓ^\pm) and the three-dimensional (3D) impact parameter vector \mathbf{n}^\pm of the charged particle, defined as the directional distance of closest approach of the charged particle's track

to the reconstructed primary vertex (PV) of the event. The four-vectors of the track momentum q_μ^\pm and the impact parameter $n_\mu^\pm = (0, \mathbf{n}^\pm)$, initially defined and measured in the laboratory frame, are boosted to the rest frame of the two charged decay particles (the visible di- τ ZMF, denoted by $*$). The boosted and normalised impact parameter vector $\hat{\mathbf{n}}^{*\pm}$ is then decomposed into components which are parallel and transverse ($\hat{\mathbf{n}}_\perp^{*\pm}$) to the direction of the associated normalised spatial momentum vector $\hat{\mathbf{q}}^{*\pm}$. Using these vectors, an angle φ^* and a CP -odd triple correlation O_{CP}^* are defined as

$$\varphi^* = \arccos(\hat{\mathbf{n}}_\perp^{*+} \cdot \hat{\mathbf{n}}_\perp^{*-}) \quad \text{and} \quad O_{CP}^* = \hat{\mathbf{q}}^{*-} \cdot (\hat{\mathbf{n}}_\perp^{*+} \times \hat{\mathbf{n}}_\perp^{*-}),$$

and both are incorporated in a single observable φ_{CP}^* ($0 \leq \varphi_{CP}^* \leq 360^\circ$) defined by

$$\varphi_{CP}^* = \begin{cases} \varphi^* & \text{if } O_{CP}^* \geq 0 \\ 360^\circ - \varphi^* & \text{if } O_{CP}^* < 0. \end{cases} \quad (1)$$

In the case of leptonic decay, due to a different sign in the spectral function for the leptonic τ decays [20, 29], an additional shift by 180° is applied to synchronise the phase in φ_{CP}^* with the other decays.

3.2 ρ -decay plane (ρ) method

The ρ method is applied to construct φ_{CP}^* in events with $1p1n-1p1n$ or $1p1n-1pXn$ decay mode combinations. In the case of consecutive decays $\tau^\pm \rightarrow \rho^\pm \nu$, $\rho^\pm \rightarrow \pi^\pm \pi^0$, the τ -lepton decay plane can be formed from the spatial momentum vectors of the charged pion (\mathbf{q}^\pm) and neutral pion ($\mathbf{q}^{0\pm}$). The four-momentum vectors of the π^\pm and π^0 are boosted to the rest frame of the ρ -meson pair (the visible τ -lepton-pair ZMF). The angle φ^* and triple correlation O_{CP}^* are then defined in the same way as in the IP method using the unit spatial vectors, but replacing the impact parameter component with the neutral-pion vector,

$$\varphi^* = \arccos(\hat{\mathbf{q}}_\perp^{*0+} \cdot \hat{\mathbf{q}}_\perp^{*0-}) \quad \text{and} \quad O_{CP}^* = \hat{\mathbf{q}}^{*-} \cdot (\hat{\mathbf{q}}_\perp^{*0+} \times \hat{\mathbf{q}}_\perp^{*0-}),$$

where $\hat{\mathbf{q}}_\perp^{*0+}$ and $\hat{\mathbf{q}}_\perp^{*0-}$ are the normalised vectors transverse to the direction of the associated charged pion for each neutral pion. A signed observable $\varphi^{*'}$ is defined similarly to Eq. (1),

$$\varphi^{*'} = \begin{cases} \varphi^* & \text{if } O_{CP}^* \geq 0 \\ 360^\circ - \varphi^* & \text{if } O_{CP}^* < 0. \end{cases}$$

An additional requirement that depends on the sign of the product of τ -lepton spin-analysing functions $y_\pm^\rho = (E_{\pi^\pm} - E_{\pi^0}) / (E_{\pi^\pm} + E_{\pi^0})$, where $E_{\pi^\pm,0}$ is the pion energy in the laboratory frame, is needed to define the observable φ_{CP}^* sensitive to the CP -mixing angle as

$$\varphi_{CP}^* = \begin{cases} \varphi^{*'} & \text{if } y_+^\rho y_-^\rho \geq 0 \\ \varphi^{*'} + 180^\circ & \text{if } y_+^\rho y_-^\rho < 0. \end{cases} \quad (2)$$

In the case of $1pXn$ decays (e.g. $\tau^\pm \rightarrow a_1^\pm \nu \rightarrow \pi^\pm 2\pi^0 \nu$), the sum of the four-momenta of all neutral pions is taken as the neutral component in the ρ method.

3.3 Combined IP and ρ (IP- ρ) method

For events with the combinations 1p0n-1p1n, 1p0n-1pXn, ℓ -1p1n, and ℓ -1pXn, the IP method and the ρ method are combined to compute the φ_{CP}^* angle. In the case of $H \rightarrow \tau\tau \rightarrow \pi^\mp \nu \rho^\pm \nu$, $\rho^\pm \rightarrow \pi^\pm \pi^0$ (1p0n-1p1n) events, φ_{CP}^* is defined in the visible τ -lepton-pair ZMF by using the $\pi\rho$ rest frame. One of the decay planes is defined using the IP method and the other with the ρ method. The quantities φ^* , \mathcal{O}_{CP}^* and $\varphi^{*'}$ are calculated in a way analogous to that in Section 3.2, but with the one-neutral-pion component replaced with the impact parameter vector defined in Section 3.1. The φ_{CP}^* observable is defined as

$$\varphi_{CP}^* = \begin{cases} \varphi^{*'} & \text{if } y^\rho \geq 0 \\ \varphi^{*'} + 180^\circ & \text{if } y^\rho < 0, \end{cases} \quad (3)$$

with a phase shift of 180° depending on the sign of y^ρ .

3.4 a_1 -decay (a_1) method

The a_1 method is an extension of the ρ method discussed in Section 3.2, and is used for $\tau^\pm \rightarrow a_1^\pm \nu$, $a_1^\pm \rightarrow \pi^\pm \pi^+ \pi^-$. The τ -lepton decay plane is defined by the charged pion (π_1^\pm) with the highest transverse momentum and the vector sum of the other two π momenta. The observable y_\pm^ρ used in the ρ method is modified to take the effect of the π masses into account, and is defined by $y_\pm^{a_1}$ adopting the convention in Ref. [36] as

$$y_\pm^{a_1} = \frac{E_{2\pi} - E_{\pi_1^\pm}}{E_{2\pi} + E_{\pi_1^\pm}} - \frac{m_{3\pi}^2 - m_{\pi_1^\pm}^2 + m_{2\pi}^2}{2m_{3\pi}^2},$$

where $m_{3\pi}$ is the invariant mass of the three charged pions from the a_1^\pm decay, and $m_{2\pi}$ ($E_{2\pi}$) refers to the invariant mass (energy) of the system of the two π in the τ decay that do not have the highest transverse momentum.

Similarly to Section 3.3, the a_1 method is combined with the IP method for the ℓ -3p0n events and with the ρ method for the 1p1n-3p0n events in the $\tau_{\text{lep}}\tau_{\text{had}}$ and $\tau_{\text{had}}\tau_{\text{had}}$ channels, respectively. In the ℓ -3p0n case, φ_{CP}^* is defined similarly to Eq. (3), but with y^ρ replaced by y^{a_1} . For 1p1n-3p0n, the φ_{CP}^* computation is analogous to Eq. (2), except that the product $y_\pm^\rho y_\mp^{a_1}$ is used to determine whether the 180° shift is applied.

4 Data and simulated event samples

This analysis uses 139 fb^{-1} of $\sqrt{s} = 13 \text{ TeV}$ pp collision data recorded by ATLAS with good operating conditions [37] in 2015–2018. The data were collected using single-lepton or di-hadronic τ triggers [38–41]. Events used in the $\tau_{\text{lep}}\tau_{\text{had}}$ channel were accepted by single-lepton triggers with p_T thresholds of 24 GeV (26 GeV) and 20 GeV (26 GeV) for electron and muon candidates, respectively, in the 2015 (2016–2018) dataset. Events used in the $\tau_{\text{had}}\tau_{\text{had}}$ analysis channel were accepted by di-hadronic τ -lepton triggers, with a p_T threshold of 35 GeV for the leading τ candidate and 25 GeV for the sub-leading τ candidate. Due to rising instantaneous luminosity, the di-hadronic τ triggers used in the 2016–2018 data-taking period required an additional first-level triggered jet with $p_T > 25 \text{ GeV}$ and $|\eta| < 3.2$.

The analysis considers the four main Higgs boson production processes at the LHC: gluon–gluon fusion (ggF), vector-boson fusion (VBF), associated production with a vector boson (VH), and associated production with top-quark pair ($t\bar{t}H$). The POWHEG NNLOPS program [42–46] was used to model ggF Higgs boson production with next-to-next-leading-order (NNLO) accuracy. The VBF and VH production processes were simulated with POWHEG at NLO accuracy in QCD. The production of $t\bar{t}H$ events was simulated using POWHEG BOX v2 [44–48] at NLO with the NNPDF3.0_{NLO} [49] PDF set. In all signal events, the decays of τ -leptons were modelled by PYTHIA 8 [50] with no spin correlations. The spin correlations are reintroduced with event-by-event weights modelling CP -mixing-dependent transverse spin correlations, using the TauSpinner package [51–53]. Background samples of $V + \text{jets}$ and diboson events were generated by SHERPA 2.2.1 [54] (including τ -lepton decays), and $t\bar{t}$ and single-top samples were generated by POWHEG+PYTHIA 8, with PYTHIA also performing τ -lepton decays. The simulated event samples are shared with the cross-section measurement in the $H \rightarrow \tau\tau$ decay channel [55].

All samples of simulated events were passed through a full simulation of the ATLAS detector response [56] using GEANT4 [57]. The effects of multiple interactions in the same or neighbouring bunch crossings (pile-up) were modelled by overlaying each hard-scatter event with minimum-bias events, simulated using the soft QCD processes of PYTHIA 8. The simulated events were then weighted such that the distribution of the average number of interactions per bunch crossing matches the one observed in data.

5 Event selection and background estimation

The analysis of CP -mixing in the $H \rightarrow \tau\tau$ channel requires the selection of signal events characterised by the presence of isolated leptons, visible decay products in hadronic τ decays, jets and missing transverse momentum. Events with an isolated lepton (electron or muon) and a hadronic τ decay are used for the $\tau_{\text{lep}}\tau_{\text{had}}$ analysis channel, whereas events with two hadronic τ decays are used for the $\tau_{\text{had}}\tau_{\text{had}}$ channel. Additional jets, the invariant mass and the transverse momenta of the τ lepton pairs are used for event categorisation (Section 5.2). Various kinematic and identification requirements are used to suppress the background.

5.1 Objects and decay mode reconstruction

The analysis shares the same object reconstruction and identification algorithms as the $H \rightarrow \tau\tau$ cross-section measurement [55]. Here the most important features specific to this CP measurement are recalled:

- Tracks measured in the ID are used to reconstruct interaction vertices [58], of which the one with the highest sum of squared transverse momenta $\sum p_{\text{T}}^2$ of the associated tracks is selected as the primary vertex of the hard interaction.
- Electrons are reconstructed from topological clusters of energy deposits in the electromagnetic calorimeter which are matched to a track reconstructed in the ID [59] and are required to satisfy ‘loose’ isolation and ‘medium’ identification criteria.
- Muons are reconstructed from signals in the muon spectrometer matched with tracks inside the ID. They are required to satisfy ‘loose’ identification and ‘tight’ isolation criteria based on track information [60].

- Jets are reconstructed using a particle-flow algorithm [61]. It applies an anti- k_t algorithm [62, 63] with distance parameter $R = 0.4$ to noise-suppressed positive-energy topological clusters in the calorimeter after subtracting energy deposits associated with primary-vertex-matched tracks, and including the track momenta instead in the clustering, thereby improving the jet energy measurement. Cleaning criteria are used to identify jets arising from non-collision backgrounds or noise in the calorimeters [64]. A dedicated jet-vertex-tagger algorithm [65] is used to remove jets that are identified as not being associated with the primary vertex of the hard interaction. Similarly, a dedicated algorithm is used to suppress pile-up jets in the forward region [66].
- Hadronic τ -lepton decays are reconstructed from the visible decay products (neutral pions or charged pions/kaons). The reconstruction is seeded by jets reconstructed with an anti- k_t algorithm using calibrated topological clusters [67] as inputs and a distance parameter of $R = 0.4$ [68]. Reconstructed nearby tracks are matched to a hadronic τ candidate ($\tau_{\text{had-vis}}$) if they exceed the value required for a multivariate discriminant determining the likelihood that the tracks are produced from the $\tau_{\text{had-vis}}$ decay. A recurrent neural network identification algorithm [69] is trained to separate the $\tau_{\text{had-vis}}$ candidates from jets initiated by quarks or gluons, and boosted decision tree (BDT) discriminants are used to help reject misidentified hadronic τ decays due to electrons. In both cases, the $\tau_{\text{had-vis}}$ is required to satisfy ‘medium’ criteria. Reconstructed $\tau_{\text{had-vis}}$ objects are required to have one or three associated tracks, and have $p_T > 20$ GeV and $|\eta| < 2.47$, excluding the transition region between the barrel and endcap electromagnetic calorimeters ($1.37 < |\eta| < 1.52$).
- The missing transverse momentum (with magnitude E_T^{miss}) is reconstructed as the negative vector sum of the transverse momenta of leptons, $\tau_{\text{had-vis}}$ objects, jets, and a ‘soft-term’. The ‘soft-term’ is calculated as the vector sum of the p_T of tracks matched to the primary vertex but not associated with reconstructed leptons, $\tau_{\text{had-vis}}$ objects, or jets [70].
- The invariant mass of the τ -lepton-pair system, $m_{\tau\tau}^{\text{MMC}}$, is estimated with an advanced likelihood-based algorithm named the Missing Mass Calculator (MMC) [55, 71].

The transverse (longitudinal) impact parameter d_0 (z_0) of a charged-particle track is defined as the distance in the transverse plane (z direction) from the primary vertex to the track’s point of closest approach in the transverse plane. The impact parameters are used in the calculation of the φ_{CP}^* observable in the cases involving single-pion or leptonic decays (Section 3.1), as well as in one of the variables defining the signal regions (Section 5.2).

An important addition in the CP analysis is that it requires the τ -lepton reconstruction algorithms to categorise the hadronic τ -lepton decays by using the number of reconstructed tracks and the capability to distinguish between single- π^0 and multi- π^0 clusters. This allows the τ_{had} candidates to be classified as being from the 1p0n, 1p1n, 1pXn or 3p0n decay modes. For this measurement it is crucial to identify each decay mode with good efficiency and purity, and to measure the momenta of the charged and neutral pions. This is achieved through the ‘ τ_{had} Particle Flow’ reconstruction algorithm [72], in which the four-momenta of the charged and neutral pions from the τ decay are determined by combining measurements from the tracking detector and the calorimeter. The decay mode classification is performed by counting the number of charged and neutral pions, exploiting the kinematic properties of the τ -lepton decay products and the number of reconstructed photons by using BDTs. Three BDTs are built respectively for the 1p0n vs 1p1n, 1p1n vs 1pXn and 3p0n vs 3pXn decay modes to improve the determination of the number of neutral pions in each case. The efficiency (purity) of the classification is about 80% (70%–80%) for the dominant decay modes 1p0n and 1p1n; for the 3p0n decay mode the efficiency is over 90%, with 90% purity.

5.2 Event selection

Events are selected by requiring at least one hadronic τ -lepton decay in the signature. For events in the $\tau_{\text{lep}}\tau_{\text{had}}$ channel, a $\tau_{\text{had-vis}}$ with $p_{\text{T}} > 30$ GeV and an electron or muon with $p_{\text{T}} > 21.0\text{--}27.3$ GeV are required, with the latter p_{T} cut depending on the data-taking period. In the $\tau_{\text{had}}\tau_{\text{had}}$ channel, two $\tau_{\text{had-vis}}$ objects are required with p_{T} above 40 and 30 GeV. The p_{T} requirements are chosen to be above the p_{T} thresholds of the respective single-lepton and hadronic τ triggers to ensure trigger operation at the plateau efficiency. The $\tau_{\text{had-vis}}$ and the lepton are required to match geometrically with their trigger counterparts in the $\tau_{\text{had}}\tau_{\text{had}}$ and $\tau_{\text{lep}}\tau_{\text{had}}$ channels, respectively. In both channels the two τ -lepton candidates are required to have opposite electric charges. The angular distances between the τ -lepton candidates are required to be $\Delta R_{\tau\tau} < 2.5$ and $|\Delta\eta_{\tau\tau}| < 1.5$ ($0.6 < \Delta R_{\tau\tau} < 2.5$ and $|\Delta\eta_{\tau\tau}| < 1.5$) to reject non-resonant events in the $\tau_{\text{lep}}\tau_{\text{had}}$ ($\tau_{\text{had}}\tau_{\text{had}}$) channel. All events require at least one jet with $p_{\text{T}} > 40$ GeV. Due to triggering conditions, this selection is tightened to $p_{\text{T}} > 70$ GeV and $|\eta| < 3.2$ in the $\tau_{\text{had}}\tau_{\text{had}}$ channel. The $E_{\text{T}}^{\text{miss}}$ is required to be greater than 20 GeV, and requirements on the fraction of the τ -lepton momentum carried by its visible decay products are applied to further improve the invariant mass estimation. In the $\tau_{\text{lep}}\tau_{\text{had}}$ channel, the transverse mass m_{T} of the lepton-plus- $E_{\text{T}}^{\text{miss}}$ system is required to be less than 70 GeV in order to efficiently reject W + jets processes. These preselection criteria are the same as in the $H \rightarrow \tau\tau$ cross-section measurement [55].

Events are further categorised to target the vector-boson fusion (VBF category) and gluon–gluon fusion (Boost category) Higgs boson production modes. The VBF category contains events with a second high- p_{T} jet with $p_{\text{T}}^{j_2} > 30$ GeV. The two leading jets are required to satisfy the following kinematics: $|\Delta\eta_{jj}| > 3.0$, $\eta_{j_1} \cdot \eta_{j_2} < 0$, and $m_{jj} > 400$ GeV, with the pseudorapidity values of τ_{lep} or τ_{had} lying between those of the two leading jets (yielding ‘central τ -leptons’). This kinematic selection is enhanced by splitting the VBF category into two regions, VBF_1 and VBF_0, based on the output of a BDT-based VBF tagger [55], with the VBF_1 region having an enhanced fraction of VBF Higgs boson production events. The Boost category targets events where the Higgs boson recoils against jets. The p_{T} of the Higgs boson ($p_{\text{T}}^{\tau\tau}$) is computed as the magnitude of the vector sum of the transverse momenta of the τ -leptons’ visible decay products and the missing transverse momentum. Events with $p_{\text{T}}^{\tau\tau} > 100$ GeV that do not pass the VBF selection form the Boost category. These events are further separated into those with $\Delta R_{\tau\tau} < 1.5$ and $p_{\text{T}}^{\tau\tau} > 140$ GeV (Boost_1) and those not passing these selections (Boost_0). The event categorisation is applied to both the $\tau_{\text{lep}}\tau_{\text{had}}$ and $\tau_{\text{had}}\tau_{\text{had}}$ channels, as summarised in Table 3.

For each category, a Higgs-enriched signal region is defined with $110 < m_{\tau\tau}^{\text{MMC}} < 150$ GeV, and a $Z \rightarrow \tau\tau$ control region (CR) is defined with $60 < m_{\tau\tau}^{\text{MMC}} < 110$ GeV, with the other selection criteria for each category remaining the same. Two additional control regions are defined using events with $\tau^{\pm} \rightarrow \rho^{\pm}\nu \rightarrow \pi^{\pm}\pi^0\nu$ decay in the $60 < m_{\tau\tau}^{\text{MMC}} < 110$ GeV range: one region with $\ell\text{--}1\text{p}1\text{n}$ events for the $\tau_{\text{lep}}\tau_{\text{had}}$ channel, and the other with $1\text{p}1\text{n}\text{--}1\text{p}1\text{n}$ events for the $\tau_{\text{had}}\tau_{\text{had}}$ channel. The events in these regions are defined so as to be statistically independent of the four $Z \rightarrow \tau\tau$ control regions in Table 3. The use of the control regions is described in Section 7.

Table 3: Summary of selection criteria for the VBF and Boost categories in this analysis. The criteria are common to the $\tau_{\text{lep}}\tau_{\text{had}}$ and $\tau_{\text{had}}\tau_{\text{had}}$ decay channels.

VBF		Boost	
$p_{\text{T}}^{j_2} > 30 \text{ GeV}$ $m_{jj} > 400 \text{ GeV}$ $ \Delta\eta_{jj} > 3.0$ $\eta_{j_1} \cdot \eta_{j_2} < 0$ Central τ -leptons		Not VBF $p_{\text{T}}^{\tau\tau} > 100 \text{ GeV}$	
Signal region ($110 < m_{\tau\tau}^{\text{MMC}} < 150 \text{ GeV}$)			
VBF_1	VBF_0	Boost_1	Boost_0
BDT(VBF) > 0	BDT(VBF) < 0	$\Delta R_{\tau\tau} < 1.5$ and $p_{\text{T}}^{\tau\tau} > 140 \text{ GeV}$	$\Delta R_{\tau\tau} > 1.5$ or $p_{\text{T}}^{\tau\tau} < 140 \text{ GeV}$
$Z \rightarrow \tau\tau$ control region ($60 < m_{\tau\tau}^{\text{MMC}} < 110 \text{ GeV}$)			
VBF_1 Z CR	VBF_0 Z CR	Boost_1 Z CR	Boost_0 Z CR

Depending on the decay mode combination, different additional selection criteria are applied to enhance the sensitivity of the φ_{CP}^* construction method. The φ_{CP}^* from the IP method is less effective in discriminating between different ϕ_τ values when the impact parameter vector has a magnitude smaller than, or similar to, its resolution. The sensitivity of this method can be enhanced by using events with high significance of the track impact parameter in the transverse plane, d_0^{sig} , defined as the transverse impact parameter d_0 divided by its resolution $\sigma(d_0)$. Events are therefore separated into two groups based on the value of $|d_0^{\text{sig}}|$ of the lepton in τ_{lep} or the pion in τ_{had} . In the ρ method, events with larger absolute values of the product $|y_+^\rho y_-^\rho|$ are more sensitive to ϕ_τ . This quantity is also used to separate the events into two groups. In the case of the combined IP- ρ method, the sensitivity of φ_{CP}^* is enhanced by separating the events based on the values $|d_0^{\text{sig}}|$ and $|y^\rho|$. For the IP- a_1 and ρ - a_1 methods the separation is based on $|y_\pm^{a_1}|$. Details of the additional selection criteria are summarised in Tables 4 and 5.

Among the τ -lepton pair decays used in this analysis, the most sensitive (‘dominant’) decay mode combinations are $1p0n$ - $1p1n$, $1p1n$ - $1p1n$, and $1p0n$ - $1p0n$ in the $\tau_{\text{had}}\tau_{\text{had}}$ decay channel, and ℓ - $1p1n$ and ℓ - $1p0n$ in the $\tau_{\text{lep}}\tau_{\text{had}}$ decay channel, while the other combinations involving $1pXn$ and $3p0n$ are subdominant due to their weaker spin analysing power and smaller decay fractions. The events are therefore divided into three groups, the ‘High’, ‘Medium’ and ‘Low’ signal regions, which characterise the different levels of sensitivity. Events satisfying the additional selection criteria for the dominant and subdominant decay mode combinations define the High and Medium signal regions, respectively, while the rest are grouped into the Low signal region. This allows the φ_{CP}^* distributions from the decay mode combinations with similar sensitivity to CP -mixing to be merged to increase the statistical precision of the distribution templates within each signal region, allowing the use of finer binning in the φ_{CP}^* distributions for the regions with better sensitivity. The splitting of the signal regions summarised in Tables 4 and 5 is applied in each of the VBF and Boost categories (VBF_1, VBF_0, Boost_1 and Boost_0).

In this configuration, there are 12 signal regions in each of the $\tau_{\text{lep}}\tau_{\text{had}}$ and $\tau_{\text{had}}\tau_{\text{had}}$ decay channels, leading to 24 signal regions in total. Each signal or control region is orthogonal to the others.

Table 4: Summary of additional selection criteria for the signal regions in the $\tau_{\text{lep}}\tau_{\text{had}}$ channel.

Channel	Signal region	Decay mode combination	Selection criteria
$\tau_{\text{lep}}\tau_{\text{had}}$	High	$\ell-1p0n$	$ d_0^{\text{sig}}(e) > 2.5$ or $ d_0^{\text{sig}}(\mu) > 2.0$ $ d_0^{\text{sig}}(\tau_{1p0n}) > 1.5$
		$\ell-1p1n$	$ d_0^{\text{sig}}(e) > 2.5$ or $ d_0^{\text{sig}}(\mu) > 2.0$ $ y^\rho(\tau_{1p1n}) > 0.1$
	Medium	$\ell-1pXn$	$ d_0^{\text{sig}}(e) > 2.5$ or $ d_0^{\text{sig}}(\mu) > 2.0$ $ y^\rho(\tau_{1pXn}) > 0.1$
		$\ell-3p0n$	$ d_0^{\text{sig}}(e) > 2.5$ or $ d_0^{\text{sig}}(\mu) > 2.0$ $ y^{\alpha_1}(\tau_{3p0n}) > 0.6$
	Low	All above	Not satisfying selection criteria

Table 5: Summary of additional selection criteria for the signal regions in the $\tau_{\text{had}}\tau_{\text{had}}$ channel.

Channel	Signal region	Decay mode combination	Selection criteria
$\tau_{\text{had}}\tau_{\text{had}}$	High	$1p0n-1p0n$	$ d_0^{\text{sig}}(\tau_1) > 1.5$ $ d_0^{\text{sig}}(\tau_2) > 1.5$
		$1p0n-1p1n$	$ d_0^{\text{sig}}(\tau_{1p0n}) > 1.5$ $ y^\rho(\tau_{1p1n}) > 0.1$
		$1p1n-1p1n$	$ y^\rho(\tau_1)y^\rho(\tau_2) > 0.2$
	Medium	$1p0n-1pXn$	$ d_0^{\text{sig}}(\tau_{1p0n}) > 1.5$ $ y^\rho(\tau_{1pXn}) > 0.1$
		$1p1n-1pXn$	$ y^\rho(\tau_{1p1n})y^\rho(\tau_{1pXn}) > 0.2$
	Low	All above	Not satisfying selection criteria

5.3 Background estimation

Expected SM processes other than the $H \rightarrow \tau\tau$ signal are evaluated using a mixture of simulation and data-driven techniques. Processes with true τ -leptons and prompt light leptons are estimated through simulation. Among those the $Z(\rightarrow \tau\tau) + \text{jets}$ process is the dominant one, and dedicated control regions with $60 < m_{\tau\tau}^{\text{MMC}} < 110$ GeV (Section 5.2) are used to extract its normalisation (Section 7).

The second most significant background contribution arises from jets misidentified as hadronically decaying τ -leptons (τ_{had}), referred to as ‘misidentified- τ background’. It is determined by a data-driven approach using fake factors, as described in detail in Ref. [55]. The misidentified- τ background consists mostly

of $W + \text{jets}$, QCD multijet, and top-quark events in the $\tau_{\text{lep}}\tau_{\text{had}}$ channel, while in the $\tau_{\text{had}}\tau_{\text{had}}$ channel it originates mainly from multijet events. The fake factors are calculated as the ratio of the number of events passing the τ identification requirements to the number failing them in dedicated QCD and $W + \text{jets}$ -enriched regions, defined by inverting the lepton isolation or m_{T} requirement, respectively. The fake factors are estimated in each hadronic τ decay mode considered in the analysis, separately for VBF and Boost region events. To estimate both the shape and the normalisation of the misidentified- τ background, distributions in the regions failing the τ identification are multiplied by the fake factors to correct for the different efficiencies to pass or fail the τ identification selection. In the ‘failed τ identification’ regions, events not corresponding to misidentified- τ background from jets are subtracted using simulated event samples. For the $\tau_{\text{had}}\tau_{\text{had}}$ final state the fake-factor method is modified slightly: the τ_{had} objects are matched to their trigger counterparts and the estimate covers processes with one or two jets misidentified as τ_{had} . The misidentified- τ background contribution is estimated for each di- τ decay combination considered (Section 3) in the preselection region for the $\tau_{\text{had}}\tau_{\text{had}}$ events.

Smaller background contributions are due to diboson, $Z(\rightarrow \ell\ell) + \text{jets}$ and $H \rightarrow WW^*$ processes in both decay channels, while $W + \text{jets}$ and top production also make small contributions in the $\tau_{\text{had}}\tau_{\text{had}}$ channel. These are estimated from simulation and are normalised to their theoretical expectations.

6 Systematic uncertainties

Systematic uncertainties generally affect the yield in the signal and control regions as well as the shape of the φ_{CP}^* distribution, on which the fit is performed. They are grouped into three types: the experimental uncertainties, the theoretical uncertainties, and the τ -lepton decay reconstruction uncertainties.

The experimental uncertainties include those from the trigger, reconstruction, identification and isolation requirements of the final-state particle candidates (electrons, muons, τ -leptons, jets, $E_{\text{T}}^{\text{miss}}$, b -tagging), as well as uncertainties from misidentified- τ background estimation and the luminosity measurement [73, 74].

The uncertainties on the jet energy resolution and scale [75] affect the acceptance of the signal and background contributions through their impact on $E_{\text{T}}^{\text{miss}}$, and thus $m_{\tau\tau}^{\text{MMC}}$ [76]. They also directly affect the jet selection for the event categorisation in the VBF and Boost regions [76]. The jet energy scale uncertainty for central jets ($|\eta| < 1.2$) varies from 1% for a wide range of jet p_{T} ($250 \text{ GeV} < p_{\text{T}} < 2000 \text{ GeV}$) to 5% for very low p_{T} jets ($p_{\text{T}} < 20 \text{ GeV}$), and 3.5% for very high p_{T} jets ($p_{\text{T}} > 2.5 \text{ TeV}$), and forward jets exhibit uncertainties of similar size. The relative jet energy resolution ranges from $(24 \pm 1.5)\%$ to $(6 \pm 0.5)\%$ for jets with p_{T} of 20 GeV to 300 GeV, respectively [75]. Other jet-related uncertainties have smaller impacts.

Uncertainties from the misidentified- τ background estimation arise from sample statistics of the events used for estimating the fake factors, subtraction of residual contributions from processes without misidentified- τ , and uncertainties in the flavour composition taken from comparisons between the predicted and observed backgrounds in a dedicated validation region. The uncertainties are assigned per τ -lepton-pair decay combination in the $\tau_{\text{lep}}\tau_{\text{had}}$ and $\tau_{\text{had}}\tau_{\text{had}}$ channels. The total expected uncertainties in the yield of the misidentified- τ events in the signal regions are typically 20% (20%–40%) in the Boost (VBF) region in the $\tau_{\text{lep}}\tau_{\text{had}}$ channel, and 15%–30% in the $\tau_{\text{had}}\tau_{\text{had}}$ channel.

Theoretical uncertainties are applied to $Z + \text{jets}$ background and signal processes. For the $Z + \text{jets}$ background, uncertainties are considered for the renormalisation and factorisation scales, the resummation

scale, the jet-to-parton matching scheme, the choice of value for the strong coupling constant α_s , and the choice of PDF. Only distribution shapes and migrations between analysis regions are considered for these uncertainties since the absolute normalisation of $Z \rightarrow \tau\tau$ is determined at the fit level. For the signal, uncertainties are considered for the QCD scale because of missing higher orders in the matrix element calculation, for the parton shower and hadronisation model, and for renormalisation and factorisation scales and the PDF. These are applied to the production cross-sections for the ggF, VBF and VH processes, and do not have large impacts on the measurement as they only affect the signal normalisation, which is also determined in the fit, and not the shape of the φ_{CP}^* distribution.

The τ -lepton decay reconstruction uncertainties primarily affect the shape of the φ_{CP}^* distributions. These concern the classification of the hadronic τ -lepton decay modes as well as measurement uncertainties of the track impact parameters, pion track momentum, and neutral pion momentum. The uncertainties in the classification of the hadronic τ -lepton decay modes are derived from a τ -lepton decay mode classification efficiency and correction factor measurement, using a tag-and-probe analysis in the μ - τ_{had} final state performed on part of the Run 2 dataset. These uncertainties include those in the decay mode reconstruction efficiencies and in the event migration between decay modes. The size of the uncertainties ranges from 6% to 20% depending on the decay modes and their cross migrations. The uncertainties affecting the impact parameters and track measurements include those in alignment effects and in impact parameter resolution, and they account for differences between data and simulation.

The uncertainties in the π^0 angular resolution and energy scale are estimated in situ in the analysis. The π^0 energy and momentum direction are initially varied in accordance with the energy response of the calorimeter to charged pions [77] and the measured π^0 angular resolution [72], respectively. These variations in the π^0 energy scale and angular resolution are found to affect the shape of the distribution of the reconstructed invariant mass of the $\pi^\pm\pi^0$ system, $m(\pi^\pm, \pi^0)$, in $\tau^\pm \rightarrow \rho^\pm\nu \rightarrow \pi^\pm\pi^0\nu$ decays. Dedicated $Z \rightarrow \tau\tau$ control regions with exclusive 1p1n decays, namely the ℓ -1p1n and 1p1n-1p1n events, are defined in the $\tau_{\text{lep}}\tau_{\text{had}}$ and $\tau_{\text{had}}\tau_{\text{had}}$ decay channels, respectively, as described in Section 5.2. The $m(\pi^\pm, \pi^0)$ distribution is used as the observable in these control regions in the combined fit, so that the final size of the π^0 angular resolution and energy scale uncertainties in the ϕ_τ measurement are determined from data. Figure 3 shows the post-fit distributions of $m(\pi^\pm, \pi^0)$ in the $Z \rightarrow \tau\tau$ control regions in the $\tau_{\text{lep}}\tau_{\text{had}}$ and $\tau_{\text{had}}\tau_{\text{had}}$ channels using ℓ -1p1n and 1p1n-1p1n events, respectively. For the 1p1n-1p1n events in the $\tau_{\text{had}}\tau_{\text{had}}$ channel, only the leading τ_{had} is selected for the $m(\pi^\pm, \pi^0)$ distribution. The $m(\pi^\pm, \pi^0)$ data distributions show good agreement with the prediction.

7 Statistical analysis

To measure the CP -mixing angle ϕ_τ , a simultaneous fit to the data is performed using a likelihood function that depends on the CP -mixing angle ϕ_τ as the parameter-of-interest, and the nuisance parameters that account for the systematic uncertainties and the floating normalisations for the Higgs boson signal and for the background. The likelihood function is constructed as a product of Poisson probability terms over the bins of the input distributions, and the parameter-of-interest is estimated by maximising the likelihood. The likelihood comprises 24 signal regions and 10 control regions. Constraints on the nuisance parameters are assigned with a Gaussian term, and bin-by-bin statistical fluctuations in the simulated background samples are included in the fit with a Poisson probability term.

In the fit the normalisation of the $Z \rightarrow \tau\tau$ events is left to float freely in the eight control regions (described in Section 5.2) to account for the $Z \rightarrow \tau\tau$ modelling in the different signal regions. Four normalisation

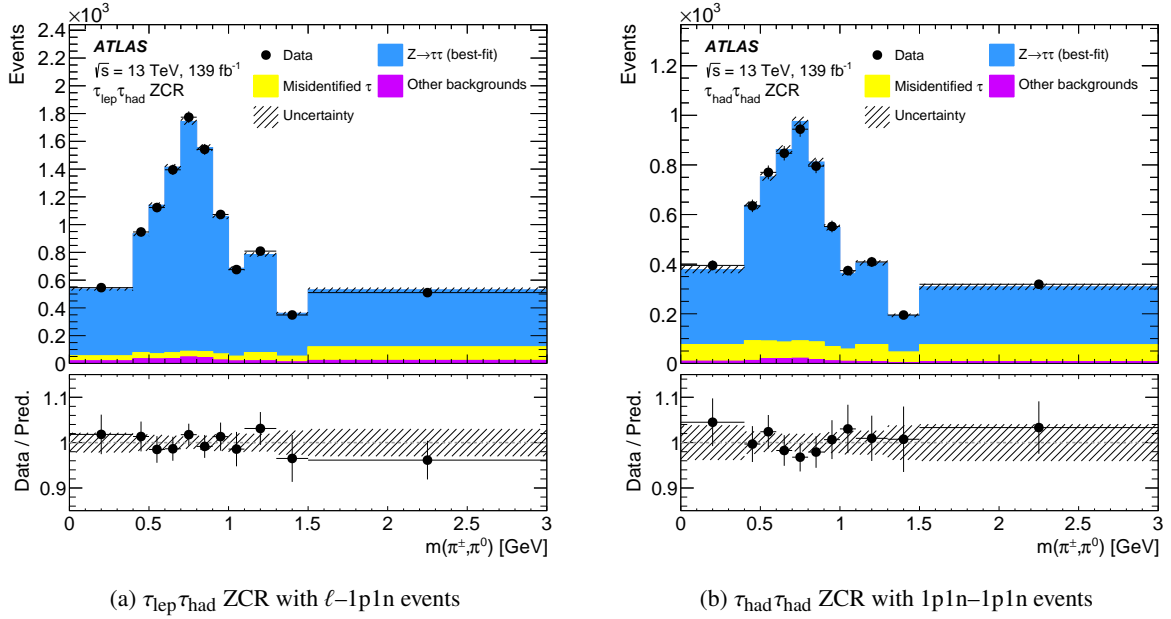


Figure 3: Post-fit distributions of the $\pi^\pm\pi^0$ invariant mass, $m(\pi^\pm, \pi^0)$, in the $Z \rightarrow \tau\tau$ control regions in the (a) $\tau_{\text{lep}}\tau_{\text{had}}$ and (b) $\tau_{\text{had}}\tau_{\text{had}}$ channels. The $\ell-1p1n$ ($1p1n-1p1n$) events are used in the $\tau_{\text{lep}}\tau_{\text{had}}$ ($\tau_{\text{had}}\tau_{\text{had}}$) channel in this control region. For the $\tau_{\text{had}}\tau_{\text{had}}$ channel only the $m(\pi^\pm, \pi^0)$ value of the leading τ_{had} is selected. ‘Other backgrounds’ include W , diboson, top, $Z \rightarrow \ell\ell$ and $H \rightarrow WW^*$. The hatched uncertainty band includes all sources of uncertainty after the fit to data.

factors (NF) are defined to control the $Z \rightarrow \tau\tau$ background events in the Boost_0, Boost_1, VBF_0, VBF_1 categories, respectively. Each factor is shared between the $\tau_{\text{lep}}\tau_{\text{had}}$ and $\tau_{\text{had}}\tau_{\text{had}}$ channels, and is also shared between a control region and the corresponding signal region in the same category. Other backgrounds are normalised to their expected number of events estimated from the MC simulation.

Two control regions using events with a $\tau^\pm \rightarrow \rho^\pm \nu \rightarrow \pi^\pm \pi^0 \nu$ decay ($\ell-1p1n$ in $\tau_{\text{lep}}\tau_{\text{had}}$ and $1p1n-1p1n$ in $\tau_{\text{had}}\tau_{\text{had}}$) are defined from the $Z \rightarrow \tau\tau$ control region events (Section 5.2). The distribution of the $\pi^\pm\pi^0$ invariant mass, $m(\pi^\pm, \pi^0)$, is employed in these control regions to control the π^0 -related uncertainties by using the data, as described in Section 6.

The Higgs boson signal strength $\mu_{\tau\tau}$ (defined as the ratio of the measured signal yield to the SM expectation) is also left unconstrained in the fit, such that the signal normalisation does not depend on the SM assumption and only the shape of the φ_{CP}^* distribution is exploited in the estimation of ϕ_τ . Model-dependence of the cross-section on CP -mixing scenarios is not exploited. The φ_{CP}^* distributions in the signal regions are binned to maximise the measurement sensitivity, taking into account the associated uncertainties. In general, finer binnings are used in the signal regions associated with higher sensitivity (High and Medium SRs), with coarser binning in the Low signal region. A smoothing procedure is applied in the signal regions to remove potentially large local fluctuations in the systematic variations of the φ_{CP}^* distributions because of the limited size of the MC samples used to build the templates. The test statistic is based on a profile likelihood ratio and the asymptotic approximation [78] is used for statistical interpretations.

8 Results

Figure 4 shows the post-fit φ_{CP}^* distributions for the data as well as the prediction in the High, Medium and Low signal regions in the $\tau_{lep}\tau_{had}$ and $\tau_{had}\tau_{had}$ channels, respectively. In each distribution, the φ_{CP}^* bins are counted incrementally through all VBF and Boost categories and cover the range $[0, 360]^\circ$ for each category. The observed and expected negative log-likelihood ($\Delta \ln L$) scans in ϕ_τ are shown in Figure 5. The observed (expected) value of ϕ_τ is $9^\circ \pm 16^\circ$ ($0^\circ \pm 28^\circ$) at the 68% confidence level (CL), and $\pm 34^\circ$ (${}^{+75^\circ}_{-70^\circ}$) at the 2σ level. The data disfavours the pure CP -odd hypothesis at the 3.4σ level, while the expected exclusion level is 2.1σ . The fitted signal and background normalisations are shown in Table 6. The results are compatible with the SM expectation within the measured uncertainties.

The total uncertainty is dominated by the statistical uncertainties of the data sample. The dominant contributions to the systematic uncertainties are from jets, followed by limited sample size of the background simulations, uncertainties from the free-floating normalisation factors, and theory uncertainties. The uncertainties in the τ -lepton decay reconstruction have small impacts of less than 1° on ϕ_τ . The effects from the π^0 uncertainties measured in situ are compared with those from a set of simulated event samples with systematically varied modelling of the hadronic response in the calorimeter, and the latter are found to have a similar impact on the ϕ_τ measurement. Effects from other sources are negligible. The impact of the uncertainties is summarised in Table 7.

The difference between the observed and expected sensitivities of the ϕ_τ measurement can be attributed to a statistical fluctuation in data. The uncertainties of the ϕ_τ measurement are highly dependent on the size of the modulation amplitude of the φ_{CP}^* distributions. In the measured data, there are more distortions of the φ_{CP}^* shape due to bins fluctuating from their expected values, resulting in overall larger modulation amplitudes than the predicted shape. A set of pseudo-experiments is performed (with the condition $\mu_{\tau\tau} = 1$) that shows that the probability of obtaining the observed distribution, given the expectation, is about 4%.

The present measurement is compatible with the recent measurement of the same mixing-angle parameter by the CMS Collaboration [24], for which an observed (expected) mixing-angle value of $-1^\circ \pm 19^\circ$ ($0^\circ \pm 21^\circ$) at the 68% CL was reported.

The expected sensitivities of the $\tau_{had}\tau_{had}$ and $\tau_{lep}\tau_{had}$ channels in excluding a pure CP -odd $H\tau\tau$ coupling are 1.7σ and 1.1σ , respectively. The ‘High’ signal regions contribute the most, with 1.4σ and 1.0σ in the $\tau_{had}\tau_{had}$ and $\tau_{lep}\tau_{had}$ channels, respectively. Other signal regions have expected sensitivities below 1σ .

A 2D scan of $\Delta \ln L$ as a function of the signal strength $\mu_{\tau\tau}$ versus ϕ_τ is shown in Figure 6. The 1σ and 2σ 2D confidence levels correspond to $\Delta \ln L$ values of 1.15 and 3.09, respectively. No strong correlation between $\mu_{\tau\tau}$ and ϕ_τ is observed. The SM prediction of $\mu_{\tau\tau} = 1$ and $\phi_\tau = 0$ is compatible with the measurement within the 1σ confidence region.

Figure 7 shows the data distribution of φ_{CP}^* with all signal regions in both the $\tau_{lep}\tau_{had}$ and $\tau_{had}\tau_{had}$ channels combined, together with the best-fit $H \rightarrow \tau\tau$ signal, pure CP -even and pure CP -odd hypotheses. The events in each signal region are weighted with $\ln(1 + S/B)$, where S and B are the event yields for the signal and the total background, respectively. The background is subtracted from data in the figure. The distribution illustrates that the data disfavours the pure CP -odd scenario.

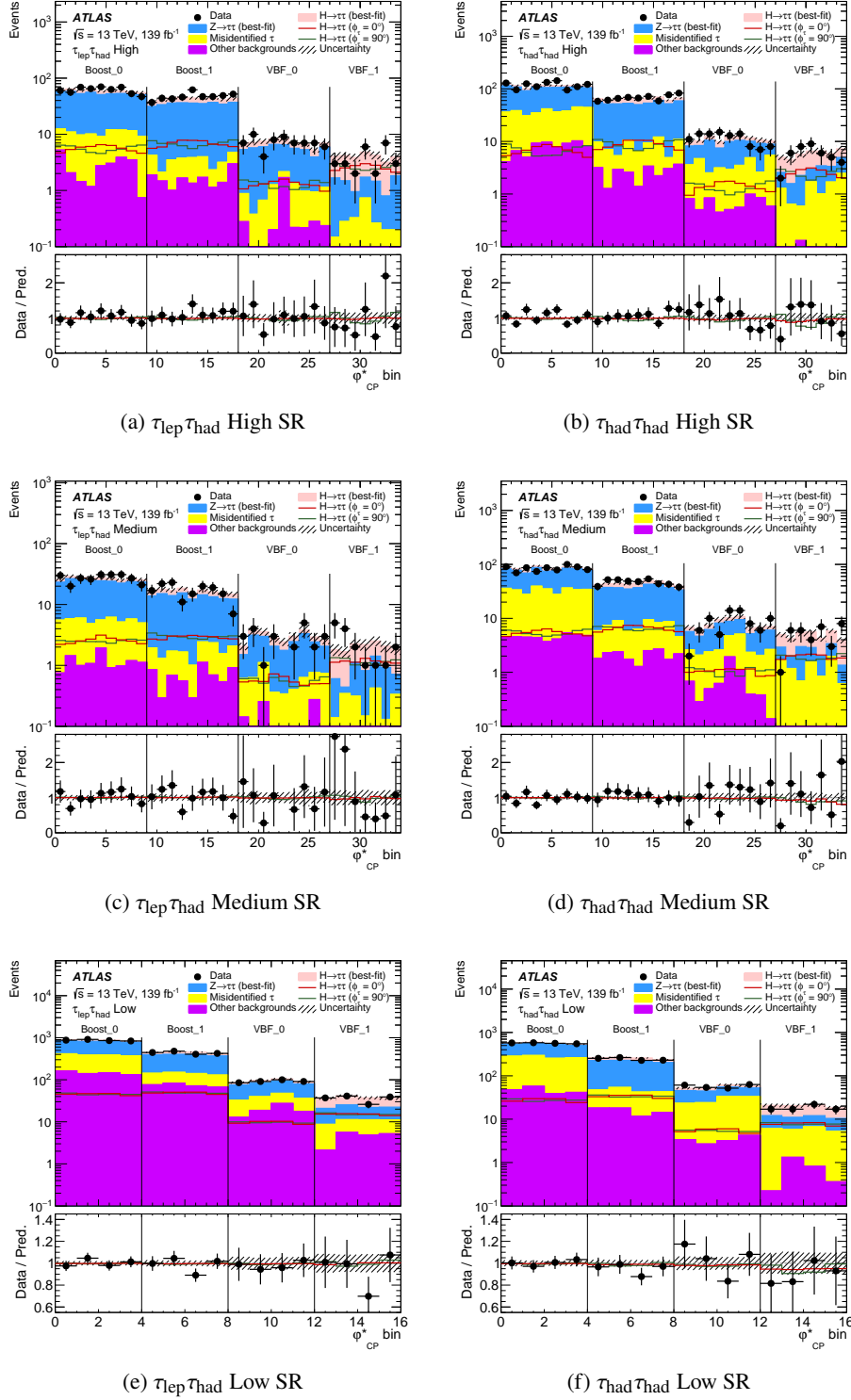


Figure 4: Post-fit distributions of φ_{CP}^* in the signal regions (SRs), showing (a) $\tau_{\text{lep}}\tau_{\text{had}}$ High SR, (b) $\tau_{\text{had}}\tau_{\text{had}}$ High SR, (c) $\tau_{\text{lep}}\tau_{\text{had}}$ Medium SR, (d) $\tau_{\text{had}}\tau_{\text{had}}$ Medium SR, (e) $\tau_{\text{lep}}\tau_{\text{had}}$ Low SR, and (f) $\tau_{\text{had}}\tau_{\text{had}}$ Low SR. The φ_{CP}^* bins are counted incrementally through all VBF and Boost categories and cover the range $[0, 360]^\circ$ for each category. The best-fit $H \rightarrow \tau\tau$ signal is shown in solid pink, while the red and green lines indicate the predictions for the pure CP -even (scalar, SM) and pure CP -odd (pseudoscalar) hypotheses, scaled to the predicted signal yield. ‘Other backgrounds’ include W , diboson, top, $Z \rightarrow \ell\ell$ and $H \rightarrow WW^*$. The hatched uncertainty band includes all sources of uncertainty after the fit to data.

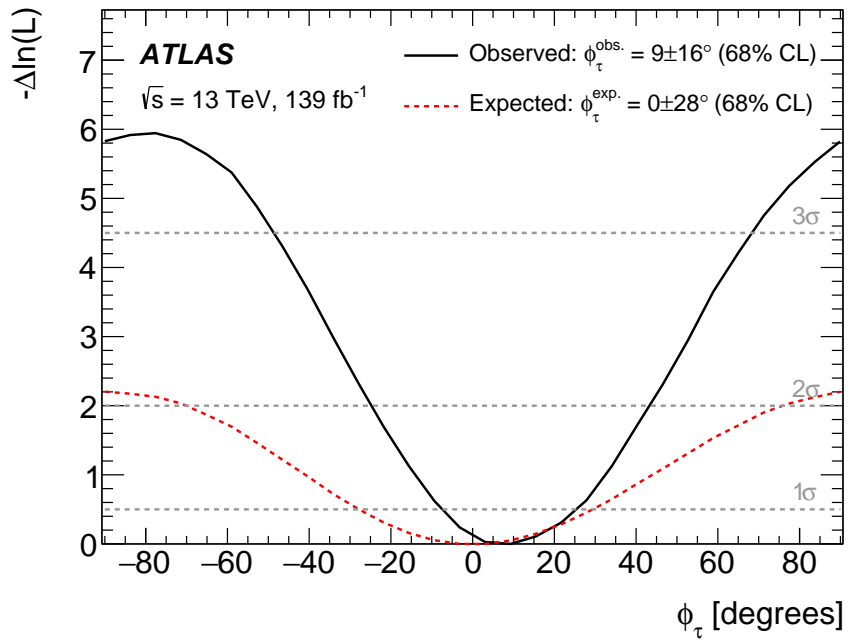


Figure 5: One-dimensional likelihood scan of the CP -mixing angle ϕ_{τ} . The observed (expected) value of ϕ_{τ} is $9^{\circ} \pm 16^{\circ}$ ($0^{\circ} \pm 28^{\circ}$) at the 68% confidence level (CL), and $\pm 34^{\circ}$ ($^{+75^{\circ}}_{-70^{\circ}}$) at the 2σ level. The CP -odd hypothesis is rejected at the 3.4σ (2.1σ expected) level.

Table 6: Free-floating parameters in the measurement. Observed and expected values are shown for the CP -mixing angle (ϕ_τ), the signal strength ($\mu_{\tau\tau}$) and various background normalisations for $Z \rightarrow \tau\tau$ ($NF_{Z \rightarrow \tau\tau}$) corresponding to different signal phase-space regions.

Fitted parameters	Observed	Expected
ϕ_τ	$9^\circ \pm 16^\circ$	$0^\circ \pm 28^\circ$
$\mu_{\tau\tau}$	$1.02^{+0.20}_{-0.20}$	$1.00^{+0.21}_{-0.21}$
$NF_{Z \rightarrow \tau\tau}^{\text{Boost}_1}$	1.01 ± 0.05	1.00 ± 0.04
$NF_{Z \rightarrow \tau\tau}^{\text{Boost}_0}$	1.02 ± 0.05	1.00 ± 0.05
$NF_{Z \rightarrow \tau\tau}^{\text{VBF}_1}$	1.04 ± 0.08	1.00 ± 0.08
$NF_{Z \rightarrow \tau\tau}^{\text{VBF}_0}$	0.95 ± 0.07	1.00 ± 0.08

Table 7: Impact of different sources of uncertainty on the ϕ_τ measurement.

Set of nuisance parameters	Impact on ϕ_τ [degrees]
Jet energy scale	3.4
Jet energy resolution	2.5
Pile-up jet tagging	0.5
Jet flavour tagging	0.2
E_T^{miss}	0.4
Electron	0.3
Muon	0.9
τ_{had} reconstruction	1.0
Misidentified τ	0.6
τ_{had} decay mode classification	0.3
π^0 angular resolution and energy scale	0.2
Track (π^\pm , impact parameter)	0.7
Luminosity	0.1
Theory uncertainty in $H \rightarrow \tau\tau$ processes	1.5
Theory uncertainty in $Z \rightarrow \tau\tau$ processes	1.1
Simulated background sample statistics	1.4
Signal normalisation	1.4
Background normalisation	0.6
Total systematic uncertainty	5.2
Data sample statistics	15.6
Total	16.4

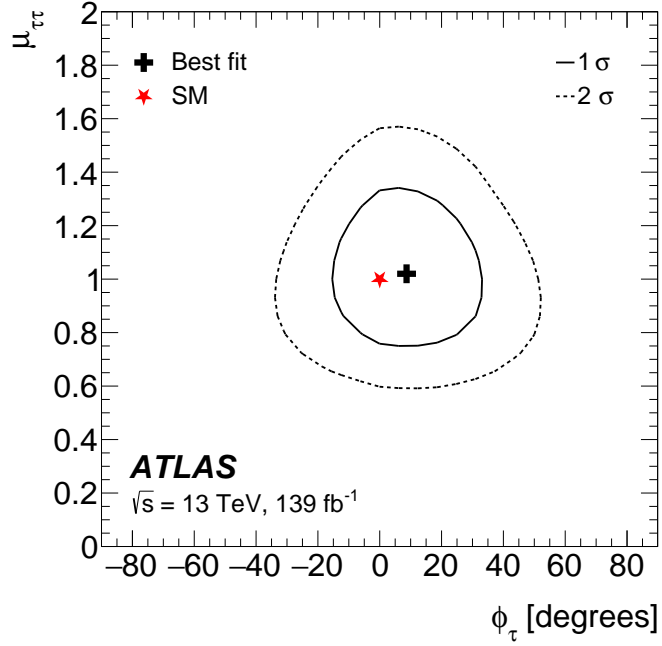


Figure 6: A 2D likelihood scan of the observed signal strength $\mu_{\tau\tau}$ versus the CP -mixing angle ϕ_{τ} . The 1σ and 2σ confidence regions are shown.

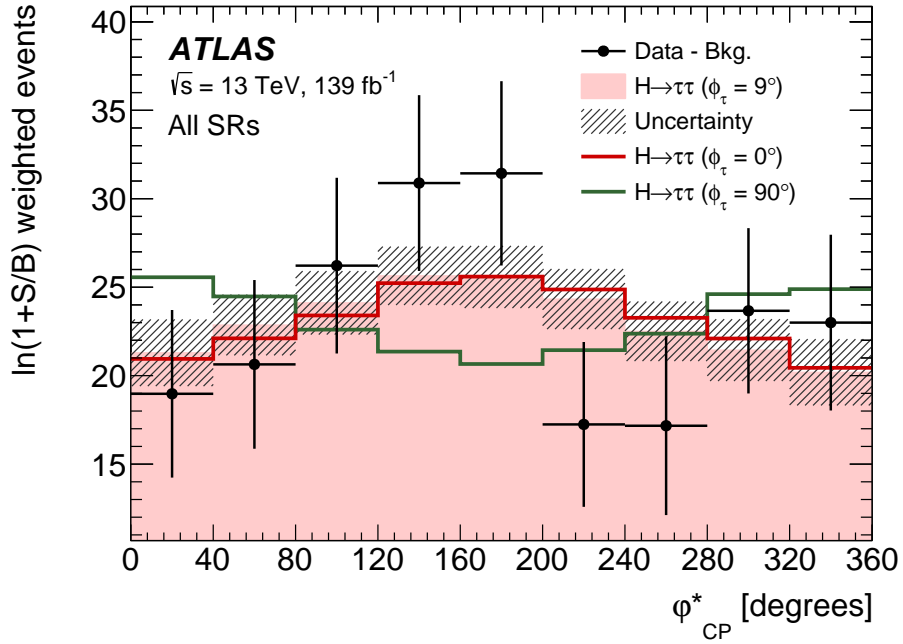


Figure 7: Combined post-fit distribution of φ_{CP}^* from all signal regions in both the $\tau_{lep}\tau_{had}$ and $\tau_{had}\tau_{had}$ channels. Events are weighted with $\ln(1+S/B)$ for the corresponding signal region. The background is subtracted from data. The best-fit $H \rightarrow \tau\tau$ signal is shown in solid pink, while the red and green lines indicate the predictions for the pure CP -even (scalar, SM) and pure CP -odd (pseudoscalar) hypotheses, respectively, all scaled to the best-fit $H \rightarrow \tau\tau$ signal yield. The hatched uncertainty band includes all sources of uncertainty after the fit to data, and represents the same uncertainty in the total signal and background predictions as in Figure 4.

9 Conclusion

A measurement of the CP properties of the interaction between the Higgs boson and τ -leptons is presented. In the generalised Yukawa interaction, a single mixing parameter ϕ_τ parameterises CP -violating interactions between the Higgs boson and τ -leptons. The measurement is performed using 139 fb^{-1} of proton–proton collision data recorded at a centre-of-mass energy of $\sqrt{s} = 13 \text{ TeV}$ with the ATLAS detector at the Large Hadron Collider. The measurement is based on a maximum-likelihood fit to the CP -sensitive angular observable φ_{CP}^* defined by the visible decay products in the $\tau_{\text{lep}}\tau_{\text{had}}$ and $\tau_{\text{had}}\tau_{\text{had}}$ decay channels. Depending on the decay channels, different methods are used to reconstruct the φ_{CP}^* distributions. The sensitivity is optimised by applying decay-mode-dependent kinematic selections. The observed (expected) value of ϕ_τ is $9^\circ \pm 16^\circ$ ($0^\circ \pm 28^\circ$) at the 68% confidence level, and $\pm 34^\circ$ ($^{+75^\circ}_{-70^\circ}$) at the 2σ level. The pure CP -odd hypothesis is disfavoured at a level of 3.4 standard deviations. The analysis precision is limited by the statistical uncertainty of the data sample. The measurement is consistent with the Standard Model expectation.

Acknowledgements

We thank CERN for the very successful operation of the LHC, as well as the support staff from our institutions without whom ATLAS could not be operated efficiently.

We acknowledge the support of ANPCyT, Argentina; YerPhI, Armenia; ARC, Australia; BMWFW and FWF, Austria; ANAS, Azerbaijan; CNPq and FAPESP, Brazil; NSERC, NRC and CFI, Canada; CERN; ANID, Chile; CAS, MOST and NSFC, China; Minciencias, Colombia; MEYS CR, Czech Republic; DNRF and DNSRC, Denmark; IN2P3-CNRS and CEA-DRF/IRFU, France; SRNSFG, Georgia; BMBF, HGF and MPG, Germany; GSRI, Greece; RGC and Hong Kong SAR, China; ISF and Benoziyo Center, Israel; INFN, Italy; MEXT and JSPS, Japan; CNRST, Morocco; NWO, Netherlands; RCN, Norway; MEiN, Poland; FCT, Portugal; MNE/IFA, Romania; MESTD, Serbia; MSSR, Slovakia; ARRS and MIZŠ, Slovenia; DSI/NRF, South Africa; MICINN, Spain; SRC and Wallenberg Foundation, Sweden; SERI, SNSF and Cantons of Bern and Geneva, Switzerland; MOST, Taiwan; TENMAK, Türkiye; STFC, United Kingdom; DOE and NSF, United States of America. In addition, individual groups and members have received support from BCKDF, CANARIE, Compute Canada and CRC, Canada; PRIMUS 21/SCI/017 and UNCE SCI/013, Czech Republic; COST, ERC, ERDF, Horizon 2020 and Marie Skłodowska-Curie Actions, European Union; Investissements d’Avenir Labex, Investissements d’Avenir IDEX and ANR, France; DFG and AvH Foundation, Germany; Herakleitos, Thales and Aristeia programmes co-financed by EU-ESF and the Greek NSRF, Greece; BSF-NSF and MINERVA, Israel; Norwegian Financial Mechanism 2014–2021, Norway; NCN and NAWA, Poland; La Caixa Banking Foundation, CERCA Programme Generalitat de Catalunya and PROMETEO and GenT Programmes Generalitat Valenciana, Spain; Göran Gustafssons Stiftelse, Sweden; The Royal Society and Leverhulme Trust, United Kingdom.

The crucial computing support from all WLCG partners is acknowledged gratefully, in particular from CERN, the ATLAS Tier-1 facilities at TRIUMF (Canada), NDGF (Denmark, Norway, Sweden), CC-IN2P3 (France), KIT/GridKA (Germany), INFN-CNAF (Italy), NL-T1 (Netherlands), PIC (Spain), ASGC (Taiwan), RAL (UK) and BNL (USA), the Tier-2 facilities worldwide and large non-WLCG resource providers. Major contributors of computing resources are listed in Ref. [79].

References

- [1] ATLAS Collaboration, *Evidence for the Higgs-boson Yukawa coupling to tau leptons with the ATLAS detector*, *JHEP* **04** (2015) 117, arXiv: [1501.04943 \[hep-ex\]](#).
- [2] CMS Collaboration, *Evidence for the 125 GeV Higgs boson decaying to a pair of τ leptons*, *JHEP* **05** (2014) 104, arXiv: [1401.5041 \[hep-ex\]](#).
- [3] ATLAS and CMS Collaborations, *Measurements of the Higgs boson production and decay rates and constraints on its couplings from a combined ATLAS and CMS analysis of the LHC pp collision data at $\sqrt{s} = 7$ and 8 TeV*, *JHEP* **08** (2016) 045, arXiv: [1606.02266 \[hep-ex\]](#).
- [4] ATLAS Collaboration, *Test of CP Invariance in vector-boson fusion production of the Higgs boson using the Optimal Observable method in the ditau decay channel with the ATLAS detector*, *Eur. Phys. J. C* **76** (2016) 658, arXiv: [1602.04516 \[hep-ex\]](#).
- [5] ATLAS Collaboration, *Measurement of the Higgs boson coupling properties in the $H \rightarrow ZZ^* \rightarrow 4\ell$ decay channel at $\sqrt{s} = 13$ TeV with the ATLAS detector*, *JHEP* **03** (2018) 095, arXiv: [1712.02304 \[hep-ex\]](#).
- [6] ATLAS Collaboration, *Measurements of Higgs boson properties in the diphoton decay channel with 36fb^{-1} of pp collision data at $\sqrt{s} = 13$ TeV with the ATLAS detector*, *Phys. Rev. D* **98** (2018) 052005, arXiv: [1802.04146 \[hep-ex\]](#).
- [7] CMS Collaboration, *Combined search for anomalous pseudoscalar HVV couplings in $VH(H \rightarrow b\bar{b})$ production and $H \rightarrow VV$ decay*, *Phys. Lett. B* **759** (2016) 672, arXiv: [1602.04305 \[hep-ex\]](#).
- [8] CMS Collaboration, *Measurements of the Higgs boson width and anomalous HVV couplings from on-shell and off-shell production in the four-lepton final state*, *Phys. Rev. D* **99** (2019) 112003, arXiv: [1901.00174 \[hep-ex\]](#).
- [9] CMS Collaboration, *Constraints on anomalous HVV couplings from the production of Higgs bosons decaying to τ lepton pairs*, *Phys. Rev. D* **100** (2019) 112002, arXiv: [1903.06973 \[hep-ex\]](#).
- [10] C. Zhang and S. Willenbrock, *Effective-field-theory approach to top-quark production and decay*, *Phys. Rev. D* **83** (2011) 034006, arXiv: [1008.3869 \[hep-ph\]](#).
- [11] ATLAS Collaboration, *CP Properties of Higgs Boson Interactions with Top Quarks in the $t\bar{t}H$ and tH Processes Using $H \rightarrow \gamma\gamma$ with the ATLAS Detector*, *Phys. Rev. Lett.* **125** (2020) 061802, arXiv: [2004.04545 \[hep-ex\]](#).
- [12] CMS Collaboration, *Measurements of $t\bar{t}H$ Production and the CP Structure of the Yukawa Interaction between the Higgs Boson and Top Quark in the Diphoton Decay Channel*, *Phys. Rev. Lett.* **125** (2020) 061801, arXiv: [2003.10866 \[hep-ex\]](#).
- [13] J. R. Dell'Aquila and C. A. Nelson, *Usage of the $\tau\tau$ or $t\bar{t}$ Decay Mode to Distinguish an Intermediate Mass Higgs Boson From a Technipion*, *Nucl. Phys. B* **320** (1989) 86.
- [14] M. Krämer, J. H. Kühn, M. L. Stong and P. M. Zerwas, *Prospects of measuring the parity of Higgs particles*, *Z. Phys. C* **64** (1994) 21, arXiv: [hep-ph/9404280](#).

- [15] G. R. Bower, T. Pierzchala, Z. Was and M. Worek, *Measuring the Higgs boson's parity using tau \rightarrow rho nu*, *Phys. Lett. B* **543** (2002) 227, arXiv: [hep-ph/0204292](#).
- [16] K. Desch, A. Imhof, Z. Was and M. Worek, *Probing the CP nature of the Higgs boson at linear colliders with tau spin correlations: the case of mixed scalar - pseudoscalar couplings*, *Phys. Lett. B* **579** (2004) 157, arXiv: [hep-ph/0307331](#).
- [17] S. Berge, W. Bernreuther and H. Spiesberger, *Higgs CP properties using the τ decay modes at the ILC*, *Phys. Lett.* **B727** (2013) 488, arXiv: [1308.2674 \[hep-ph\]](#).
- [18] S. Berge, W. Bernreuther and J. Ziethe, *Determining the CP parity of Higgs bosons at the LHC in their tau decay channels*, *Phys. Rev. Lett.* **100** (2008) 171605, arXiv: [0801.2297 \[hep-ph\]](#).
- [19] S. Berge and W. Bernreuther, *Determining the CP parity of Higgs bosons at the LHC in the tau to 1-prong decay channels*, *Phys. Lett. B* **671** (2009) 470, arXiv: [0812.1910 \[hep-ph\]](#).
- [20] S. Berge, W. Bernreuther, B. Niepelt and H. Spiesberger, *How to pin down the CP quantum numbers of a Higgs boson in its tau decays at the LHC*, *Phys. Rev. D* **84** (2011) 116003, arXiv: [1108.0670 \[hep-ph\]](#).
- [21] S. Berge, W. Bernreuther and S. Kirchner, *Determination of the Higgs CP-mixing angle in the tau decay channels at the LHC including the Drell-Yan background*, *Eur. Phys. J.* **C74** (2014) 3164, arXiv: [1408.0798 \[hep-ph\]](#).
- [22] S. Berge, W. Bernreuther and S. Kirchner, *Determination of the Higgs CP-mixing angle in the tau decay channels*, *Nucl. Part. Phys. Proc.* **273-275** (2016) 841, arXiv: [1410.6362 \[hep-ph\]](#).
- [23] S. Berge, W. Bernreuther and S. Kirchner, *Prospects of constraining the Higgs boson's CP nature in the tau decay channel at the LHC*, *Phys. Rev. D* **92** (2015) 096012, arXiv: [1510.03850 \[hep-ph\]](#).
- [24] CMS Collaboration, *Analysis of the CP structure of the Yukawa coupling between the Higgs boson and τ leptons in proton-proton collisions at $\sqrt{s} = 13$ TeV*, *JHEP* **06** (2022) 012, arXiv: [2110.04836 \[hep-ex\]](#).
- [25] S. Jadach and Z. Was, *Monte Carlo simulation of the process $e^+e^- \rightarrow \tau^+\tau^-$, $\tau \rightarrow X^\pm$ including radiative $O(\alpha^3)$ QED corrections, mass and spin*, *Comput. Phys. Commun.* **36** (1985) 191.
- [26] J. H. Kühn and F. Wagner, *Semileptonic Decays of the tau Lepton*, *Nucl. Phys. B* **236** (1984) 16.
- [27] S. Jadach, Z. Was, R. Decker and J. H. Kühn, *The tau decay library TAUOLA: Version 2.4*, *Comput. Phys. Commun.* **76** (1993) 361.
- [28] N. Davidson, G. Nanava, T. Przedzinski, E. Richter-Was and Z. Was, *Universal interface of TAUOLA: Technical and physics documentation*, *Comput. Phys. Commun.* **183** (2012) 821, arXiv: [1002.0543 \[hep-ph\]](#).
- [29] Y.-S. Tsai, *Decay Correlations of Heavy Leptons in $e^+e^- \rightarrow$ Lepton+ Lepton-*, *Phys. Rev. D* **4** (1971) 2821, [Erratum: *Phys.Rev.D* 13, 771 (1976)].
- [30] Particle Data Group, *Review of Particle Physics*, *PTEP* **2020** (2020) 083C01.

- [31] ATLAS Collaboration, *The ATLAS Experiment at the CERN Large Hadron Collider*, [JINST 3 \(2008\) S08003](#).
- [32] ATLAS Collaboration, *ATLAS Insertable B-Layer: Technical Design Report*, ATLAS-TDR-19; CERN-LHCC-2010-013, 2010, URL: <https://cds.cern.ch/record/1291633>, Addendum: ATLAS-TDR-19-ADD-1; CERN-LHCC-2012-009, 2012, URL: <https://cds.cern.ch/record/1451888>.
- [33] B. Abbott et al., *Production and integration of the ATLAS Insertable B-Layer*, [JINST 13 \(2018\) T05008](#), arXiv: [1803.00844 \[physics.ins-det\]](#).
- [34] ATLAS Collaboration, *Performance of the ATLAS trigger system in 2015*, [Eur. Phys. J. C 77 \(2017\) 317](#), arXiv: [1611.09661 \[hep-ex\]](#).
- [35] ATLAS Collaboration, *The ATLAS Collaboration Software and Firmware*, ATL-SOFT-PUB-2021-001, 2021, URL: <https://cds.cern.ch/record/2767187>.
- [36] R. Józefowicz, E. Richter-Was and Z. Was, *Potential for optimizing the Higgs boson CP measurement in $H \rightarrow \tau\tau$ decays at the LHC including machine learning techniques*, [Phys. Rev. D 94 \(2016\) 093001](#), arXiv: [1608.02609 \[hep-ph\]](#).
- [37] ATLAS Collaboration, *ATLAS data quality operations and performance for 2015–2018 data-taking*, [JINST 15 \(2020\) P04003](#), arXiv: [1911.04632 \[physics.ins-det\]](#).
- [38] ATLAS Collaboration, *Performance of electron and photon triggers in ATLAS during LHC Run 2*, [Eur. Phys. J. C 80 \(2020\) 47](#), arXiv: [1909.00761 \[hep-ex\]](#).
- [39] ATLAS Collaboration, *Performance of the ATLAS muon triggers in Run 2*, [JINST 15 \(2020\) P09015](#), arXiv: [2004.13447 \[hep-ex\]](#).
- [40] ATLAS Collaboration, *The ATLAS Inner Detector Trigger performance in pp collisions at 13 TeV during LHC Run 2*, [Eur. Phys. J. C 82 \(2021\) 206](#), arXiv: [2107.02485 \[hep-ex\]](#).
- [41] ATLAS Collaboration, *Performance of the ATLAS Level-1 topological trigger in Run 2*, [Eur. Phys. J. C 82 \(2021\) 7](#), arXiv: [2105.01416 \[hep-ex\]](#).
- [42] K. Hamilton, P. Nason, E. Re and G. Zanderighi, *NNLOPS simulation of Higgs boson production*, [JHEP 10 \(2013\) 222](#), arXiv: [1309.0017 \[hep-ph\]](#).
- [43] K. Hamilton, P. Nason and G. Zanderighi, *Finite quark-mass effects in the NNLOPS POWHEG+MiNLO Higgs generator*, [JHEP 05 \(2015\) 140](#), arXiv: [1501.04637 \[hep-ph\]](#).
- [44] S. Alioli, P. Nason, C. Oleari and E. Re, *A general framework for implementing NLO calculations in shower Monte Carlo programs: the POWHEG BOX*, [JHEP 06 \(2010\) 043](#), arXiv: [1002.2581 \[hep-ph\]](#).
- [45] P. Nason, *A new method for combining NLO QCD with shower Monte Carlo algorithms*, [JHEP 11 \(2004\) 040](#), arXiv: [hep-ph/0409146](#).
- [46] S. Frixione, P. Nason and C. Oleari, *Matching NLO QCD computations with Parton Shower simulations: the POWHEG method*, [JHEP 11 \(2007\) 070](#), arXiv: [0709.2092 \[hep-ph\]](#).
- [47] S. Frixione, P. Nason and G. Ridolfi, *A positive-weight next-to-leading-order Monte Carlo for heavy flavour hadroproduction*, [JHEP 09 \(2007\) 126](#), arXiv: [0707.3088 \[hep-ph\]](#).

- [48] H. B. Hartanto, B. Jäger, L. Reina and D. Wackerroth, *Higgs boson production in association with top quarks in the POWHEG BOX*, *Phys. Rev. D* **91** (2015) 094003, arXiv: [1501.04498 \[hep-ph\]](#).
- [49] NNPDF Collaboration, R.D. Ball et al., *Parton distributions for the LHC Run II*, *JHEP* **04** (2015) 040, arXiv: [1410.8849 \[hep-ph\]](#).
- [50] T. Sjöstrand et al., *An introduction to PYTHIA 8.2*, *Comput. Phys. Commun.* **191** (2015) 159, arXiv: [1410.3012 \[hep-ph\]](#).
- [51] Z. Czcycula, T. Przedzinski and Z. Was, *TauSpinner program for studies on spin effect in tau production at the LHC*, *Eur. Phys. J. C* **72** (2012) 1988, arXiv: [1201.0117 \[hep-ph\]](#).
- [52] T. Przedzinski, E. Richter-Was and Z. Was, *Documentation of TauSpinner algorithms: program for simulating spin effects in τ -lepton production at LHC*, *Eur. Phys. J. C* **79** (2019) 91, arXiv: [1802.05459 \[hep-ph\]](#).
- [53] T. Przedzinski, E. Richter-Was and Z. Was, *TauSpinner: a tool for simulating CP effects in $H \rightarrow \tau\tau$ decays at LHC*, *Eur. Phys. J. C* **74** (2014) 3177, arXiv: [1406.1647 \[hep-ph\]](#).
- [54] E. Bothmann et al., *Event Generation with Sherpa 2.2*, *SciPost Phys.* **7** (2019) 034, arXiv: [1905.09127 \[hep-ph\]](#).
- [55] ATLAS Collaboration, *Measurements of Higgs boson production cross-sections in the $H \rightarrow \tau^+\tau^-$ decay channel in pp collisions at $\sqrt{s} = 13$ TeV with the ATLAS detector*, *JHEP* **08** (2022) 175, arXiv: [2201.08269 \[hep-ex\]](#).
- [56] ATLAS Collaboration, *The ATLAS Simulation Infrastructure*, *Eur. Phys. J. C* **70** (2010) 823, arXiv: [1005.4568 \[physics.ins-det\]](#).
- [57] GEANT4 Collaboration, S. Agostinelli et al., *GEANT4 – a simulation toolkit*, *Nucl. Instrum. Meth. A* **506** (2003) 250.
- [58] ATLAS Collaboration, *Reconstruction of primary vertices at the ATLAS experiment in Run 1 proton–proton collisions at the LHC*, *Eur. Phys. J. C* **77** (2017) 332, arXiv: [1611.10235 \[hep-ex\]](#).
- [59] ATLAS Collaboration, *Electron and photon performance measurements with the ATLAS detector using the 2015–2017 LHC proton–proton collision data*, *JINST* **14** (2019) P12006, arXiv: [1908.00005 \[hep-ex\]](#).
- [60] ATLAS Collaboration, *Muon reconstruction and identification efficiency in ATLAS using the full Run 2 pp collision data set at $\sqrt{s} = 13$ TeV*, *Eur. Phys. J. C* **81** (2021) 578, arXiv: [2012.00578 \[hep-ex\]](#).
- [61] ATLAS Collaboration, *Jet reconstruction and performance using particle flow with the ATLAS Detector*, *Eur. Phys. J. C* **77** (2017) 466, arXiv: [1703.10485 \[hep-ex\]](#).
- [62] M. Cacciari, G. P. Salam and G. Soyez, *The anti- k_t jet clustering algorithm*, *JHEP* **04** (2008) 063, arXiv: [0802.1189 \[hep-ph\]](#).
- [63] M. Cacciari, G. P. Salam and G. Soyez, *FastJet user manual*, *Eur. Phys. J. C* **72** (2012) 1896, arXiv: [1111.6097 \[hep-ph\]](#).

- [64] ATLAS Collaboration, *Selection of jets produced in 13 TeV proton–proton collisions with the ATLAS detector*, ATLAS-CONF-2015-029, 2015, URL: <https://cds.cern.ch/record/2037702>.
- [65] ATLAS Collaboration, *Performance of pile-up mitigation techniques for jets in pp collisions at $\sqrt{s} = 8$ TeV using the ATLAS detector*, *Eur. Phys. J. C* **76** (2016) 581, arXiv: [1510.03823](https://arxiv.org/abs/1510.03823) [hep-ex].
- [66] ATLAS Collaboration, *Identification and rejection of pile-up jets at high pseudorapidity with the ATLAS detector*, *Eur. Phys. J. C* **77** (2017) 580, arXiv: [1705.02211](https://arxiv.org/abs/1705.02211) [hep-ex], Erratum: *Eur. Phys. J. C* **77** (2017) 712.
- [67] ATLAS Collaboration, *Topological cell clustering in the ATLAS calorimeters and its performance in LHC Run 1*, *Eur. Phys. J. C* **77** (2017) 490, arXiv: [1603.02934](https://arxiv.org/abs/1603.02934) [hep-ex].
- [68] ATLAS Collaboration, *Measurement of the tau lepton reconstruction and identification performance in the ATLAS experiment using pp collisions at $\sqrt{s} = 13$ TeV*, ATLAS-CONF-2017-029, 2017, URL: <https://cds.cern.ch/record/2261772>.
- [69] ATLAS Collaboration, *Identification of hadronic tau lepton decays using neural networks in the ATLAS experiment*, ATL-PHYS-PUB-2019-033, 2019, URL: <https://cds.cern.ch/record/2688062>.
- [70] ATLAS Collaboration, *Performance of missing transverse momentum reconstruction with the ATLAS detector using proton–proton collisions at $\sqrt{s} = 13$ TeV*, *Eur. Phys. J. C* **78** (2018) 903, arXiv: [1802.08168](https://arxiv.org/abs/1802.08168) [hep-ex].
- [71] A. Elagin, P. Murat, A. Pranko and A. Safonov, *A New Mass Reconstruction Technique for Resonances Decaying to di-tau*, *Nucl. Instrum. Meth. A* **654** (2011) 481, arXiv: [1012.4686](https://arxiv.org/abs/1012.4686) [hep-ex].
- [72] ATLAS Collaboration, *Reconstruction of hadronic decay products of tau leptons with the ATLAS experiment*, *Eur. Phys. J. C* **76** (2016) 295, arXiv: [1512.05955](https://arxiv.org/abs/1512.05955) [hep-ex].
- [73] ATLAS Collaboration, *Luminosity determination in pp collisions at $\sqrt{s} = 13$ TeV using the ATLAS detector at the LHC*, ATLAS-CONF-2019-021, 2019, URL: <https://cds.cern.ch/record/2677054>.
- [74] G. Avoni et al., *The new LUCID-2 detector for luminosity measurement and monitoring in ATLAS*, *JINST* **13** (2018) P07017.
- [75] ATLAS Collaboration, *Jet energy scale and resolution measured in proton–proton collisions at $\sqrt{s} = 13$ TeV with the ATLAS detector*, *Eur. Phys. J. C* **81** (2020) 689, arXiv: [2007.02645](https://arxiv.org/abs/2007.02645) [hep-ex].
- [76] ATLAS Collaboration, *Cross-section measurements of the Higgs boson decaying into a pair of τ -leptons in proton–proton collisions at $\sqrt{s} = 13$ TeV with the ATLAS detector*, *Phys. Rev. D* **99** (2019) 072001, arXiv: [1811.08856](https://arxiv.org/abs/1811.08856) [hep-ex].
- [77] ATLAS Collaboration, *Measurement of the energy response of the ATLAS calorimeter to charged pions from $W^\pm \rightarrow \tau^\pm (\rightarrow \pi^\pm \nu_\tau) \nu_\tau$ events in Run 2 data*, *Eur. Phys. J. C* **82** (2021) 223, arXiv: [2108.09043](https://arxiv.org/abs/2108.09043) [hep-ex].

- [78] G. Cowan, K. Cranmer, E. Gross and O. Vitells,
Asymptotic formulae for likelihood-based tests of new physics, *Eur. Phys. J. C* **71** (2011) 1554,
arXiv: [1007.1727](https://arxiv.org/abs/1007.1727) [[physics.data-an](https://arxiv.org/archive/physics)], Erratum: *Eur. Phys. J. C* **73** (2013) 2501.
- [79] ATLAS Collaboration, *ATLAS Computing Acknowledgements*, ATL-SOFT-PUB-2021-003, 2021,
URL: <https://cds.cern.ch/record/2776662>.

The ATLAS Collaboration

G. Aad ¹⁰¹, B. Abbott ¹¹⁹, D.C. Abbott ¹⁰², K. Abeling ⁵⁵, S.H. Abidi ²⁹, A. Aboulhorma ^{35e}, H. Abramowicz ¹⁵⁰, H. Abreu ¹⁴⁹, Y. Abulaiti ¹¹⁶, A.C. Abusleme Hoffman ^{136a}, B.S. Acharya ^{68a,68b,p}, B. Achkar ⁵⁵, C. Adam Bourdarios ⁴, L. Adamczyk ^{84a}, L. Adamek ¹⁵⁴, S.V. Addepalli ²⁶, J. Adelman ¹¹⁴, A. Adiguzel ^{21c}, S. Adorni ⁵⁶, T. Adye ¹³³, A.A. Affolder ¹³⁵, Y. Afik ³⁶, M.N. Agaras ¹³, J. Agarwala ^{72a,72b}, A. Aggarwal ⁹⁹, C. Agheorghiesei ^{27c}, J.A. Aguilar-Saavedra ^{129f}, A. Ahmad ³⁶, F. Ahmadov ^{38,z}, W.S. Ahmed ¹⁰³, S. Ahuja ⁹⁴, X. Ai ⁴⁸, G. Aielli ^{75a,75b}, I. Aizenberg ¹⁶⁸, M. Akbiyik ⁹⁹, T.P.A. Åkesson ⁹⁷, A.V. Akimov ³⁷, K. Al Khoury ⁴¹, G.L. Alberghi ^{23b}, J. Albert ¹⁶⁴, P. Albicocco ⁵³, M.J. Alconada Verzini ⁸⁹, S. Alderweireldt ⁵², M. Aleksa ³⁶, I.N. Aleksandrov ³⁸, C. Alexa ^{27b}, T. Alexopoulos ¹⁰, A. Alfonsi ¹¹³, F. Alfonsi ^{23b}, M. Alhroob ¹¹⁹, B. Ali ¹³¹, S. Ali ¹⁴⁷, M. Aliev ³⁷, G. Alimonti ^{70a}, W. Alkakhri ⁵⁵, C. Allaire ³⁶, B.M.M. Allbrooke ¹⁴⁵, P.P. Allport ²⁰, A. Aloisio ^{71a,71b}, F. Alonso ⁸⁹, C. Alpigiani ¹³⁷, E. Alunno Camelia ^{75a,75b}, M. Alvarez Estevez ⁹⁸, M.G. Alvigi ^{71a,71b}, Y. Amaral Coutinho ^{81b}, A. Ambler ¹⁰³, C. Amelung ³⁶, C.G. Ames ¹⁰⁸, D. Amidei ¹⁰⁵, S.P. Amor Dos Santos ^{129a}, S. Amoroso ⁴⁸, K.R. Amos ¹⁶², C.S. Amrouche ⁵⁶, V. Ananiev ¹²⁴, C. Anastopoulos ¹³⁸, T. Andeen ¹¹, J.K. Anders ¹⁹, S.Y. Andrean ^{47a,47b}, A. Andreazza ^{70a,70b}, S. Angelidakis ⁹, A. Angerami ^{41,ac}, A.V. Anisenkov ³⁷, A. Annovi ^{73a}, C. Antel ⁵⁶, M.T. Anthony ¹³⁸, E. Antipov ¹²⁰, M. Antonelli ⁵³, D.J.A. Antrim ^{17a}, F. Anulli ^{74a}, M. Aoki ⁸², T. Aoki ¹⁵², J.A. Aparisi Pozo ¹⁶², M.A. Aparo ¹⁴⁵, L. Aperio Bella ⁴⁸, C. Appelt ¹⁸, N. Aranzabal ³⁶, V. Araujo Ferraz ^{81a}, C. Arcangeletti ⁵³, A.T.H. Arce ⁵¹, E. Arena ⁹¹, J-F. Arguin ¹⁰⁷, S. Argyropoulos ⁵⁴, J.-H. Arling ⁴⁸, A.J. Armbruster ³⁶, O. Arnaez ¹⁵⁴, H. Arnold ¹¹³, Z.P. Arrubarrena Tame ¹⁰⁸, G. Artoni ^{74a,74b}, H. Asada ¹¹⁰, K. Asai ¹¹⁷, S. Asai ¹⁵², N.A. Asbah ⁶¹, J. Assahsah ^{35d}, K. Assamagan ²⁹, R. Astalos ^{28a}, R.J. Atkin ^{33a}, M. Atkinson ¹⁶¹, N.B. Atlay ¹⁸, H. Atmani ^{62b}, P.A. Atmasiddha ¹⁰⁵, K. Augsten ¹³¹, S. Auricchio ^{71a,71b}, A.D. Auriol ²⁰, V.A. Austrup ¹⁷⁰, G. Avner ¹⁴⁹, G. Avolio ³⁶, K. Axiotis ⁵⁶, M.K. Ayoub ^{14c}, G. Azuelos ^{107,ag}, D. Babal ^{28a}, H. Bachacou ¹³⁴, K. Bachas ^{151,s}, A. Bachiu ³⁴, F. Backman ^{47a,47b}, A. Badea ⁶¹, P. Bagnaia ^{74a,74b}, M. Bahmani ¹⁸, A.J. Bailey ¹⁶², V.R. Bailey ¹⁶¹, J.T. Baines ¹³³, C. Bakalis ¹⁰, O.K. Baker ¹⁷¹, P.J. Bakker ¹¹³, E. Bakos ¹⁵, D. Bakshi Gupta ⁸, S. Balaji ¹⁴⁶, R. Balasubramanian ¹¹³, E.M. Baldin ³⁷, P. Balek ¹³², E. Ballabene ^{70a,70b}, F. Balli ¹³⁴, L.M. Bales ^{63a}, W.K. Balunas ³², J. Balz ⁹⁹, E. Banas ⁸⁵, M. Bandieramonte ¹²⁸, A. Bandyopadhyay ²⁴, S. Bansal ²⁴, L. Barak ¹⁵⁰, E.L. Barberio ¹⁰⁴, D. Barberis ^{57b,57a}, M. Barbero ¹⁰¹, G. Barbour ⁹⁵, K.N. Barends ^{33a}, T. Barillari ¹⁰⁹, M-S. Barisits ³⁶, T. Barklow ¹⁴², R.M. Barnett ^{17a}, P. Baron ¹²¹, D.A. Baron Moreno ¹⁰⁰, A. Baroncelli ^{62a}, G. Barone ²⁹, A.J. Barr ¹²⁵, L. Barranco Navarro ^{47a,47b}, F. Barreiro ⁹⁸, J. Barreiro Guimarães da Costa ^{14a}, U. Barron ¹⁵⁰, M.G. Barros Teixeira ^{129a}, S. Barsov ³⁷, F. Bartels ^{63a}, R. Bartoldus ¹⁴², A.E. Barton ⁹⁰, P. Bartos ^{28a}, A. Basalaeu ⁴⁸, A. Basan ⁹⁹, M. Baselga ⁴⁹, I. Bashta ^{76a,76b}, A. Bassalat ^{66,b}, M.J. Basso ¹⁵⁴, C.R. Basson ¹⁰⁰, R.L. Bates ⁵⁹, S. Batlamous ^{35e}, J.R. Batley ³², B. Batool ¹⁴⁰, M. Battaglia ¹³⁵, D. Battulga ¹⁸, M. Baucé ^{74a,74b}, P. Bauer ²⁴, A. Bayirli ^{21a}, J.B. Beacham ⁵¹, T. Beau ¹²⁶, P.H. Beauchemin ¹⁵⁷, F. Becherer ⁵⁴, P. Bechtel ²⁴, H.P. Beck ^{19,r}, K. Becker ¹⁶⁶, C. Becot ⁴⁸, A.J. Beddall ^{21d}, V.A. Bednyakov ³⁸, C.P. Bee ¹⁴⁴, L.J. Beemster ¹⁵, T.A. Beermann ³⁶, M. Begalli ^{81d}, M. Begel ²⁹, A. Behera ¹⁴⁴, J.K. Behr ⁴⁸, C. Beirao Da Cruz E Silva ³⁶, J.F. Beirer ^{55,36}, F. Beisiegel ²⁴, M. Belfkir ¹⁵⁸, G. Bella ¹⁵⁰, L. Bellagamba ^{23b}, A. Bellerive ³⁴, P. Bellos ²⁰, K. Beloborodov ³⁷, K. Belotskiy ³⁷, N.L. Belyaev ³⁷, D. Benckekroun ^{35a}, F. Bendebba ^{35a}, Y. Benhammou ¹⁵⁰, D.P. Benjamin ²⁹,

M. Benoit ²⁹, J.R. Bensinger ²⁶, S. Bentvelsen ¹¹³, L. Beresford ³⁶, M. Beretta ⁵³, D. Berge ¹⁸,
E. Bergeaas Kuutmann ¹⁶⁰, N. Berger ⁴, B. Bergmann ¹³¹, J. Beringer ^{17a}, S. Berlendis ⁷,
G. Bernardi ⁵, C. Bernius ¹⁴², F.U. Bernlochner ²⁴, T. Berry ⁹⁴, P. Berta ¹³², A. Berthold ⁵⁰,
I.A. Bertram ⁹⁰, S. Bethke ¹⁰⁹, A. Betti ^{74a,74b}, A.J. Bevan ⁹³, M. Bhamjee ^{33c}, S. Bhatta ¹⁴⁴,
D.S. Bhattacharya ¹⁶⁵, P. Bhattarai ²⁶, V.S. Bhopatkar ¹²⁰, R. Bi ^{29,aj}, R.M. Bianchi ¹²⁸,
O. Biebel ¹⁰⁸, R. Bielski ¹²², M. Biglietti ^{76a}, T.R.V. Billoud ¹³¹, M. Bindi ⁵⁵, A. Bingul ^{21b},
C. Bini ^{74a,74b}, S. Biondi ^{23b,23a}, A. Biondini ⁹¹, C.J. Birch-sykes ¹⁰⁰, G.A. Bird ^{20,133},
M. Birman ¹⁶⁸, T. Bisanz ³⁶, E. Bisceglie ^{43b,43a}, D. Biswas ^{169,1}, A. Bitadze ¹⁰⁰, K. Bjørke ¹²⁴,
I. Bloch ⁴⁸, C. Blocker ²⁶, A. Blue ⁵⁹, U. Blumenschein ⁹³, J. Blumenthal ⁹⁹, G.J. Bobbink ¹¹³,
V.S. Bobrovnikov ³⁷, M. Boehler ⁵⁴, D. Bogavac ³⁶, A.G. Bogdanchikov ³⁷, C. Bohm ^{47a},
V. Boisvert ⁹⁴, P. Bokan ⁴⁸, T. Bold ^{84a}, M. Bomben ⁵, M. Bona ⁹³, M. Boonekamp ¹³⁴,
C.D. Booth ⁹⁴, A.G. Borbély ⁵⁹, H.M. Borecka-Bielska ¹⁰⁷, L.S. Borgna ⁹⁵, G. Borissov ⁹⁰,
D. Bortoletto ¹²⁵, D. Boscherini ^{23b}, M. Bosman ¹³, J.D. Bossio Sola ³⁶, K. Bouaouda ^{35a},
J. Boudreau ¹²⁸, E.V. Bouhova-Thacker ⁹⁰, D. Boumediene ⁴⁰, R. Bouquet ⁵, A. Boveia ¹¹⁸,
J. Boyd ³⁶, D. Boye ²⁹, I.R. Boyko ³⁸, J. Bracinik ²⁰, N. Brahimy ^{62d}, G. Brandt ¹⁷⁰,
O. Brandt ³², F. Braren ⁴⁸, B. Brau ¹⁰², J.E. Brau ¹²², K. Brendlinger ⁴⁸, R. Brenner ¹⁶⁸,
L. Brenner ³⁶, R. Brenner ¹⁶⁰, S. Bressler ¹⁶⁸, B. Brickwedde ⁹⁹, D. Britton ⁵⁹, D. Britzger ¹⁰⁹,
I. Brock ²⁴, G. Brooijmans ⁴¹, W.K. Brooks ^{136f}, E. Brost ²⁹, T.L. Bruckler ¹²⁵,
P.A. Bruckman de Renstrom ⁸⁵, B. Brüers ⁴⁸, D. Bruncko ^{28b,*}, A. Bruni ^{23b}, G. Bruni ^{23b},
M. Bruschi ^{23b}, N. Bruscinò ^{74a,74b}, L. Bryngemark ¹⁴², T. Buanes ¹⁶, Q. Buat ¹³⁷,
P. Buchholz ¹⁴⁰, A.G. Buckley ⁵⁹, I.A. Budagov ^{38,*}, M.K. Bugge ¹²⁴, O. Bulekov ³⁷,
B.A. Bullard ⁶¹, S. Burdin ⁹¹, C.D. Burgard ⁴⁸, A.M. Burger ⁴⁰, B. Burghgrave ⁸, J.T.P. Burr ³²,
C.D. Burton ¹¹, J.C. Burzynski ¹⁴¹, E.L. Busch ⁴¹, V. Büscher ⁹⁹, P.J. Bussey ⁵⁹, J.M. Butler ²⁵,
C.M. Buttar ⁵⁹, J.M. Butterworth ⁹⁵, W. Buttinger ¹³³, C.J. Buxo Vazquez ¹⁰⁶, A.R. Buzykaev ³⁷,
G. Cabras ^{23b}, S. Cabrera Urbán ¹⁶², D. Caforio ⁵⁸, H. Cai ¹²⁸, Y. Cai ^{14a,14d}, V.M.M. Cairo ³⁶,
O. Cakir ^{3a}, N. Calace ³⁶, P. Calafiura ^{17a}, G. Calderini ¹²⁶, P. Calfayan ⁶⁷, G. Callea ⁵⁹,
L.P. Caloba ^{81b}, D. Calvet ⁴⁰, S. Calvet ⁴⁰, T.P. Calvet ¹⁰¹, M. Calvetti ^{73a,73b},
R. Camacho Toro ¹²⁶, S. Camarda ³⁶, D. Camarero Munoz ²⁶, P. Camarri ^{75a,75b},
M.T. Camerlingo ^{76a,76b}, D. Cameron ¹²⁴, C. Camincher ¹⁶⁴, M. Campanelli ⁹⁵, A. Camplani ⁴²,
V. Canale ^{71a,71b}, A. Canesse ¹⁰³, M. Cano Bret ⁷⁹, J. Cantero ¹⁶², Y. Cao ¹⁶¹, F. Capocasa ²⁶,
M. Capua ^{43b,43a}, A. Carbone ^{70a,70b}, R. Cardarelli ^{75a}, J.C.J. Cardenas ⁸, F. Cardillo ¹⁶²,
T. Carli ³⁶, G. Carlino ^{71a}, J.I. Carlotto ¹³, B.T. Carlson ^{128,t}, E.M. Carlson ^{164,155a},
L. Carminati ^{70a,70b}, M. Carnesale ^{74a,74b}, S. Caron ¹¹², E. Carquin ^{136f}, S. Carrá ^{70a,70b},
G. Carratta ^{23b,23a}, F. Carri Argos ^{33g}, J.W.S. Carter ¹⁵⁴, T.M. Carter ⁵², M.P. Casado ^{13,i},
A.F. Casha ¹⁵⁴, E.G. Castiglia ¹⁷¹, F.L. Castillo ^{63a}, L. Castillo Garcia ¹³, V. Castillo Gimenez ¹⁶²,
N.F. Castro ^{129a,129e}, A. Catinaccio ³⁶, J.R. Catmore ¹²⁴, V. Cavaliere ²⁹, N. Cavalli ^{23b,23a},
V. Cavasinni ^{73a,73b}, E. Celebi ^{21a}, F. Celli ¹²⁵, M.S. Centonze ^{69a,69b}, K. Cerny ¹²¹,
A.S. Cerqueira ^{81a}, A. Cerri ¹⁴⁵, L. Cerrito ^{75a,75b}, F. Cerutti ^{17a}, A. Cervelli ^{23b}, S.A. Cetin ^{21d},
Z. Chadi ^{35a}, D. Chakraborty ¹¹⁴, M. Chala ^{129f}, J. Chan ¹⁶⁹, W.Y. Chan ¹⁵², J.D. Chapman ³²,
B. Chargeishvili ^{148b}, D.G. Charlton ²⁰, T.P. Charman ⁹³, M. Chatterjee ¹⁹, S. Chekanov ⁶,
S.V. Chekulaev ^{155a}, G.A. Chelkov ^{38,a}, A. Chen ¹⁰⁵, B. Chen ¹⁵⁰, B. Chen ¹⁶⁴, C. Chen ^{62a},
H. Chen ^{14c}, H. Chen ²⁹, J. Chen ^{62c}, J. Chen ²⁶, S. Chen ¹⁵², S.J. Chen ^{14c}, X. Chen ^{62c},
X. Chen ^{14b,af}, Y. Chen ^{62a}, C.L. Cheng ¹⁶⁹, H.C. Cheng ^{64a}, A. Cheplakov ³⁸,
E. Cheremushkina ⁴⁸, E. Cherepanova ¹¹³, R. Cherkaoui El Moursli ^{35e}, E. Cheu ⁷, K. Cheung ⁶⁵,
L. Chevalier ¹³⁴, V. Chiarella ⁵³, G. Chiarelli ^{73a}, N. Chiedde ¹⁰¹, G. Chiodini ^{69a},
A.S. Chisholm ²⁰, A. Chitan ^{27b}, M. Chitishvili ¹⁶², Y.H. Chiu ¹⁶⁴, M.V. Chizhov ³⁸, K. Choi ¹¹,
A.R. Chomont ^{74a,74b}, Y. Chou ¹⁰², E.Y.S. Chow ¹¹³, T. Chowdhury ^{33g}, L.D. Christopher ^{33g},

K.L. Chu^{64a}, M.C. Chu^{64a}, X. Chu^{14a,14d}, J. Chudoba¹³⁰, J.J. Chwastowski⁸⁵, D. Cieri¹⁰⁹,
 K.M. Ciesla^{84a}, V. Cindro⁹², A. Ciocio^{17a}, F. Cirotto^{71a,71b}, Z.H. Citron^{168,m}, M. Citterio^{70a},
 D.A. Ciubotaru^{27b}, B.M. Ciungu¹⁵⁴, A. Clark⁵⁶, P.J. Clark⁵², J.M. Clavijo Columbie⁴⁸,
 S.E. Clawson¹⁰⁰, C. Clement^{47a,47b}, J. Clercx⁴⁸, L. Clissa^{23b,23a}, Y. Coadou¹⁰¹,
 M. Cobal^{68a,68c}, A. Coccaro^{57b}, R.F. Coelho Barrue^{129a}, R. Coelho Lopes De Sa¹⁰²,
 S. Coelli^{70a}, H. Cohen¹⁵⁰, A.E.C. Coimbra^{70a,70b}, B. Cole⁴¹, J. Collot⁶⁰,
 P. Conde Muiño^{129a,129g}, M.P. Connell^{33c}, S.H. Connell^{33c}, I.A. Connelly⁵⁹, E.I. Conroy¹²⁵,
 F. Conventi^{71a,ah}, H.G. Cooke²⁰, A.M. Cooper-Sarkar¹²⁵, F. Cormier¹⁶³, L.D. Corpe³⁶,
 M. Corradi^{74a,74b}, E.E. Corrigan⁹⁷, F. Corriveau^{103,y}, A. Cortes-Gonzalez¹⁸, M.J. Costa¹⁶²,
 F. Costanza⁴, D. Costanzo¹³⁸, B.M. Cote¹¹⁸, G. Cowan⁹⁴, J.W. Cowley³², K. Cranmer¹¹⁶,
 S. Crépe-Renaudin⁶⁰, F. Crescioli¹²⁶, M. Cristinziani¹⁴⁰, M. Cristoforetti^{77a,77b,d}, V. Croft¹⁵⁷,
 G. Crosetti^{43b,43a}, A. Cueto³⁶, T. Cuhadar Donszelmann¹⁵⁹, H. Cui^{14a,14d}, Z. Cui⁷,
 A.R. Cukierman¹⁴², W.R. Cunningham⁵⁹, F. Curcio^{43b,43a}, P. Czodrowski³⁶, M.M. Czurylo^{63b},
 M.J. Da Cunha Sargedas De Sousa^{62a}, J.V. Da Fonseca Pinto^{81b}, C. Da Via¹⁰⁰, W. Dabrowski^{84a},
 T. Dado⁴⁹, S. Dahbi^{33g}, T. Dai¹⁰⁵, C. Dallapiccola¹⁰², M. Dam⁴², G. D'amen²⁹,
 V. D'Amico¹⁰⁸, J. Damp⁹⁹, J.R. Dandoy¹²⁷, M.F. Daneri³⁰, M. Danninger¹⁴¹, V. Dao³⁶,
 G. Darbo^{57b}, S. Darmora⁶, S.J. Das^{29,aj}, S. D'Auria^{70a,70b}, C. David^{155b}, T. Davidek¹³²,
 D.R. Davis⁵¹, B. Davis-Purcell³⁴, I. Dawson⁹³, K. De⁸, R. De Asmundis^{71a},
 M. De Beurs¹¹³, N. De Biase⁴⁸, S. De Castro^{23b,23a}, N. De Groot¹¹², P. de Jong¹¹³,
 H. De la Torre¹⁰⁶, A. De Maria^{14c}, A. De Salvo^{74a}, U. De Sanctis^{75a,75b}, A. De Santo¹⁴⁵,
 J.B. De Vivie De Regie⁶⁰, D.V. Dedovich³⁸, J. Degens¹¹³, A.M. Deiana⁴⁴, F. Del Corso^{23b,23a},
 J. Del Peso⁹⁸, F. Del Rio^{63a}, F. Deliot¹³⁴, C.M. Delitzsch⁴⁹, M. Della Pietra^{71a,71b},
 D. Della Volpe⁵⁶, A. Dell'Acqua³⁶, L. Dell'Asta^{70a,70b}, M. Delmastro⁴, P.A. Delsart⁶⁰,
 S. Demers¹⁷¹, M. Demichev³⁸, S.P. Denisov³⁷, L. D'Eramo¹¹⁴, D. Derendarz⁸⁵, F. Derue¹²⁶,
 P. Dervan⁹¹, K. Desch²⁴, K. Dette¹⁵⁴, C. Deutsch²⁴, P.O. Deviveiros³⁶, F.A. Di Bello^{74a,74b},
 A. Di Ciaccio^{75a,75b}, L. Di Ciaccio⁴, A. Di Domenico^{74a,74b}, C. Di Donato^{71a,71b},
 A. Di Girolamo³⁶, G. Di Gregorio^{73a,73b}, A. Di Luca^{77a,77b}, B. Di Micco^{76a,76b},
 R. Di Nardo^{76a,76b}, C. Diaconu¹⁰¹, F.A. Dias¹¹³, T. Dias Do Vale¹⁴¹, M.A. Diaz^{136a,136b},
 F.G. Diaz Capriles²⁴, M. Didenko¹⁶², E.B. Diehl¹⁰⁵, L. Diehl⁵⁴, S. Díez Cornell⁴⁸,
 C. Díez Pardos¹⁴⁰, C. Dimitriadi^{24,160}, A. Dimitrievska^{17a}, W. Ding^{14b}, J. Dingfelder²⁴,
 I-M. Dinu^{27b}, S.J. Dittmeier^{63b}, F. Dittus³⁶, F. Djama¹⁰¹, T. Djobava^{148b}, J.I. Djuvsland¹⁶,
 C. Doglioni^{100,97}, J. Dolejsi¹³², Z. Dolezal¹³², M. Donadelli^{81c}, B. Dong^{62c}, J. Donini⁴⁰,
 A. D'Onofrio^{14c}, M. D'Onofrio⁹¹, J. Dopke¹³³, A. Doria^{71a}, M.T. Dova⁸⁹, A.T. Doyle⁵⁹,
 M.A. Draguet¹²⁵, E. Drechsler¹⁴¹, E. Dreyer¹⁶⁸, I. Drivas-koulouris¹⁰, A.S. Drobac¹⁵⁷,
 M. Drozdova⁵⁶, D. Du^{62a}, T.A. du Pree¹¹³, F. Dubinin³⁷, M. Dubovsky^{28a}, E. Duchovni¹⁶⁸,
 G. Duckeck¹⁰⁸, O.A. Ducu^{27b}, D. Duda¹⁰⁹, A. Dudarev³⁶, M. D'uffizi¹⁰⁰, L. Duflost⁶⁶,
 M. Dührssen³⁶, C. Dülsen¹⁷⁰, A.E. Dumitriu^{27b}, M. Dunford^{63a}, S. Dungs⁴⁹,
 K. Dunne^{47a,47b}, A. Duperrin¹⁰¹, H. Duran Yildiz^{3a}, M. Düren⁵⁸, A. Durglishvili^{148b},
 B.L. Dwyer¹¹⁴, G.I. Dyckes^{17a}, M. Dyndal^{84a}, S. Dysch¹⁰⁰, B.S. Dziedzic⁸⁵,
 Z.O. Earnshaw¹⁴⁵, B. Eckerova^{28a}, M.G. Eggleston⁵¹, E. Egidio Purcino De Souza^{81b},
 L.F. Ehrke⁵⁶, G. Eigen¹⁶, K. Einsweiler^{17a}, T. Ekelof¹⁶⁰, P.A. Ekman⁹⁷, Y. El Ghazali^{35b},
 H. El Jarrari^{35e,147}, A. El Moussaouy^{35a}, V. Ellajosyula¹⁶⁰, M. Ellert¹⁶⁰, F. Ellinghaus¹⁷⁰,
 A.A. Elliot⁹³, N. Ellis³⁶, J. Elmsheuser²⁹, M. Elsing³⁶, D. Emelianov¹³³, A. Emerman⁴¹,
 Y. Enari¹⁵², I. Ene^{17a}, S. Epari¹³, J. Erdmann⁴⁹, A. Ereditato¹⁹, P.A. Erland⁸⁵,
 M. Errenst¹⁷⁰, M. Escalier⁶⁶, C. Escobar¹⁶², E. Etzion¹⁵⁰, G. Evans^{129a}, H. Evans⁶⁷,
 M.O. Evans¹⁴⁵, A. Ezhilov³⁷, S. Ezzarqtouni^{35a}, F. Fabbri⁵⁹, L. Fabbri^{23b,23a}, G. Facini⁹⁵,
 V. Fadeyev¹³⁵, R.M. Fakhrutdinov³⁷, S. Falciano^{74a}, P.J. Falke²⁴, S. Falke³⁶, J. Faltova¹³²,

Y. Fan [id](#)^{14a}, Y. Fang [id](#)^{14a,14d}, G. Fanourakis [id](#)⁴⁶, M. Fanti [id](#)^{70a,70b}, M. Faraj [id](#)^{68a,68b}, A. Farbin [id](#)⁸,
 A. Farilla [id](#)^{76a}, T. Farooque [id](#)¹⁰⁶, S.M. Farrington [id](#)⁵², F. Fassi [id](#)^{35e}, D. Fassouliotis [id](#)⁹,
 M. Faucci Giannelli [id](#)^{75a,75b}, W.J. Fawcett [id](#)³², L. Fayard [id](#)⁶⁶, P. Federicova [id](#)¹³⁰, O.L. Fedin [id](#)^{37,a},
 G. Fedotov [id](#)³⁷, M. Feickert [id](#)¹⁶¹, L. Feligioni [id](#)¹⁰¹, A. Fell [id](#)¹³⁸, D.E. Fellers [id](#)¹²², C. Feng [id](#)^{62b},
 M. Feng [id](#)^{14b}, Z. Feng [id](#)¹¹³, M.J. Fenton [id](#)¹⁵⁹, A.B. Fenyuk [id](#)³⁷, L. Ferencz [id](#)⁴⁸, S.W. Ferguson [id](#)⁴⁵,
 J. Ferrando [id](#)⁴⁸, A. Ferrari [id](#)¹⁶⁰, P. Ferrari [id](#)¹¹³, R. Ferrari [id](#)^{72a}, D. Ferrere [id](#)⁵⁶, C. Ferretti [id](#)¹⁰⁵,
 F. Fiedler [id](#)⁹⁹, A. Filipčič [id](#)⁹², E.K. Filmer [id](#)¹, F. Filthaut [id](#)¹¹², M.C.N. Fiolhais [id](#)^{129a,129c,c},
 L. Fiorini [id](#)¹⁶², F. Fischer [id](#)¹⁴⁰, W.C. Fisher [id](#)¹⁰⁶, T. Fitschen [id](#)²⁰, I. Fleck [id](#)¹⁴⁰, P. Fleischmann [id](#)¹⁰⁵,
 T. Flick [id](#)¹⁷⁰, L. Flores [id](#)¹²⁷, M. Flores [id](#)^{33d,ad}, L.R. Flores Castillo [id](#)^{64a}, F.M. Follega [id](#)^{77a,77b},
 N. Fomin [id](#)¹⁶, J.H. Foo [id](#)¹⁵⁴, B.C. Forland [id](#)⁶⁷, A. Formica [id](#)¹³⁴, A.C. Forti [id](#)¹⁰⁰, E. Fortin [id](#)¹⁰¹,
 A.W. Fortman [id](#)⁶¹, M.G. Foti [id](#)^{17a}, L. Fountas [id](#)^{9,j}, D. Fournier [id](#)⁶⁶, H. Fox [id](#)⁹⁰, P. Francavilla [id](#)^{73a,73b},
 S. Francescato [id](#)⁶¹, M. Franchini [id](#)^{23b,23a}, S. Franchino [id](#)^{63a}, D. Francis [id](#)³⁶, L. Franco [id](#)¹¹²,
 L. Franconi [id](#)¹⁹, M. Franklin [id](#)⁶¹, G. Frattari [id](#)²⁶, A.C. Freegard [id](#)⁹³, P.M. Freeman [id](#)²⁰, W.S. Freund [id](#)^{81b},
 N. Fritzsche [id](#)⁵⁰, A. Froch [id](#)⁵⁴, D. Froidevaux [id](#)³⁶, J.A. Frost [id](#)¹²⁵, Y. Fu [id](#)^{62a}, M. Fujimoto [id](#)¹¹⁷,
 E. Fullana Torregrosa [id](#)^{162,*}, J. Fuster [id](#)¹⁶², A. Gabrielli [id](#)^{23b,23a}, A. Gabrielli [id](#)¹⁵⁴, P. Gadow [id](#)⁴⁸,
 G. Gagliardi [id](#)^{57b,57a}, L.G. Gagnon [id](#)^{17a}, G.E. Gallardo [id](#)¹²⁵, E.J. Gallas [id](#)¹²⁵, B.J. Gallop [id](#)¹³³,
 R. Gamboa Goni [id](#)⁹³, K.K. Gan [id](#)¹¹⁸, S. Ganguly [id](#)¹⁵², J. Gao [id](#)^{62a}, Y. Gao [id](#)⁵²,
 F.M. Garay Walls [id](#)^{136a,136b}, B. Garcia [id](#)^{29,aj}, C. García [id](#)¹⁶², J.E. García Navarro [id](#)¹⁶²,
 J.A. García Pascual [id](#)^{14a}, M. Garcia-Sciveres [id](#)^{17a}, R.W. Gardner [id](#)³⁹, D. Garg [id](#)⁷⁹, R.B. Garg [id](#)^{142,q},
 S. Gargiulo [id](#)⁵⁴, C.A. Garner [id](#)¹⁵⁴, V. Garonne [id](#)²⁹, S.J. Gasiorowski [id](#)¹³⁷, P. Gaspar [id](#)^{81b}, G. Gaudio [id](#)^{72a},
 V. Gautam [id](#)¹³, P. Gauzzi [id](#)^{74a,74b}, I.L. Gavrilenko [id](#)³⁷, A. Gavrilyuk [id](#)³⁷, C. Gay [id](#)¹⁶³, G. Gaycken [id](#)⁴⁸,
 E.N. Gazis [id](#)¹⁰, A.A. Geanta [id](#)^{27b,27e}, C.M. Gee [id](#)¹³⁵, J. Geisen [id](#)⁹⁷, M. Geisen [id](#)⁹⁹, C. Gemme [id](#)^{57b},
 M.H. Genest [id](#)⁶⁰, S. Gentile [id](#)^{74a,74b}, S. George [id](#)⁹⁴, W.F. George [id](#)²⁰, T. Geralis [id](#)⁴⁶, L.O. Gerlach [id](#)⁵⁵,
 P. Gessinger-Befurt [id](#)³⁶, M. Ghasemi Bostanabad [id](#)¹⁶⁴, M. Ghneimat [id](#)¹⁴⁰, A. Ghosal [id](#)¹⁴⁰,
 A. Ghosh [id](#)¹⁵⁹, A. Ghosh [id](#)⁷, B. Giacobbe [id](#)^{23b}, S. Giagu [id](#)^{74a,74b}, N. Giangiacomi [id](#)¹⁵⁴,
 P. Giannetti [id](#)^{73a}, A. Giannini [id](#)^{62a}, S.M. Gibson [id](#)⁹⁴, M. Gignac [id](#)¹³⁵, D.T. Gil [id](#)^{84b}, A.K. Gilbert [id](#)^{84a},
 B.J. Gilbert [id](#)⁴¹, D. Gillberg [id](#)³⁴, G. Gilles [id](#)¹¹³, N.E.K. Gillwald [id](#)⁴⁸, L. Ginabat [id](#)¹²⁶,
 D.M. Gingrich [id](#)^{2,ag}, M.P. Giordani [id](#)^{68a,68c}, P.F. Giraud [id](#)¹³⁴, G. Giugliarelli [id](#)^{68a,68c}, D. Giugni [id](#)^{70a},
 F. Giuli [id](#)³⁶, I. Gkialas [id](#)^{9,j}, L.K. Gladilin [id](#)³⁷, C. Glasman [id](#)⁹⁸, G.R. Gledhill [id](#)¹²², M. Glisic [id](#)¹²²,
 I. Gnesi [id](#)^{43b,f}, Y. Go [id](#)^{29,aj}, M. Goblirsch-Kolb [id](#)²⁶, D. Godin [id](#)¹⁰⁷, S. Goldfarb [id](#)¹⁰⁴, T. Golling [id](#)⁵⁶,
 M.G.D. Gololo [id](#)^{33g}, D. Golubkov [id](#)³⁷, J.P. Gombas [id](#)¹⁰⁶, A. Gomes [id](#)^{129a,129b}, G. Gomes Da Silva [id](#)¹⁴⁰,
 A.J. Gomez Delegido [id](#)¹⁶², R. Goncalves Gama [id](#)⁵⁵, R. Gonçalves [id](#)^{129a,129c}, G. Gonella [id](#)¹²²,
 L. Gonella [id](#)²⁰, A. Gongadze [id](#)³⁸, F. Gonnella [id](#)²⁰, J.L. Gonski [id](#)⁴¹, R.Y. González Andana [id](#)⁵²,
 S. González de la Hoz [id](#)¹⁶², S. Gonzalez Fernandez [id](#)¹³, R. Gonzalez Lopez [id](#)⁹¹,
 C. Gonzalez Renteria [id](#)^{17a}, R. Gonzalez Suarez [id](#)¹⁶⁰, S. Gonzalez-Sevilla [id](#)⁵⁶,
 G.R. Gonzalvo Rodriguez [id](#)¹⁶², L. Goossens [id](#)³⁶, N.A. Gorasia [id](#)²⁰, P.A. Gorbounov [id](#)³⁷, B. Gorini [id](#)³⁶,
 E. Gorini [id](#)^{69a,69b}, A. Gorišek [id](#)⁹², A.T. Goshaw [id](#)⁵¹, M.I. Gostkin [id](#)³⁸, C.A. Gottardo [id](#)³⁶,
 M. Goughri [id](#)^{35b}, V. Goumarre [id](#)⁴⁸, A.G. Goussiou [id](#)¹³⁷, N. Govender [id](#)^{33c}, C. Goy [id](#)⁴,
 I. Grabowska-Bold [id](#)^{84a}, K. Graham [id](#)³⁴, E. Gramstad [id](#)¹²⁴, S. Grancagnolo [id](#)¹⁸, M. Grandi [id](#)¹⁴⁵,
 V. Gratchev [id](#)^{37,*}, P.M. Gravila [id](#)^{27f}, F.G. Gravili [id](#)^{69a,69b}, H.M. Gray [id](#)^{17a}, M. Greco [id](#)^{69a,69b},
 C. Grefe [id](#)²⁴, I.M. Gregor [id](#)⁴⁸, P. Grenier [id](#)¹⁴², C. Grieco [id](#)¹³, A.A. Grillo [id](#)¹³⁵, K. Grimm [id](#)^{31,n},
 S. Grinstein [id](#)^{13,v}, J.-F. Grivaz [id](#)⁶⁶, E. Gross [id](#)¹⁶⁸, J. Grosse-Knetter [id](#)⁵⁵, C. Grud [id](#)¹⁰⁵, A. Grummer [id](#)¹¹¹,
 J.C. Grundy [id](#)¹²⁵, L. Guan [id](#)¹⁰⁵, W. Guan [id](#)¹⁶⁹, C. Gubbels [id](#)¹⁶³, J.G.R. Guerrero Rojas [id](#)¹⁶²,
 G. Guerrieri [id](#)^{68a,68b}, F. Guescini [id](#)¹⁰⁹, R. Gugel [id](#)⁹⁹, J.A.M. Guhit [id](#)¹⁰⁵, A. Guida [id](#)⁴⁸, T. Guillemin [id](#)⁴,
 E. Guilloton [id](#)^{166,133}, S. Guindon [id](#)³⁶, F. Guo [id](#)^{14a,14d}, J. Guo [id](#)^{62c}, L. Guo [id](#)⁶⁶, Y. Guo [id](#)¹⁰⁵,
 R. Gupta [id](#)⁴⁸, S. Gurbuz [id](#)²⁴, S.S. Gurdasani [id](#)⁵⁴, G. Gustavino [id](#)³⁶, M. Guth [id](#)⁵⁶, P. Gutierrez [id](#)¹¹⁹,
 L.F. Gutierrez Zagazeta [id](#)¹²⁷, C. Gutschow [id](#)⁹⁵, C. Guyot [id](#)¹³⁴, C. Gwenlan [id](#)¹²⁵, C.B. Gwilliam [id](#)⁹¹,

E.S. Haaland ¹²⁴, A. Haas ¹¹⁶, M. Habedank ⁴⁸, C. Haber ^{17a}, H.K. Hadavand ⁸, A. Hadeif ⁹⁹,
 S. Hadzic ¹⁰⁹, M. Haleem ¹⁶⁵, J. Haley ¹²⁰, J.J. Hall ¹³⁸, G.D. Hallewell ¹⁰¹, L. Halser ¹⁹,
 K. Hamano ¹⁶⁴, H. Hamdaoui ^{35e}, M. Hamer ²⁴, G.N. Hamity ⁵², J. Han ^{62b}, K. Han ^{62a},
 L. Han ^{14c}, L. Han ^{62a}, S. Han ^{17a}, Y.F. Han ¹⁵⁴, K. Hanagaki ⁸², M. Hance ¹³⁵,
 D.A. Hangal ^{41,ac}, H. Hanif ¹⁴¹, M.D. Hank ³⁹, R. Hankache ¹⁰⁰, J.B. Hansen ⁴²,
 J.D. Hansen ⁴², P.H. Hansen ⁴², K. Hara ¹⁵⁶, D. Harada ⁵⁶, T. Harenberg ¹⁷⁰, S. Harkusha ³⁷,
 Y.T. Harris ¹²⁵, N.M. Harrison ¹¹⁸, P.F. Harrison ¹⁶⁶, N.M. Hartman ¹⁴², N.M. Hartmann ¹⁰⁸,
 Y. Hasegawa ¹³⁹, A. Hasib ⁵², S. Haug ¹⁹, R. Hauser ¹⁰⁶, M. Havranek ¹³¹, C.M. Hawkes ²⁰,
 R.J. Hawkings ³⁶, S. Hayashida ¹¹⁰, D. Hayden ¹⁰⁶, C. Hayes ¹⁰⁵, R.L. Hayes ¹⁶³, C.P. Hays ¹²⁵,
 J.M. Hays ⁹³, H.S. Hayward ⁹¹, F. He ^{62a}, Y. He ¹⁵³, Y. He ¹²⁶, M.P. Heath ⁵², V. Hedberg ⁹⁷,
 A.L. Heggelund ¹²⁴, N.D. Hehir ⁹³, C. Heidegger ⁵⁴, K.K. Heidegger ⁵⁴, W.D. Heidorn ⁸⁰,
 J. Heilmann ³⁴, S. Heim ⁴⁸, T. Heim ^{17a}, J.G. Heinlein ¹²⁷, J.J. Heinrich ¹²², L. Heinrich ^{109,ae},
 J. Hejbal ¹³⁰, L. Helary ⁴⁸, A. Held ¹⁶⁹, S. Hellesund ¹²⁴, C.M. Helling ¹⁶³, S. Hellman ^{47a,47b},
 C. Helsens ³⁶, R.C.W. Henderson ⁹⁰, L. Henkelmann ³², A.M. Henriques Correia ³⁶, H. Herde ¹⁴²,
 Y. Hernández Jiménez ¹⁴⁴, M.G. Herrmann ¹⁰⁸, T. Herrmann ⁵⁰, G. Herten ⁵⁴,
 R. Hertenberger ¹⁰⁸, L. Hervás ³⁶, N.P. Hesse ^{155a}, H. Hibi ⁸³, E. Higón-Rodríguez ¹⁶²,
 S.J. Hillier ²⁰, I. Hinchliffe ^{17a}, F. Hinterkeuser ²⁴, M. Hirose ¹²³, S. Hirose ¹⁵⁶,
 D. Hirschbuehl ¹⁷⁰, T.G. Hitchings ¹⁰⁰, B. Hiti ⁹², J. Hobbs ¹⁴⁴, R. Hobincu ^{27e}, N. Hod ¹⁶⁸,
 M.C. Hodgkinson ¹³⁸, B.H. Hodgkinson ³², A. Hoecker ³⁶, J. Hofer ⁴⁸, D. Hohn ⁵⁴, T. Holm ²⁴,
 M. Holzbock ¹⁰⁹, L.B.A.H. Hommels ³², B.P. Honan ¹⁰⁰, J. Hong ^{62c}, T.M. Hong ¹²⁸,
 Y. Hong ⁵⁵, J.C. Honig ⁵⁴, A. Hönle ¹⁰⁹, B.H. Hooberman ¹⁶¹, W.H. Hopkins ⁶, Y. Horii ¹¹⁰,
 S. Hou ¹⁴⁷, A.S. Howard ⁹², J. Howarth ⁵⁹, J. Hoya ⁶, M. Hrabovsky ¹²¹, A. Hrynevich ³⁷,
 T. Hryn'ova ⁴, P.J. Hsu ⁶⁵, S.-C. Hsu ¹³⁷, Q. Hu ^{41,ac}, Y.F. Hu ^{14a,14d,ai}, D.P. Huang ⁹⁵,
 S. Huang ^{64b}, X. Huang ^{14c}, Y. Huang ^{62a}, Y. Huang ^{14a}, Z. Huang ¹⁰⁰, Z. Hubacek ¹³¹,
 M. Huebner ²⁴, F. Huegging ²⁴, T.B. Huffman ¹²⁵, M. Huhtinen ³⁶, S.K. Huiberts ¹⁶,
 R. Hulsken ¹⁰³, N. Huseynov ^{12,a}, J. Huston ¹⁰⁶, J. Huth ⁶¹, R. Hyneman ¹⁴², S. Hyrych ^{28a},
 G. Iacobucci ⁵⁶, G. Iakovidis ²⁹, I. Ibragimov ¹⁴⁰, L. Iconomidou-Fayard ⁶⁶, P. Iengo ^{71a,71b},
 R. Iguchi ¹⁵², T. Iizawa ⁵⁶, Y. Ikegami ⁸², A. Ilg ¹⁹, N. Ilic ¹⁵⁴, H. Imam ^{35a},
 T. Ingebretsen Carlson ^{47a,47b}, G. Introzzi ^{72a,72b}, M. Iodice ^{76a}, V. Ippolito ^{74a,74b}, M. Ishino ¹⁵²,
 W. Islam ¹⁶⁹, C. Issever ^{18,48}, S. Istin ^{21a,al}, H. Ito ¹⁶⁷, J.M. Iturbe Ponce ^{64a}, R. Iuppa ^{77a,77b},
 A. Ivina ¹⁶⁸, J.M. Izen ⁴⁵, V. Izzo ^{71a}, P. Jacka ^{130,131}, P. Jackson ¹, R.M. Jacobs ⁴⁸,
 B.P. Jaeger ¹⁴¹, C.S. Jagfeld ¹⁰⁸, G. Jäkel ¹⁷⁰, K. Jakobs ⁵⁴, T. Jakoubek ¹⁶⁸, J. Jamieson ⁵⁹,
 K.W. Janas ^{84a}, G. Jarlskog ⁹⁷, A.E. Jaspan ⁹¹, M. Javurkova ¹⁰², F. Jeanneau ¹³⁴, L. Jeanty ¹²²,
 J. Jejelava ^{148a,aa}, P. Jenni ^{54,g}, C.E. Jessiman ³⁴, S. Jézéquel ⁴, J. Jia ¹⁴⁴, X. Jia ⁶¹,
 X. Jia ^{14a,14d}, Z. Jia ^{14c}, Y. Jiang ^{62a}, S. Jiggins ⁵², J. Jimenez Pena ¹⁰⁹, S. Jin ^{14c}, A. Jinaru ^{27b},
 O. Jinnouchi ¹⁵³, P. Johansson ¹³⁸, K.A. Johns ⁷, D.M. Jones ³², E. Jones ¹⁶⁶, P. Jones ³²,
 R.W.L. Jones ⁹⁰, T.J. Jones ⁹¹, R. Joshi ¹¹⁸, J. Jovicevic ¹⁵, X. Ju ^{17a}, J.J. Junggeburth ³⁶,
 A. Juste Rozas ^{13,v}, S. Kabana ^{136e}, A. Kaczmarzka ⁸⁵, M. Kado ^{74a,74b}, H. Kagan ¹¹⁸,
 M. Kagan ¹⁴², A. Kahn ⁴¹, A. Kahn ¹²⁷, C. Kahra ⁹⁹, T. Kaji ¹⁶⁷, E. Kajomovitz ¹⁴⁹,
 N. Kakati ¹⁶⁸, C.W. Kalderon ²⁹, A. Kamenshchikov ¹⁵⁴, S. Kanayama ¹⁵³, N.J. Kang ¹³⁵,
 Y. Kano ¹¹⁰, D. Kar ^{33g}, K. Karava ¹²⁵, M.J. Kareem ^{155b}, E. Karentzos ⁵⁴, I. Karkanias ¹⁵¹,
 S.N. Karpov ³⁸, Z.M. Karpova ³⁸, V. Kartvelishvili ⁹⁰, A.N. Karyukhin ³⁷, E. Kasimi ¹⁵¹,
 C. Kato ^{62d}, J. Katzy ⁴⁸, S. Kaur ³⁴, K. Kawade ¹³⁹, K. Kawagoe ⁸⁸, T. Kawamoto ¹³⁴,
 G. Kawamura ⁵⁵, E.F. Kay ¹⁶⁴, F.I. Kaya ¹⁵⁷, S. Kazakos ¹³, V.F. Kazanin ³⁷, Y. Ke ¹⁴⁴,
 J.M. Keaveney ^{33a}, R. Keeler ¹⁶⁴, G.V. Kehris ⁶¹, J.S. Keller ³⁴, A.S. Kelly ⁹⁵, D. Kelsey ¹⁴⁵,
 J.J. Kempster ²⁰, K.E. Kennedy ⁴¹, O. Kepka ¹³⁰, B.P. Kerridge ¹⁶⁶, S. Kersten ¹⁷⁰,
 B.P. Kerševan ⁹², S. Keshri ⁶⁶, L. Keszeghova ^{28a}, S. Ketabchi Haghighat ¹⁵⁴, M. Khandoga ¹²⁶,

A. Khanov ¹²⁰, A.G. Kharlamov ³⁷, T. Kharlamova ³⁷, E.E. Khoda ¹³⁷, T.J. Khoo ¹⁸,
 G. Khorauli ¹⁶⁵, J. Khubua ^{148b}, Y.A.R. Khwaira ⁶⁶, M. Kiehn ³⁶, A. Kilgallon ¹²²,
 D.W. Kim ^{47a,47b}, E. Kim ¹⁵³, Y.K. Kim ³⁹, N. Kimura ⁹⁵, A. Kirchhoff ⁵⁵, D. Kirchmeier ⁵⁰,
 C. Kirfel ²⁴, J. Kirk ¹³³, A.E. Kiryunin ¹⁰⁹, T. Kishimoto ¹⁵², D.P. Kisliuk ¹⁵⁴, C. Kitsaki ¹⁰,
 O. Kivernyk ²⁴, M. Klassen ^{63a}, C. Klein ³⁴, L. Klein ¹⁶⁵, M.H. Klein ¹⁰⁵, M. Klein ⁹¹,
 S.B. Klein ⁵⁶, U. Klein ⁹¹, P. Klimek ³⁶, A. Klimentov ²⁹, F. Klimpel ¹⁰⁹, T. Klingl ²⁴,
 T. Klioutchnikova ³⁶, F.F. Klitzner ¹⁰⁸, P. Kluit ¹¹³, S. Kluth ¹⁰⁹, E. Kneringer ⁷⁸,
 T.M. Knight ¹⁵⁴, A. Knue ⁵⁴, D. Kobayashi⁸⁸, R. Kobayashi ⁸⁶, M. Kocian ¹⁴², P. Kodyš ¹³²,
 D.M. Koeck ¹⁴⁵, P.T. Koenig ²⁴, T. Koffas ³⁴, N.M. Köhler ³⁶, M. Kolb ¹³⁴, I. Koletsou ⁴,
 T. Komarek ¹²¹, K. Köneke ⁵⁴, A.X.Y. Kong ¹, T. Kono ¹¹⁷, N. Konstantinidis ⁹⁵, B. Konya ⁹⁷,
 R. Kopeliansky ⁶⁷, S. Koperny ^{84a}, K. Korcyl ⁸⁵, K. Kordas ¹⁵¹, G. Koren ¹⁵⁰, A. Korn ⁹⁵,
 S. Korn ⁵⁵, I. Korolkov ¹³, N. Korotkova ³⁷, B. Kortman ¹¹³, O. Kortner ¹⁰⁹, S. Kortner ¹⁰⁹,
 W.H. Kostecka ¹¹⁴, V.V. Kostyukhin ¹⁴⁰, A. Kotsokechagia ¹³⁴, A. Kotwal ⁵¹, A. Koulouris ³⁶,
 A. Kourkoumeli-Charalampidi ^{72a,72b}, C. Kourkoumelis ⁹, E. Kourlitis ⁶, O. Kovanda ¹⁴⁵,
 R. Kowalewski ¹⁶⁴, W. Kozanecki ¹³⁴, A.S. Kozhin ³⁷, V.A. Kramarenko ³⁷, G. Kramberger ⁹²,
 P. Kramer ⁹⁹, M.W. Krasny ¹²⁶, A. Krasznahorkay ³⁶, J.A. Kremer ⁹⁹, T. Kresse ⁵⁰,
 J. Kretschmar ⁹¹, K. Kreul ¹⁸, P. Krieger ¹⁵⁴, F. Krieter ¹⁰⁸, S. Krishnamurthy ¹⁰²,
 A. Krishnan ^{63b}, M. Krivos ¹³², K. Krizka ^{17a}, K. Kroeninger ⁴⁹, H. Kroha ¹⁰⁹, J. Kroll ¹³⁰,
 J. Kroll ¹²⁷, K.S. Krowpman ¹⁰⁶, U. Kruchonak ³⁸, H. Krüger ²⁴, N. Krumnack⁸⁰, M.C. Kruse ⁵¹,
 J.A. Krzysiak ⁸⁵, A. Kubota ¹⁵³, O. Kuchinskaia ³⁷, S. Kuday ^{3a}, D. Kuechler ⁴⁸,
 J.T. Kuechler ⁴⁸, S. Kuehn ³⁶, T. Kuhl ⁴⁸, V. Kukhtin ³⁸, Y. Kulchitsky ^{37,a},
 S. Kuleshov ^{136d,136b}, M. Kumar ^{33g}, N. Kumari ¹⁰¹, M. Kuna ⁶⁰, A. Kupco ¹³⁰, T. Kupfer⁴⁹,
 A. Kupich ³⁷, O. Kuprash ⁵⁴, H. Kurashige ⁸³, L.L. Kurchaninov ^{155a}, Y.A. Kurochkin ³⁷,
 A. Kurova ³⁷, E.S. Kuwertz ³⁶, M. Kuze ¹⁵³, A.K. Kvam ¹⁰², J. Kvita ¹²¹, T. Kwan ¹⁰³,
 K.W. Kwok ^{64a}, N.G. Kyriacou ¹⁰⁵, L.A.O. Laatu ¹⁰¹, C. Lacasta ¹⁶², F. Lacava ^{74a,74b},
 H. Lacker ¹⁸, D. Lacour ¹²⁶, N.N. Lad ⁹⁵, E. Ladygin ³⁸, B. Laforge ¹²⁶, T. Lagouri ^{136e},
 S. Lai ⁵⁵, I.K. Lakomic ^{84a}, N. Lalloue ⁶⁰, J.E. Lambert ¹¹⁹, S. Lammers ⁶⁷, W. Lampl ⁷,
 C. Lampoudis ¹⁵¹, A.N. Lancaster ¹¹⁴, E. Lançon ²⁹, U. Landgraf ⁵⁴, M.P.J. Landon ⁹³,
 V.S. Lang ⁵⁴, R.J. Langenberg ¹⁰², A.J. Lankford ¹⁵⁹, F. Lanni ³⁶, K. Lantzsch ²⁴, A. Lanza ^{72a},
 A. Lapertosa ^{57b,57a}, J.F. Laporte ¹³⁴, T. Lari ^{70a}, F. Lasagni Manghi ^{23b}, M. Lassnig ³⁶,
 V. Latonova ¹³⁰, T.S. Lau ^{64a}, A. Laudrain ⁹⁹, A. Laurier ³⁴, S.D. Lawlor ⁹⁴, Z. Lawrence ¹⁰⁰,
 M. Lazzaroni ^{70a,70b}, B. Le¹⁰⁰, B. Leban ⁹², A. Lebedev ⁸⁰, M. LeBlanc ³⁶, T. LeCompte ⁶,
 F. Ledroit-Guillon ⁶⁰, A.C.A. Lee⁹⁵, G.R. Lee ¹⁶, L. Lee ⁶¹, S.C. Lee ¹⁴⁷, S. Lee ^{47a,47b},
 T.F. Lee ⁹¹, L.L. Leeuw ^{33c}, H.P. Lefebvre ⁹⁴, M. Lefebvre ¹⁶⁴, C. Leggett ^{17a}, K. Lehmann ¹⁴¹,
 G. Lehmann Miotto ³⁶, M. Leigh ⁵⁶, W.A. Leight ¹⁰², A. Leisos ^{151,u}, M.A.L. Leite ^{81c},
 C.E. Leitgeb ⁴⁸, R. Leitner ¹³², K.J.C. Leney ⁴⁴, T. Lenz ²⁴, S. Leone ^{73a}, C. Leonidopoulos ⁵²,
 A. Leopold ¹⁴³, C. Leroy ¹⁰⁷, R. Les ¹⁰⁶, C.G. Lester ³², M. Levchenko ³⁷, J. Levêque ⁴,
 D. Levin ¹⁰⁵, L.J. Levinson ¹⁶⁸, M.P. Lewicki ⁸⁵, D.J. Lewis ²⁰, B. Li ^{14b}, B. Li ^{62b}, C. Li^{62a},
 C-Q. Li ^{62c}, H. Li ^{62a}, H. Li ^{62b}, H. Li ^{14c}, H. Li ^{62b}, J. Li ^{62c}, K. Li ¹³⁷, L. Li ^{62c},
 M. Li ^{14a,14d}, Q.Y. Li ^{62a}, S. Li ^{62d,62c,e}, T. Li ^{62b}, X. Li ¹⁰³, Z. Li ^{62b}, Z. Li ¹²⁵, Z. Li ¹⁰³,
 Z. Li ⁹¹, Z. Li ^{14a,14d}, Z. Liang ^{14a}, M. Liberatore ⁴⁸, B. Liberti ^{75a}, K. Lie ^{64c},
 J. Lieber Marin ^{81b}, K. Lin ¹⁰⁶, R.A. Linck ⁶⁷, R.E. Lindley ⁷, J.H. Lindon ², A. Linss ⁴⁸,
 E. Lipeles ¹²⁷, A. Lipniacka ¹⁶, A. Lister ¹⁶³, J.D. Little ⁴, B. Liu ^{14a}, B.X. Liu ¹⁴¹,
 D. Liu ^{62d,62c}, J.B. Liu ^{62a}, J.K.K. Liu ³², K. Liu ^{62d,62c}, M. Liu ^{62a}, M.Y. Liu ^{62a}, P. Liu ^{14a},
 Q. Liu ^{62d,137,62c}, X. Liu ^{62a}, Y. Liu ⁴⁸, Y. Liu ^{14c,14d}, Y.L. Liu ¹⁰⁵, Y.W. Liu ^{62a},
 M. Livan ^{72a,72b}, J. Llorente Merino ¹⁴¹, S.L. Lloyd ⁹³, E.M. Lobodzinska ⁴⁸, P. Loch ⁷,
 S. Loffredo ^{75a,75b}, T. Lohse ¹⁸, K. Lohwasser ¹³⁸, M. Lokajicek ^{130,*}, J.D. Long ¹⁶¹,

I. Longarini ^{74a,74b}, L. Longo ^{69a,69b}, R. Longo ¹⁶¹, I. Lopez Paz ³⁶, A. Lopez Solis ⁴⁸,
 J. Lorenz ¹⁰⁸, N. Lorenzo Martinez ⁴, A.M. Lory ¹⁰⁸, A. Lösle ⁵⁴, X. Lou ^{47a,47b}, X. Lou ^{14a,14d},
 A. Lounis ⁶⁶, J. Love ⁶, P.A. Love ⁹⁰, J.J. Lozano Bahilo ¹⁶², G. Lu ^{14a,14d}, M. Lu ⁷⁹,
 S. Lu ¹²⁷, Y.J. Lu ⁶⁵, H.J. Lubatti ¹³⁷, C. Luci ^{74a,74b}, F.L. Lucio Alves ^{14c}, A. Lucotte ⁶⁰,
 F. Luehring ⁶⁷, I. Luise ¹⁴⁴, O. Lukianchuk ⁶⁶, O. Lundberg ¹⁴³, B. Lund-Jensen ¹⁴³,
 N.A. Luongo ¹²², M.S. Lutz ¹⁵⁰, D. Lynn ²⁹, H. Lyons ⁹¹, R. Lysak ¹³⁰, E. Lytken ⁹⁷, F. Lyu ^{14a},
 V. Lyubushkin ³⁸, T. Lyubushkina ³⁸, H. Ma ²⁹, L.L. Ma ^{62b}, Y. Ma ⁹⁵, D.M. Mac Donell ¹⁶⁴,
 G. Maccarrone ⁵³, J.C. MacDonald ¹³⁸, R. Madar ⁴⁰, W.F. Mader ⁵⁰, J. Maeda ⁸³, T. Maeno ²⁹,
 M. Maerker ⁵⁰, V. Magerl ⁵⁴, J. Magro ^{68a,68c}, H. Maguire ¹³⁸, D.J. Mahon ⁴¹,
 C. Maidantchik ^{81b}, A. Maio ^{129a,129b,129d}, K. Maj ^{84a}, O. Majersky ^{28a}, S. Majewski ¹²²,
 N. Makovec ⁶⁶, V. Maksimovic ¹⁵, B. Malaescu ¹²⁶, Pa. Malecki ⁸⁵, V.P. Maleev ³⁷,
 F. Malek ⁶⁰, D. Malito ^{43b,43a}, U. Mallik ⁷⁹, C. Malone ³², S. Maltezos ¹⁰, S. Malyukov ³⁸,
 J. Mamuzic ¹³, G. Mancini ⁵³, G. Manco ^{72a,72b}, J.P. Mandalia ⁹³, I. Mandić ⁹²,
 L. Manhaes de Andrade Filho ^{81a}, I.M. Maniatis ¹⁵¹, M. Manisha ¹³⁴, J. Manjarres Ramos ⁵⁰,
 D.C. Mankad ¹⁶⁸, A. Mann ¹⁰⁸, B. Mansoulie ¹³⁴, S. Manzoni ³⁶, A. Marantis ^{151,u},
 G. Marchiori ⁵, M. Marcisovsky ¹³⁰, L. Marcoccia ^{75a,75b}, C. Marcon ^{70a,70b}, M. Marinescu ²⁰,
 M. Marjanovic ¹¹⁹, Z. Marshall ^{17a}, S. Marti-Garcia ¹⁶², T.A. Martin ¹⁶⁶, V.J. Martin ⁵²,
 B. Martin dit Latour ¹⁶, L. Martinelli ^{74a,74b}, M. Martinez ^{13,v}, P. Martinez Agullo ¹⁶²,
 V.I. Martinez Outschoorn ¹⁰², P. Martinez Suarez ¹³, S. Martin-Haugh ¹³³, V.S. Martoiu ^{27b},
 A.C. Martyniuk ⁹⁵, A. Marzin ³⁶, S.R. Maschek ¹⁰⁹, L. Masetti ⁹⁹, T. Mashimo ¹⁵²,
 J. Masik ¹⁰⁰, A.L. Maslennikov ³⁷, L. Massa ^{23b}, P. Massarotti ^{71a,71b}, P. Mastrandrea ^{73a,73b},
 A. Mastroberardino ^{43b,43a}, T. Masubuchi ¹⁵², T. Mathisen ¹⁶⁰, N. Matsuzawa ¹⁵², J. Maurer ^{27b},
 B. Maček ⁹², D.A. Maximov ³⁷, R. Mazini ¹⁴⁷, I. Maznas ¹⁵¹, M. Mazza ¹⁰⁶, S.M. Mazza ¹³⁵,
 C. Mc Ginn ²⁹, J.P. Mc Gowan ¹⁰³, S.P. Mc Kee ¹⁰⁵, T.G. McCarthy ¹⁰⁹, W.P. McCormack ^{17a},
 E.F. McDonald ¹⁰⁴, A.E. McDougall ¹¹³, J.A. Mcfayden ¹⁴⁵, G. Mchedlidze ^{148b},
 R.P. Mckenzie ^{33g}, T.C. Mclachlan ⁴⁸, D.J. Mclaughlin ⁹⁵, K.D. McLean ¹⁶⁴, S.J. McMahon ¹³³,
 P.C. McNamara ¹⁰⁴, C.M. Mcpartland ⁹¹, R.A. McPherson ^{164,y}, T. Megy ⁴⁰, S. Mehlhase ¹⁰⁸,
 A. Mehta ⁹¹, B. Meirose ⁴⁵, D. Melini ¹⁴⁹, B.R. Mellado Garcia ^{33g}, A.H. Melo ⁵⁵,
 F. Meloni ⁴⁸, E.D. Mendes Gouveia ^{129a}, A.M. Mendes Jacques Da Costa ²⁰, H.Y. Meng ¹⁵⁴,
 L. Meng ⁹⁰, S. Menke ¹⁰⁹, M. Mentink ³⁶, E. Meoni ^{43b,43a}, C. Merlassino ¹²⁵,
 L. Merola ^{71a,71b}, C. Meroni ^{70a}, G. Merz ¹⁰⁵, O. Meshkov ³⁷, J.K.R. Meshreki ¹⁴⁰, J. Metcalfe ⁶,
 A.S. Mete ⁶, C. Meyer ⁶⁷, J-P. Meyer ¹³⁴, M. Michetti ¹⁸, R.P. Middleton ¹³³, L. Mijović ⁵²,
 G. Mikenberg ¹⁶⁸, M. Mikestikova ¹³⁰, M. Mikuž ⁹², H. Mildner ¹³⁸, A. Milic ¹⁵⁴,
 C.D. Milke ⁴⁴, D.W. Miller ³⁹, L.S. Miller ³⁴, A. Milov ¹⁶⁸, D.A. Milstead ^{47a,47b}, T. Min ^{14c},
 A.A. Minaenko ³⁷, I.A. Minashvili ^{148b}, L. Mince ⁵⁹, A.I. Mincer ¹¹⁶, B. Mindur ^{84a},
 M. Mineev ³⁸, Y. Mino ⁸⁶, L.M. Mir ¹³, M. Miralles Lopez ¹⁶², M. Mironova ¹²⁵, T. Mitani ¹⁶⁷,
 A. Mitra ¹⁶⁶, V.A. Mitsou ¹⁶², O. Miu ¹⁵⁴, P.S. Miyagawa ⁹³, Y. Miyazaki ⁸⁸, A. Mizukami ⁸²,
 J.U. Mjörnmark ⁹⁷, T. Mkrtchyan ^{63a}, T. Mlinarevic ⁹⁵, M. Mlynarikova ³⁶, T. Moa ^{47a,47b},
 S. Mobius ⁵⁵, K. Mochizuki ¹⁰⁷, P. Moder ⁴⁸, P. Mogg ¹⁰⁸, A.F. Mohammed ^{14a,14d},
 S. Mohapatra ⁴¹, G. Mokgatitswane ^{33g}, B. Mondal ¹⁴⁰, S. Mondal ¹³¹, K. Mönig ⁴⁸,
 E. Monnier ¹⁰¹, L. Monsonis Romero ¹⁶², J. Montejo Berlingen ³⁶, M. Montella ¹¹⁸,
 F. Monticelli ⁸⁹, N. Morange ⁶⁶, A.L. Moreira De Carvalho ^{129a}, M. Moreno Llácer ¹⁶²,
 C. Moreno Martinez ¹³, P. Morettini ^{57b}, S. Morgenstern ¹⁶⁶, M. Morii ⁶¹, M. Morinaga ¹⁵²,
 V. Morisbak ¹²⁴, A.K. Morley ³⁶, F. Morodei ^{74a,74b}, L. Morvaj ³⁶, P. Moschovakos ³⁶,
 B. Moser ³⁶, M. Mosidze ^{148b}, T. Moskalets ⁵⁴, P. Moskvitina ¹¹², J. Moss ^{31,o}, E.J.W. Moyses ¹⁰²,
 S. Muanza ¹⁰¹, J. Mueller ¹²⁸, D. Muenstermann ⁹⁰, R. Müller ¹⁹, G.A. Mullier ⁹⁷, J.J. Mullin ¹²⁷,
 D.P. Mungo ^{70a,70b}, J.L. Munoz Martinez ¹³, D. Munoz Perez ¹⁶², F.J. Munoz Sanchez ¹⁰⁰,

M. Murin ¹⁰⁰, W.J. Murray ^{166,133}, A. Murrone ^{70a,70b}, J.M. Muse ¹¹⁹, M. Muškinja ^{17a},
C. Mwewa ²⁹, A.G. Myagkov ^{37,a}, A.J. Myers ⁸, A.A. Myers ¹²⁸, G. Myers ⁶⁷, M. Myska ¹³¹,
B.P. Nachman ^{17a}, O. Nackenhorst ⁴⁹, A. Nag ⁵⁰, K. Nagai ¹²⁵, K. Nagano ⁸², J.L. Nagle ^{29,aj},
E. Nagy ¹⁰¹, A.M. Nairz ³⁶, Y. Nakahama ⁸², K. Nakamura ⁸², H. Nanjo ¹²³, R. Narayan ⁴⁴,
E.A. Narayanan ¹¹¹, I. Naryshkin ³⁷, M. Naseri ³⁴, C. Nass ²⁴, G. Navarro ^{22a},
J. Navarro-Gonzalez ¹⁶², R. Nayak ¹⁵⁰, A. Nayaz ¹⁸, P.Y. Nechaeva ³⁷, F. Nechansky ⁴⁸,
L. Nedic ¹²⁵, T.J. Neep ²⁰, A. Negri ^{72a,72b}, M. Negrini ^{23b}, C. Nellist ¹¹², C. Nelson ¹⁰³,
K. Nelson ¹⁰⁵, S. Nemecek ¹³⁰, M. Nessi ^{36,h}, M.S. Neubauer ¹⁶¹, F. Neuhaus ⁹⁹,
J. Neundorff ⁴⁸, R. Newhouse ¹⁶³, P.R. Newman ²⁰, C.W. Ng ¹²⁸, Y.S. Ng ¹⁸, Y.W.Y. Ng ¹⁵⁹,
B. Ngair ^{35e}, H.D.N. Nguyen ¹⁰⁷, R.B. Nickerson ¹²⁵, R. Nicolaidou ¹³⁴, J. Nielsen ¹³⁵,
M. Niemeyer ⁵⁵, N. Nikipforou ³⁶, V. Nikolaenko ^{37,a}, I. Nikolic-Audit ¹²⁶, K. Nikolopoulos ²⁰,
P. Nilsson ²⁹, H.R. Nindhito ⁵⁶, A. Nisati ^{74a}, N. Nishu ², R. Nisius ¹⁰⁹, J.-E. Nitschke ⁵⁰,
E.K. Nkadimeng ^{33g}, S.J. Noacco Rosende ⁸⁹, T. Nobe ¹⁵², D.L. Noel ³², Y. Noguchi ⁸⁶,
T. Nommensen ¹⁴⁶, M.A. Nomura ²⁹, M.B. Norfolk ¹³⁸, R.R.B. Norisam ⁹⁵, B.J. Norman ³⁴,
J. Novak ⁹², T. Novak ⁴⁸, O. Novgorodova ⁵⁰, L. Novotny ¹³¹, R. Novotny ¹¹¹, L. Nozka ¹²¹,
K. Ntekas ¹⁵⁹, E. Nurse ⁹⁵, F.G. Oakham ^{34,ag}, J. Ocariz ¹²⁶, A. Ochi ⁸³, I. Ochoa ^{129a},
S. Oerdek ¹⁶⁰, A. Ogrodnik ^{84a}, A. Oh ¹⁰⁰, C.C. Ohm ¹⁴³, H. Oide ¹⁵³, R. Oishi ¹⁵²,
M.L. Ojeda ⁴⁸, Y. Okazaki ⁸⁶, M.W. O'Keefe ⁹¹, Y. Okumura ¹⁵², A. Olariu ^{27b},
L.F. Oleiro Seabra ^{129a}, S.A. Olivares Pino ^{136e}, D. Oliveira Damazio ²⁹, D. Oliveira Goncalves ^{81a},
J.L. Oliver ¹⁵⁹, M.J.R. Olsson ¹⁵⁹, A. Olszewski ⁸⁵, J. Olszowska ^{85,*}, Ö.O. Öncel ⁵⁴,
D.C. O'Neil ¹⁴¹, A.P. O'Neill ¹⁹, A. Onofre ^{129a,129e}, P.U.E. Onyisi ¹¹, M.J. Oreglia ³⁹,
G.E. Orellana ⁸⁹, D. Orestano ^{76a,76b}, N. Orlando ¹³, R.S. Orr ¹⁵⁴, V. O'Shea ⁵⁹,
R. Ospanov ^{62a}, G. Otero y Garzon ³⁰, H. Otono ⁸⁸, P.S. Ott ^{63a}, G.J. Ottino ^{17a}, M. Ouchrif ^{35d},
J. Ouellette ^{29,aj}, F. Ould-Saada ¹²⁴, M. Owen ⁵⁹, R.E. Owen ¹³³, K.Y. Oyulmaz ^{21a},
V.E. Ozcan ^{21a}, N. Ozturk ⁸, S. Ozturk ^{21d}, J. Pacalt ¹²¹, H.A. Pacey ³², K. Pachal ⁵¹,
A. Pacheco Pages ¹³, C. Padilla Aranda ¹³, G. Padovano ^{74a,74b}, S. Pagan Griso ^{17a},
G. Palacino ⁶⁷, A. Palazzo ^{69a,69b}, S. Palazzo ⁵², S. Palestini ³⁶, M. Palka ^{84b}, J. Pan ¹⁷¹,
T. Pan ^{64a}, D.K. Panchal ¹¹, C.E. Pandini ¹¹³, J.G. Panduro Vazquez ⁹⁴, H. Pang ^{14b}, P. Pani ⁴⁸,
G. Panizzo ^{68a,68c}, L. Paolozzi ⁵⁶, C. Papadatos ¹⁰⁷, S. Parajuli ⁴⁴, A. Paramonov ⁶,
C. Paraskevopoulos ¹⁰, D. Paredes Hernandez ^{64b}, T.H. Park ¹⁵⁴, M.A. Parker ³², F. Parodi ^{57b,57a},
E.W. Parrish ¹¹⁴, V.A. Parrish ⁵², J.A. Parsons ⁴¹, U. Parzefall ⁵⁴, B. Pascual Dias ¹⁰⁷,
L. Pascual Dominguez ¹⁵⁰, V.R. Pascuzzi ^{17a}, F. Pasquali ¹¹³, E. Pasqualucci ^{74a}, S. Passaggio ^{57b},
F. Pastore ⁹⁴, P. Pasuwan ^{47a,47b}, P. Patel ⁸⁵, J.R. Pater ¹⁰⁰, J. Patton ⁹¹, T. Pauly ³⁶,
J. Pearkes ¹⁴², M. Pedersen ¹²⁴, R. Pedro ^{129a}, S.V. Peleganchuk ³⁷, O. Penc ³⁶, E.A. Pender ⁵²,
C. Peng ^{64b}, H. Peng ^{62a}, K.E. Pensi ¹⁰⁸, M. Penzin ³⁷, B.S. Peralva ^{81d},
A.P. Pereira Peixoto ⁶⁰, L. Pereira Sanchez ^{47a,47b}, D.V. Perepelitsa ^{29,aj}, E. Perez Codina ^{155a},
M. Perganti ¹⁰, L. Perini ^{70a,70b,*}, H. Pernegger ³⁶, S. Perrella ³⁶, A. Perrevoort ¹¹², O. Perrin ⁴⁰,
K. Peters ⁴⁸, R.F.Y. Peters ¹⁰⁰, B.A. Petersen ³⁶, T.C. Petersen ⁴², E. Petit ¹⁰¹, V. Petousis ¹³¹,
C. Petridou ¹⁵¹, A. Petrukhin ¹⁴⁰, M. Pettee ^{17a}, N.E. Pettersson ³⁶, A. Petukhov ³⁷,
K. Petukhova ¹³², A. Peyaud ¹³⁴, R. Pezoa ^{136f}, L. Pezzotti ³⁶, G. Pezzullo ¹⁷¹, T.M. Pham ¹⁶⁹,
T. Pham ¹⁰⁴, P.W. Phillips ¹³³, M.W. Phipps ¹⁶¹, G. Piacquadio ¹⁴⁴, E. Pianori ^{17a},
F. Piazza ^{70a,70b}, R. Piegaia ³⁰, D. Pietreanu ^{27b}, A.D. Pilkington ¹⁰⁰, M. Pinamonti ^{68a,68c},
J.L. Pinfold ², B.C. Pinheiro Pereira ^{129a}, C. Pitman Donaldson ⁹⁵, D.A. Pizzi ³⁴,
L. Pizzimento ^{75a,75b}, A. Pizzini ¹¹³, M.-A. Pleier ²⁹, V. Plesanovs ⁵⁴, V. Pleskot ¹³², E. Plotnikova ³⁸,
G. Poddar ⁴, R. Poettgen ⁹⁷, L. Poggioli ¹²⁶, I. Pogrebnyak ¹⁰⁶, D. Pohl ²⁴, I. Pokharel ⁵⁵,
S. Polacek ¹³², G. Polesello ^{72a}, A. Poley ^{141,155a}, R. Polifka ¹³¹, A. Polini ^{23b}, C.S. Pollard ¹²⁵,
Z.B. Pollock ¹¹⁸, V. Polychronakos ²⁹, E. Pompa Pacchi ^{74a,74b}, D. Ponomarenko ³⁷,

L. Pontecorvo ³⁶, S. Popa ^{27a}, G.A. Popeneciu ^{27d}, D.M. Portillo Quintero ^{155a}, S. Pospisil ¹³¹,
 P. Postolache ^{27c}, K. Potamianos ¹²⁵, I.N. Potrap ³⁸, C.J. Potter ³², H. Potti ¹, T. Poulsen ⁴⁸,
 J. Poveda ¹⁶², M.E. Pozo Astigarraga ³⁶, A. Prades Ibanez ¹⁶², M.M. Prapa ⁴⁶, J. Pretel ⁵⁴,
 D. Price ¹⁰⁰, M. Primavera ^{69a}, M.A. Principe Martin ⁹⁸, M.L. Proffitt ¹³⁷, N. Proklova ¹²⁷,
 K. Prokofiev ^{64c}, G. Proto ^{75a,75b}, S. Protopopescu ²⁹, J. Proudfoot ⁶, M. Przybycien ^{84a},
 J.E. Puddefoot ¹³⁸, D. Pudzha ³⁷, P. Puzo ⁶⁶, D. Pyatiizbyantseva ³⁷, J. Qian ¹⁰⁵, D. Qichen ¹⁰⁰,
 Y. Qin ¹⁰⁰, T. Qiu ⁹³, A. Quadt ⁵⁵, M. Queitsch-Maitland ¹⁰⁰, G. Quetant ⁵⁶,
 G. Rabanal Bolanos ⁶¹, D. Rafanoharana ⁵⁴, F. Ragusa ^{70a,70b}, J.L. Rainbolt ³⁹, J.A. Raine ⁵⁶,
 S. Rajagopalan ²⁹, E. Ramakoti ³⁷, K. Ran ^{48,14d}, V. Raskina ¹²⁶, D.F. Rassloff ^{63a}, S. Rave ⁹⁹,
 B. Ravina ⁵⁵, I. Ravinovich ¹⁶⁸, M. Raymond ³⁶, A.L. Read ¹²⁴, N.P. Readioff ¹³⁸,
 D.M. Rebuzzi ^{72a,72b}, G. Redlinger ²⁹, K. Reeves ⁴⁵, J.A. Reidelsturz ¹⁷⁰, D. Reikher ¹⁵⁰,
 A. Reiss ⁹⁹, A. Rej ¹⁴⁰, C. Rembser ³⁶, A. Renardi ⁴⁸, M. Renda ^{27b}, M.B. Rendel ¹⁰⁹,
 A.G. Rennie ⁵⁹, S. Resconi ^{70a}, M. Ressegotti ^{57b,57a}, E.D. Resseguie ^{17a}, S. Rettie ⁹⁵,
 B. Reynolds ¹¹⁸, E. Reynolds ^{17a}, M. Rezaei Estabragh ¹⁷⁰, O.L. Rezanova ³⁷, P. Reznicek ¹³²,
 E. Ricci ^{77a,77b}, R. Richter ¹⁰⁹, S. Richter ^{47a,47b}, E. Richter-Was ^{84b}, M. Ridel ¹²⁶, P. Rieck ¹¹⁶,
 P. Riedler ³⁶, M. Rijssenbeek ¹⁴⁴, A. Rimoldi ^{72a,72b}, M. Rimoldi ⁴⁸, L. Rinaldi ^{23b,23a},
 T.T. Rinn ²⁹, M.P. Rinnagel ¹⁰⁸, G. Ripellino ¹⁴³, I. Riu ¹³, P. Rivadeneira ⁴⁸,
 J.C. Rivera Vergara ¹⁶⁴, F. Rizatdinova ¹²⁰, E. Rizvi ⁹³, C. Rizzi ⁵⁶, B.A. Roberts ¹⁶⁶,
 B.R. Roberts ^{17a}, S.H. Robertson ^{103,y}, M. Robin ⁴⁸, D. Robinson ³², C.M. Robles Gajardo ^{136f},
 M. Robles Manzano ⁹⁹, A. Robson ⁵⁹, A. Rocchi ^{75a,75b}, C. Roda ^{73a,73b}, S. Rodriguez Bosca ^{63a},
 Y. Rodriguez Garcia ^{22a}, A. Rodriguez Rodriguez ⁵⁴, A.M. Rodríguez Vera ^{155b}, S. Roe ³⁶,
 J.T. Roemer ¹⁵⁹, A.R. Roepe-Gier ¹¹⁹, J. Roggel ¹⁷⁰, O. Røhne ¹²⁴, R.A. Rojas ¹⁶⁴, B. Roland ⁵⁴,
 C.P.A. Roland ⁶⁷, J. Roloff ²⁹, A. Romaniouk ³⁷, E. Romano ^{72a,72b}, M. Romano ^{23b},
 A.C. Romero Hernandez ¹⁶¹, N. Rompotis ⁹¹, L. Roos ¹²⁶, S. Rosati ^{74a}, B.J. Rosser ³⁹,
 E. Rossi ⁴, E. Rossi ^{71a,71b}, L.P. Rossi ^{57b}, L. Rossini ⁴⁸, R. Rosten ¹¹⁸, M. Rotaru ^{27b},
 B. Rottler ⁵⁴, D. Rousseau ⁶⁶, D. Rousso ³², G. Rovelli ^{72a,72b}, A. Roy ¹⁶¹, A. Rozanov ¹⁰¹,
 Y. Rozen ¹⁴⁹, X. Ruan ^{33g}, A. Rubio Jimenez ¹⁶², A.J. Ruby ⁹¹, V.H. Ruelas Rivera ¹⁸,
 T.A. Ruggeri ¹, F. Rühr ⁵⁴, A. Ruiz-Martinez ¹⁶², A. Rummler ³⁶, Z. Rurikova ⁵⁴,
 N.A. Rusakovich ³⁸, H.L. Russell ¹⁶⁴, J.P. Rutherford ⁷, K. Rybacki ⁹⁰, M. Rybar ¹³²,
 E.B. Rye ¹²⁴, A. Ryzhov ³⁷, J.A. Sabater Iglesias ⁵⁶, P. Sabatini ¹⁶², L. Sabetta ^{74a,74b},
 H.F-W. Sadrozinski ¹³⁵, F. Safai Tehrani ^{74a}, B. Safarzadeh Samani ¹⁴⁵, M. Safdari ¹⁴²,
 S. Saha ¹⁰³, M. Sahinsoy ¹⁰⁹, M. Saimpert ¹³⁴, M. Saito ¹⁵², T. Saito ¹⁵², D. Salamani ³⁶,
 G. Salamanna ^{76a,76b}, A. Salnikov ¹⁴², J. Salt ¹⁶², A. Salvador Salas ¹³, D. Salvatore ^{43b,43a},
 F. Salvatore ¹⁴⁵, A. Salzburger ³⁶, D. Sammel ⁵⁴, D. Sampsonidis ¹⁵¹, D. Sampsonidou ^{62d,62c},
 J. Sánchez ¹⁶², A. Sanchez Pineda ⁴, V. Sanchez Sebastian ¹⁶², H. Sandaker ¹²⁴, C.O. Sander ⁴⁸,
 J.A. Sandesara ¹⁰², M. Sandhoff ¹⁷⁰, C. Sandoval ^{22b}, D.P.C. Sankey ¹³³, A. Sansoni ⁵³,
 L. Santi ^{74a,74b}, C. Santoni ⁴⁰, H. Santos ^{129a,129b}, S.N. Santpur ^{17a}, A. Santra ¹⁶⁸,
 K.A. Saoucha ¹³⁸, J.G. Saraiva ^{129a,129d}, J. Sardain ⁷, O. Sasaki ⁸², K. Sato ¹⁵⁶, C. Sauer ^{63b},
 F. Sauerburger ⁵⁴, E. Sauvan ⁴, P. Savard ^{154,ag}, R. Sawada ¹⁵², C. Sawyer ¹³³, L. Sawyer ⁹⁶,
 I. Sayago Galvan ¹⁶², C. Sbarra ^{23b}, A. Sbrizzi ^{23b,23a}, T. Scanlon ⁹⁵, J. Schaarschmidt ¹³⁷,
 P. Schacht ¹⁰⁹, D. Schaefer ³⁹, U. Schäfer ⁹⁹, A.C. Schaffer ⁶⁶, D. Schaile ¹⁰⁸,
 R.D. Schamberger ¹⁴⁴, E. Schanet ¹⁰⁸, C. Scharf ¹⁸, V.A. Schegelsky ³⁷, D. Scheirich ¹³²,
 F. Schenck ¹⁸, M. Schernau ¹⁵⁹, C. Scheulen ⁵⁵, C. Schiavi ^{57b,57a}, Z.M. Schillaci ²⁶,
 E.J. Schioppa ^{69a,69b}, M. Schioppa ^{43b,43a}, B. Schlag ⁹⁹, K.E. Schleicher ⁵⁴, S. Schlenker ³⁶,
 K. Schmieden ⁹⁹, C. Schmitt ⁹⁹, S. Schmitt ⁴⁸, L. Schoeffel ¹³⁴, A. Schoening ^{63b},
 P.G. Scholer ⁵⁴, E. Schopf ¹²⁵, M. Schott ⁹⁹, J. Schovancova ³⁶, S. Schramm ⁵⁶,
 F. Schroeder ¹⁷⁰, H-C. Schultz-Coulon ^{63a}, M. Schumacher ⁵⁴, B.A. Schumm ¹³⁵, Ph. Schune ¹³⁴,

A. Schwartzman ¹⁴², T.A. Schwarz ¹⁰⁵, Ph. Schwemling ¹³⁴, R. Schwienhorst ¹⁰⁶,
 A. Sciandra ¹³⁵, G. Sciolla ²⁶, F. Scuri ^{73a}, F. Scutti ¹⁰⁴, C.D. Sebastiani ⁹¹, K. Sedlaczek ⁴⁹,
 P. Seema ¹⁸, S.C. Seidel ¹¹¹, A. Seiden ¹³⁵, B.D. Seidlitz ⁴¹, T. Seiss ³⁹, C. Seitz ⁴⁸,
 J.M. Seixas ^{81b}, G. Sekhniaidze ^{71a}, S.J. Sekula ⁴⁴, L. Selem ⁴, N. Semprini-Cesari ^{23b,23a},
 S. Sen ⁵¹, D. Sengupta ⁵⁶, V. Senthilkumar ¹⁶², L. Serin ⁶⁶, L. Serkin ^{68a,68b}, M. Sessa ^{76a,76b},
 H. Severini ¹¹⁹, S. Sevova ¹⁴², F. Sforza ^{57b,57a}, A. Sfyrta ⁵⁶, E. Shabalina ⁵⁵, R. Shaheen ¹⁴³,
 J.D. Shahinian ¹²⁷, N.W. Shaikh ^{47a,47b}, D. Shaked Renous ¹⁶⁸, L.Y. Shan ^{14a}, M. Shapiro ^{17a},
 A. Sharma ³⁶, A.S. Sharma ¹⁶³, P. Sharma ⁷⁹, S. Sharma ⁴⁸, P.B. Shatalov ³⁷, K. Shaw ¹⁴⁵,
 S.M. Shaw ¹⁰⁰, Q. Shen ^{62c,5}, P. Sherwood ⁹⁵, L. Shi ⁹⁵, C.O. Shimmin ¹⁷¹, Y. Shimogama ¹⁶⁷,
 J.D. Shinner ⁹⁴, I.P.J. Shipsey ¹²⁵, S. Shirabe ⁶⁰, M. Shiyakova ^{38,x}, J. Shlomi ¹⁶⁸,
 M.J. Shochet ³⁹, J. Shojaii ¹⁰⁴, D.R. Shope ¹²⁴, S. Shrestha ^{118,ak}, E.M. Shrif ^{33g},
 M.J. Shroff ¹⁶⁴, P. Sicho ¹³⁰, A.M. Sickles ¹⁶¹, E. Sideras Haddad ^{33g}, A. Sidoti ^{23b},
 F. Siegert ⁵⁰, Dj. Sijacki ¹⁵, R. Sikora ^{84a}, F. Sili ⁸⁹, J.M. Silva ²⁰, M.V. Silva Oliveira ³⁶,
 S.B. Silverstein ^{47a}, S. Simion ⁶⁶, R. Simoniello ³⁶, E.L. Simpson ⁵⁹, N.D. Simpson ⁹⁷,
 S. Simsek ^{21d}, S. Sindhu ⁵⁵, P. Sinervo ¹⁵⁴, V. Sinetckii ³⁷, S. Singh ¹⁴¹, S. Singh ¹⁵⁴,
 S. Sinha ⁴⁸, S. Sinha ^{33g}, M. Sioli ^{23b,23a}, I. Siral ¹²², S. Yu. Sivoklov ^{37,*}, J. Sjölin ^{47a,47b},
 A. Skaf ⁵⁵, E. Skorda ⁹⁷, P. Skubic ¹¹⁹, M. Slawinska ⁸⁵, V. Smakhtin ¹⁶⁸, B.H. Smart ¹³³,
 J. Smiesko ³⁶, S. Yu. Smirnov ³⁷, Y. Smirnov ³⁷, L.N. Smirnova ^{37,a}, O. Smirnova ⁹⁷,
 A.C. Smith ⁴¹, E.A. Smith ³⁹, H.A. Smith ¹²⁵, J.L. Smith ⁹¹, R. Smith ¹⁴², M. Smizanska ⁹⁰,
 K. Smolek ¹³¹, A. Smykiewicz ⁸⁵, A.A. Snesarev ³⁷, H.L. Snoek ¹¹³, S. Snyder ²⁹,
 R. Sobie ^{164,y}, A. Soffer ¹⁵⁰, C.A. Solans Sanchez ³⁶, E. Yu. Soldatov ³⁷, U. Soldevila ¹⁶²,
 A.A. Solodkov ³⁷, S. Solomon ⁵⁴, A. Soloshenko ³⁸, K. Solovieva ⁵⁴, O.V. Solovyanov ³⁷,
 V. Solovyev ³⁷, P. Sommer ³⁶, A. Sonay ¹³, W.Y. Song ^{155b}, A. Sopczak ¹³¹, A.L. Sopio ⁹⁵,
 F. Sopkova ^{28b}, V. Sothilingam ^{63a}, S. Sottocornola ^{72a,72b}, R. Soualah ^{115b}, Z. Soumami ^{35e},
 D. South ⁴⁸, S. Spagnolo ^{69a,69b}, M. Spalla ¹⁰⁹, F. Spanò ⁹⁴, D. Sperlich ⁵⁴, G. Spigo ³⁶,
 M. Spina ¹⁴⁵, S. Spinali ⁹⁰, D.P. Spiteri ⁵⁹, M. Spousta ¹³², E.J. Staats ³⁴, A. Stabile ^{70a,70b},
 R. Stamen ^{63a}, M. Stamenkovic ¹¹³, A. Stampekis ²⁰, M. Standke ²⁴, E. Stanecka ⁸⁵,
 M.V. Stange ⁵⁰, B. Stanislaus ^{17a}, M.M. Stanitzki ⁴⁸, M. Stankaityte ¹²⁵, B. Stapf ⁴⁸,
 E.A. Starchenko ³⁷, G.H. Stark ¹³⁵, J. Stark ^{101,ab}, D.M. Starko ^{155b}, P. Staroba ¹³⁰,
 P. Starovoitov ^{63a}, S. Stärz ¹⁰³, R. Staszewski ⁸⁵, G. Stavropoulos ⁴⁶, J. Steentoft ¹⁶⁰,
 P. Steinberg ²⁹, A.L. Steinhebel ¹²², B. Stelzer ^{141,155a}, H.J. Stelzer ¹²⁸, O. Stelzer-Chilton ^{155a},
 H. Stenzel ⁵⁸, T.J. Stevenson ¹⁴⁵, G.A. Stewart ³⁶, M.C. Stockton ³⁶, G. Stoicea ^{27b},
 M. Stolarski ^{129a}, S. Stonjek ¹⁰⁹, A. Straessner ⁵⁰, J. Strandberg ¹⁴³, S. Strandberg ^{47a,47b},
 M. Strauss ¹¹⁹, T. Strebler ¹⁰¹, P. Strizeneč ^{28b}, R. Ströhmer ¹⁶⁵, D.M. Strom ¹²², L.R. Strom ⁴⁸,
 R. Stroynowski ⁴⁴, A. Strubig ^{47a,47b}, S.A. Stucci ²⁹, B. Stugu ¹⁶, J. Stupak ¹¹⁹, N.A. Styles ⁴⁸,
 D. Su ¹⁴², S. Su ^{62a}, W. Su ^{62d,137,62c}, X. Su ^{62a,66}, K. Sugizaki ¹⁵², V.V. Sulin ³⁷,
 M.J. Sullivan ⁹¹, D.M.S. Sultan ^{77a,77b}, L. Sultanaliyeva ³⁷, S. Sultansoy ^{3b}, T. Sumida ⁸⁶,
 S. Sun ¹⁰⁵, S. Sun ¹⁶⁹, O. Sunneborn Gudnadottir ¹⁶⁰, M.R. Sutton ¹⁴⁵, M. Svatos ¹³⁰,
 M. Swiatlowski ^{155a}, T. Swirski ¹⁶⁵, I. Sykora ^{28a}, M. Sykora ¹³², T. Sykora ¹³², D. Ta ⁹⁹,
 K. Tackmann ^{48,w}, A. Taffard ¹⁵⁹, R. Tafirout ^{155a}, J.S. Tafuya Vargas ⁶⁶, R.H.M. Taibah ¹²⁶,
 R. Takashima ⁸⁷, K. Takeda ⁸³, E.P. Takeva ⁵², Y. Takubo ⁸², M. Talby ¹⁰¹, A.A. Talyshev ³⁷,
 K.C. Tam ^{64b}, N.M. Tamir ¹⁵⁰, A. Tanaka ¹⁵², J. Tanaka ¹⁵², R. Tanaka ⁶⁶, M. Tanasini ^{57b,57a},
 J. Tang ^{62c}, Z. Tao ¹⁶³, S. Tapia Araya ⁸⁰, S. Tapprogge ⁹⁹, A. Tarek Abouelfadl Mohamed ¹⁰⁶,
 S. Tarem ¹⁴⁹, K. Tariq ^{62b}, G. Tarna ^{27b}, G.F. Tartarelli ^{70a}, P. Tas ¹³², M. Tasevsky ¹³⁰,
 E. Tassi ^{43b,43a}, A.C. Tate ¹⁶¹, G. Tateno ¹⁵², Y. Tayalati ^{35e}, G.N. Taylor ¹⁰⁴, W. Taylor ^{155b},
 H. Teagle ⁹¹, A.S. Tee ¹⁶⁹, R. Teixeira De Lima ¹⁴², P. Teixeira-Dias ⁹⁴, J.J. Teoh ¹⁵⁴,
 K. Terashi ¹⁵², J. Terron ⁹⁸, S. Terzo ¹³, M. Testa ⁵³, R.J. Teuscher ^{154,y}, A. Thaler ⁷⁸,

O. Theiner ⁵⁶, N. Themistokleous ⁵², T. Thevenaux-Pelzer ¹⁸, O. Thielmann ¹⁷⁰, D.W. Thomas ⁹⁴, J.P. Thomas ²⁰, E.A. Thompson ⁴⁸, P.D. Thompson ²⁰, E. Thomson ¹²⁷, E.J. Thorpe ⁹³, Y. Tian ⁵⁵, V. Tikhomirov ^{37,a}, Yu.A. Tikhonov ³⁷, S. Timoshenko ³⁷, E.X.L. Ting ¹, P. Tipton ¹⁷¹, S. Tisserant ¹⁰¹, S.H. Tlou ^{33g}, A. Tnourji ⁴⁰, K. Todome ^{23b,23a}, S. Todorova-Nova ¹³², S. Todt ⁵⁰, M. Togawa ⁸², J. Tojo ⁸⁸, S. Tokár ^{28a}, K. Tokushuku ⁸², R. Tombs ³², M. Tomoto ^{82,110}, L. Tompkins ^{142,q}, K.W. Topolnicki ^{84b}, P. Tornambe ¹⁰², E. Torrence ¹²², H. Torres ⁵⁰, E. Torró Pastor ¹⁶², M. Toscani ³⁰, C. Tosciri ³⁹, D.R. Tovey ¹³⁸, A. Traeet ¹⁶, I.S. Trandafir ^{27b}, T. Trefzger ¹⁶⁵, A. Tricoli ²⁹, I.M. Trigger ^{155a}, S. Trincaz-Duvoid ¹²⁶, D.A. Trischuk ²⁶, B. Trocmé ⁶⁰, A. Trofymov ⁶⁶, C. Troncon ^{70a}, L. Truong ^{33c}, M. Trzebinski ⁸⁵, A. Trzupek ⁸⁵, F. Tsai ¹⁴⁴, M. Tsai ¹⁰⁵, A. Tsiamis ¹⁵¹, P.V. Tsiareshka ³⁷, S. Tsigaridas ^{155a}, A. Tsigiriotis ^{151,u}, V. Tsiskaridze ¹⁴⁴, E.G. Tskhadadze ^{148a}, M. Tsopoulou ¹⁵¹, Y. Tsujikawa ⁸⁶, I.I. Tsukerman ³⁷, V. Tsulaia ^{17a}, S. Tsuno ⁸², O. Tsur ¹⁴⁹, D. Tsybychev ¹⁴⁴, Y. Tu ^{64b}, A. Tudorache ^{27b}, V. Tudorache ^{27b}, A.N. Tuna ³⁶, S. Turchikhin ³⁸, I. Turk Cakir ^{3a}, R. Turra ^{70a}, T. Turtuvshin ³⁸, P.M. Tuts ⁴¹, S. Tzamarias ¹⁵¹, P. Tzanis ¹⁰, E. Tzovara ⁹⁹, K. Uchida ¹⁵², F. Ukegawa ¹⁵⁶, P.A. Ulloa Poblete ^{136c}, G. Unal ³⁶, M. Unal ¹¹, A. Undrus ²⁹, G. Unel ¹⁵⁹, J. Urban ^{28b}, P. Urquijo ¹⁰⁴, G. Usai ⁸, R. Ushioda ¹⁵³, M. Usman ¹⁰⁷, Z. Uysal ^{21b}, V. Vacek ¹³¹, B. Vachon ¹⁰³, K.O.H. Vadla ¹²⁴, T. Vafeiadis ³⁶, C. Valderanis ¹⁰⁸, E. Valdes Santurio ^{47a,47b}, M. Valente ^{155a}, S. Valentinetti ^{23b,23a}, A. Valero ¹⁶², A. Vallier ^{101,ab}, J.A. Valls Ferrer ¹⁶², T.R. Van Daalen ¹³⁷, P. Van Gemmeren ⁶, M. Van Rijnbach ^{124,36}, S. Van Stroud ⁹⁵, I. Van Vulpen ¹¹³, M. Vanadia ^{75a,75b}, W. Vandelli ³⁶, M. Vandenbroucke ¹³⁴, E.R. Vandewall ¹²⁰, D. Vannicola ¹⁵⁰, L. Vannoli ^{57b,57a}, R. Vari ^{74a}, E.W. Varnes ⁷, C. Varni ^{17a}, T. Varol ¹⁴⁷, D. Varouchas ⁶⁶, L. Varriale ¹⁶², K.E. Varvell ¹⁴⁶, M.E. Vasile ^{27b}, L. Vaslin ⁴⁰, G.A. Vasquez ¹⁶⁴, F. Vazeille ⁴⁰, T. Vazquez Schroeder ³⁶, J. Veatch ³¹, V. Vecchio ¹⁰⁰, M.J. Veen ¹⁰², I. Veliscek ¹²⁵, L.M. Veloce ¹⁵⁴, F. Veloso ^{129a,129c}, S. Veneziano ^{74a}, A. Ventura ^{69a,69b}, A. Verbitskiy ¹⁰⁹, M. Verducci ^{73a,73b}, C. Vergis ²⁴, M. Verissimo De Araujo ^{81b}, W. Verkerke ¹¹³, J.C. Vermeulen ¹¹³, C. Vernieri ¹⁴², P.J. Verschuuren ⁹⁴, M. Vessella ¹⁰², M.C. Vetterli ^{141,ag}, A. Vgenopoulos ¹⁵¹, N. Viaux Maira ^{136f}, T. Vickey ¹³⁸, O.E. Vickey Boeriu ¹³⁸, G.H.A. Viehhauser ¹²⁵, L. Vigani ^{63b}, M. Villa ^{23b,23a}, M. Villaplana Perez ¹⁶², E.M. Villhauer ⁵², E. Vilucchi ⁵³, M.G. Vincter ³⁴, G.S. Virdee ²⁰, A. Vishwakarma ⁵², C. Vittori ^{23b,23a}, I. Vivarelli ¹⁴⁵, V. Vladimirov ¹⁶⁶, E. Voevodina ¹⁰⁹, F. Vogel ¹⁰⁸, P. Vokac ¹³¹, J. Von Ahnen ⁴⁸, E. Von Toerne ²⁴, B. Vormwald ³⁶, V. Vorobel ¹³², K. Vorobev ³⁷, M. Vos ¹⁶², J.H. Vosseveld ⁹¹, M. Vozak ¹¹³, L. Vozdecky ⁹³, N. Vranjes ¹⁵, M. Vranjes Milosavljevic ¹⁵, M. Vreeswijk ¹¹³, R. Vuillermet ³⁶, O. Vujanovic ⁹⁹, I. Vukotic ³⁹, S. Wada ¹⁵⁶, C. Wagner ¹⁰², W. Wagner ¹⁷⁰, S. Wahdan ¹⁷⁰, H. Wahlberg ⁸⁹, R. Wakasa ¹⁵⁶, M. Wakida ¹¹⁰, V.M. Walbrecht ¹⁰⁹, J. Walder ¹³³, R. Walker ¹⁰⁸, W. Walkowiak ¹⁴⁰, A.M. Wang ⁶¹, A.Z. Wang ¹⁶⁹, C. Wang ^{62a}, C. Wang ^{62c}, H. Wang ^{17a}, J. Wang ^{64a}, P. Wang ⁴⁴, R.-J. Wang ⁹⁹, R. Wang ⁶¹, R. Wang ⁶, S.M. Wang ¹⁴⁷, S. Wang ^{62b}, T. Wang ^{62a}, W.T. Wang ⁷⁹, W.X. Wang ^{62a}, X. Wang ^{14c}, X. Wang ¹⁶¹, X. Wang ^{62c}, Y. Wang ^{62d}, Y. Wang ^{14c}, Z. Wang ¹⁰⁵, Z. Wang ^{62d,51,62c}, Z. Wang ¹⁰⁵, A. Warburton ¹⁰³, R.J. Ward ²⁰, N. Warrack ⁵⁹, A.T. Watson ²⁰, M.F. Watson ²⁰, G. Watts ¹³⁷, B.M. Waugh ⁹⁵, A.F. Webb ¹¹, C. Weber ²⁹, M.S. Weber ¹⁹, S.M. Weber ^{63a}, C. Wei ^{62a}, Y. Wei ¹²⁵, A.R. Weidberg ¹²⁵, J. Weingarten ⁴⁹, M. Weirich ⁹⁹, C. Weiser ⁵⁴, C.J. Wells ⁴⁸, T. Wenaus ²⁹, B. Wendland ⁴⁹, T. Wengler ³⁶, N.S. Wenke ¹⁰⁹, N. Wermes ²⁴, M. Wessels ^{63a}, K. Whalen ¹²², A.M. Wharton ⁹⁰, A.S. White ⁶¹, A. White ⁸, M.J. White ¹, D. Whiteson ¹⁵⁹, L. Wickremasinghe ¹²³, W. Wiedenmann ¹⁶⁹, C. Wiel ⁵⁰, M. Wielers ¹³³, N. Wieseotte ⁹⁹, C. Wiglesworth ⁴², L.A.M. Wiik-Fuchs ⁵⁴, D.J. Wilbern ¹¹⁹, H.G. Wilkens ³⁶, D.M. Williams ⁴¹, H.H. Williams ¹²⁷, S. Williams ³², S. Willocq ¹⁰², P.J. Windischhofer ¹²⁵, F. Winklmeier ¹²², B.T. Winter ⁵⁴,

M. Wittgen¹⁴², M. Wobisch⁹⁶, R. Wölker¹²⁵, J. Wollrath¹⁵⁹, M.W. Wolter⁸⁵, H. Wolters^{129a,129c}, V.W.S. Wong¹⁶³, A.F. Wongel⁴⁸, S.D. Worm⁴⁸, B.K. Wosiek⁸⁵, K.W. Woźniak⁸⁵, K. Wraight⁵⁹, J. Wu^{14a,14d}, M. Wu^{64a}, M. Wu¹¹², S.L. Wu¹⁶⁹, X. Wu⁵⁶, Y. Wu^{62a}, Z. Wu^{134,62a}, J. Wuerzinger¹²⁵, T.R. Wyatt¹⁰⁰, B.M. Wynne⁵², S. Xella⁴², L. Xia^{14c}, M. Xia^{14b}, J. Xiang^{64c}, X. Xiao¹⁰⁵, M. Xie^{62a}, X. Xie^{62a}, J. Xiong^{17a}, I. Xiotidis¹⁴⁵, D. Xu^{14a}, H. Xu^{62a}, H. Xu^{62a}, L. Xu^{62a}, R. Xu¹²⁷, T. Xu¹⁰⁵, W. Xu¹⁰⁵, Y. Xu^{14b}, Z. Xu^{62b}, Z. Xu¹⁴², B. Yabsley¹⁴⁶, S. Yacoob^{33a}, N. Yamaguchi⁸⁸, Y. Yamaguchi¹⁵³, H. Yamauchi¹⁵⁶, T. Yamazaki^{17a}, Y. Yamazaki⁸³, J. Yan^{62c}, S. Yan¹²⁵, Z. Yan²⁵, H.J. Yang^{62c,62d}, H.T. Yang^{17a}, S. Yang^{62a}, T. Yang^{64c}, X. Yang^{62a}, X. Yang^{14a}, Y. Yang⁴⁴, Z. Yang^{62a,105}, W-M. Yao^{17a}, Y.C. Yap⁴⁸, H. Ye^{14c}, J. Ye⁴⁴, S. Ye²⁹, X. Ye^{62a}, Y. Yeh⁹⁵, I. Yeletsikh³⁸, M.R. Yexley⁹⁰, P. Yin⁴¹, K. Yorita¹⁶⁷, C.J.S. Young⁵⁴, C. Young¹⁴², M. Yuan¹⁰⁵, R. Yuan^{62b,k}, L. Yue⁹⁵, X. Yue^{63a}, M. Zaazoua^{35e}, B. Zabinski⁸⁵, E. Zaid⁵², T. Zakareishvili^{148b}, N. Zakharchuk³⁴, S. Zambito⁵⁶, J.A. Zamora Saa^{136d}, J. Zang¹⁵², D. Zanzi⁵⁴, O. Zaplatilek¹³¹, S.V. Zeibner⁴⁹, C. Zeitnitz¹⁷⁰, J.C. Zeng¹⁶¹, D.T. Zenger Jr²⁶, O. Zenin³⁷, T. Ženiš^{28a}, S. Zenz⁹³, S. Zerradi^{35a}, D. Zerwas⁶⁶, B. Zhang^{14c}, D.F. Zhang¹³⁸, G. Zhang^{14b}, J. Zhang^{62b}, J. Zhang⁶, K. Zhang^{14a,14d}, L. Zhang^{14c}, P. Zhang^{14a,14d}, R. Zhang¹⁶⁹, S. Zhang¹⁰⁵, T. Zhang¹⁵², X. Zhang^{62c}, X. Zhang^{62b}, Z. Zhang^{17a}, Z. Zhang⁶⁶, H. Zhao¹³⁷, P. Zhao⁵¹, T. Zhao^{62b}, Y. Zhao¹³⁵, Z. Zhao^{62a}, A. Zhemchugov³⁸, X. Zheng^{62a}, Z. Zheng¹⁴², D. Zhong¹⁶¹, B. Zhou¹⁰⁵, C. Zhou¹⁶⁹, H. Zhou⁷, N. Zhou^{62c}, Y. Zhou⁷, C.G. Zhu^{62b}, C. Zhu^{14a,14d}, H.L. Zhu^{62a}, H. Zhu^{14a}, J. Zhu¹⁰⁵, Y. Zhu^{62c}, Y. Zhu^{62a}, X. Zhuang^{14a}, K. Zhukov³⁷, V. Zhulanov³⁷, N.I. Zimine³⁸, J. Zinsser^{63b}, M. Ziolkowski¹⁴⁰, L. Živković¹⁵, A. Zoccoli^{23b,23a}, K. Zoch⁵⁶, T.G. Zorbas¹³⁸, O. Zormpa⁴⁶, W. Zou⁴¹, L. Zwalinski³⁶.

¹Department of Physics, University of Adelaide, Adelaide; Australia.

²Department of Physics, University of Alberta, Edmonton AB; Canada.

³(^a)Department of Physics, Ankara University, Ankara; (^b)Division of Physics, TOBB University of Economics and Technology, Ankara; Türkiye.

⁴LAPP, Université Savoie Mont Blanc, CNRS/IN2P3, Annecy; France.

⁵APC, Université Paris Cité, CNRS/IN2P3, Paris; France.

⁶High Energy Physics Division, Argonne National Laboratory, Argonne IL; United States of America.

⁷Department of Physics, University of Arizona, Tucson AZ; United States of America.

⁸Department of Physics, University of Texas at Arlington, Arlington TX; United States of America.

⁹Physics Department, National and Kapodistrian University of Athens, Athens; Greece.

¹⁰Physics Department, National Technical University of Athens, Zografou; Greece.

¹¹Department of Physics, University of Texas at Austin, Austin TX; United States of America.

¹²Institute of Physics, Azerbaijan Academy of Sciences, Baku; Azerbaijan.

¹³Institut de Física d'Altes Energies (IFAE), Barcelona Institute of Science and Technology, Barcelona; Spain.

¹⁴(^a)Institute of High Energy Physics, Chinese Academy of Sciences, Beijing; (^b)Physics Department, Tsinghua University, Beijing; (^c)Department of Physics, Nanjing University, Nanjing; (^d)University of Chinese Academy of Science (UCAS), Beijing; China.

¹⁵Institute of Physics, University of Belgrade, Belgrade; Serbia.

¹⁶Department for Physics and Technology, University of Bergen, Bergen; Norway.

¹⁷(^a)Physics Division, Lawrence Berkeley National Laboratory, Berkeley CA; (^b)University of California, Berkeley CA; United States of America.

¹⁸Institut für Physik, Humboldt Universität zu Berlin, Berlin; Germany.

- ¹⁹Albert Einstein Center for Fundamental Physics and Laboratory for High Energy Physics, University of Bern, Bern; Switzerland.
- ²⁰School of Physics and Astronomy, University of Birmingham, Birmingham; United Kingdom.
- ²¹(^a)Department of Physics, Bogazici University, Istanbul; (^b)Department of Physics Engineering, Gaziantep University, Gaziantep; (^c)Department of Physics, Istanbul University, Istanbul; (^d)Istinye University, Sariyer, Istanbul; Türkiye.
- ²²(^a)Facultad de Ciencias y Centro de Investigaciones, Universidad Antonio Nariño, Bogotá; (^b)Departamento de Física, Universidad Nacional de Colombia, Bogotá; Colombia.
- ²³(^a)Dipartimento di Fisica e Astronomia A. Righi, Università di Bologna, Bologna; (^b)INFN Sezione di Bologna; Italy.
- ²⁴Physikalisches Institut, Universität Bonn, Bonn; Germany.
- ²⁵Department of Physics, Boston University, Boston MA; United States of America.
- ²⁶Department of Physics, Brandeis University, Waltham MA; United States of America.
- ²⁷(^a)Transilvania University of Brasov, Brasov; (^b)Horia Hulubei National Institute of Physics and Nuclear Engineering, Bucharest; (^c)Department of Physics, Alexandru Ioan Cuza University of Iasi, Iasi; (^d)National Institute for Research and Development of Isotopic and Molecular Technologies, Physics Department, Cluj-Napoca; (^e)University Politehnica Bucharest, Bucharest; (^f)West University in Timisoara, Timisoara; (^g)Faculty of Physics, University of Bucharest, Bucharest; Romania.
- ²⁸(^a)Faculty of Mathematics, Physics and Informatics, Comenius University, Bratislava; (^b)Department of Subnuclear Physics, Institute of Experimental Physics of the Slovak Academy of Sciences, Kosice; Slovak Republic.
- ²⁹Physics Department, Brookhaven National Laboratory, Upton NY; United States of America.
- ³⁰Universidad de Buenos Aires, Facultad de Ciencias Exactas y Naturales, Departamento de Física, y CONICET, Instituto de Física de Buenos Aires (IFIBA), Buenos Aires; Argentina.
- ³¹California State University, CA; United States of America.
- ³²Cavendish Laboratory, University of Cambridge, Cambridge; United Kingdom.
- ³³(^a)Department of Physics, University of Cape Town, Cape Town; (^b)iThemba Labs, Western Cape; (^c)Department of Mechanical Engineering Science, University of Johannesburg, Johannesburg; (^d)National Institute of Physics, University of the Philippines Diliman (Philippines); (^e)University of South Africa, Department of Physics, Pretoria; (^f)University of Zululand, KwaDlangezwa; (^g)School of Physics, University of the Witwatersrand, Johannesburg; South Africa.
- ³⁴Department of Physics, Carleton University, Ottawa ON; Canada.
- ³⁵(^a)Faculté des Sciences Ain Chock, Réseau Universitaire de Physique des Hautes Energies - Université Hassan II, Casablanca; (^b)Faculté des Sciences, Université Ibn-Tofail, Kénitra; (^c)Faculté des Sciences Semlalia, Université Cadi Ayyad, LPHEA-Marrakech; (^d)LPMR, Faculté des Sciences, Université Mohamed Premier, Oujda; (^e)Faculté des sciences, Université Mohammed V, Rabat; (^f)Institute of Applied Physics, Mohammed VI Polytechnic University, Ben Guerir; Morocco.
- ³⁶CERN, Geneva; Switzerland.
- ³⁷Affiliated with an institute covered by a cooperation agreement with CERN.
- ³⁸Affiliated with an international laboratory covered by a cooperation agreement with CERN.
- ³⁹Enrico Fermi Institute, University of Chicago, Chicago IL; United States of America.
- ⁴⁰LPC, Université Clermont Auvergne, CNRS/IN2P3, Clermont-Ferrand; France.
- ⁴¹Nevis Laboratory, Columbia University, Irvington NY; United States of America.
- ⁴²Niels Bohr Institute, University of Copenhagen, Copenhagen; Denmark.
- ⁴³(^a)Dipartimento di Fisica, Università della Calabria, Rende; (^b)INFN Gruppo Collegato di Cosenza, Laboratori Nazionali di Frascati; Italy.
- ⁴⁴Physics Department, Southern Methodist University, Dallas TX; United States of America.

- ⁴⁵Physics Department, University of Texas at Dallas, Richardson TX; United States of America.
- ⁴⁶National Centre for Scientific Research "Demokritos", Agia Paraskevi; Greece.
- ⁴⁷(^a)Department of Physics, Stockholm University; (^b)Oskar Klein Centre, Stockholm; Sweden.
- ⁴⁸Deutsches Elektronen-Synchrotron DESY, Hamburg and Zeuthen; Germany.
- ⁴⁹Fakultät Physik, Technische Universität Dortmund, Dortmund; Germany.
- ⁵⁰Institut für Kern- und Teilchenphysik, Technische Universität Dresden, Dresden; Germany.
- ⁵¹Department of Physics, Duke University, Durham NC; United States of America.
- ⁵²SUPA - School of Physics and Astronomy, University of Edinburgh, Edinburgh; United Kingdom.
- ⁵³INFN e Laboratori Nazionali di Frascati, Frascati; Italy.
- ⁵⁴Physikalisches Institut, Albert-Ludwigs-Universität Freiburg, Freiburg; Germany.
- ⁵⁵II. Physikalisches Institut, Georg-August-Universität Göttingen, Göttingen; Germany.
- ⁵⁶Département de Physique Nucléaire et Corpusculaire, Université de Genève, Genève; Switzerland.
- ⁵⁷(^a)Dipartimento di Fisica, Università di Genova, Genova; (^b)INFN Sezione di Genova; Italy.
- ⁵⁸II. Physikalisches Institut, Justus-Liebig-Universität Giessen, Giessen; Germany.
- ⁵⁹SUPA - School of Physics and Astronomy, University of Glasgow, Glasgow; United Kingdom.
- ⁶⁰LPSC, Université Grenoble Alpes, CNRS/IN2P3, Grenoble INP, Grenoble; France.
- ⁶¹Laboratory for Particle Physics and Cosmology, Harvard University, Cambridge MA; United States of America.
- ⁶²(^a)Department of Modern Physics and State Key Laboratory of Particle Detection and Electronics, University of Science and Technology of China, Hefei; (^b)Institute of Frontier and Interdisciplinary Science and Key Laboratory of Particle Physics and Particle Irradiation (MOE), Shandong University, Qingdao; (^c)School of Physics and Astronomy, Shanghai Jiao Tong University, Key Laboratory for Particle Astrophysics and Cosmology (MOE), SKLPPC, Shanghai; (^d)Tsung-Dao Lee Institute, Shanghai; China.
- ⁶³(^a)Kirchhoff-Institut für Physik, Ruprecht-Karls-Universität Heidelberg, Heidelberg; (^b)Physikalisches Institut, Ruprecht-Karls-Universität Heidelberg, Heidelberg; Germany.
- ⁶⁴(^a)Department of Physics, Chinese University of Hong Kong, Shatin, N.T., Hong Kong; (^b)Department of Physics, University of Hong Kong, Hong Kong; (^c)Department of Physics and Institute for Advanced Study, Hong Kong University of Science and Technology, Clear Water Bay, Kowloon, Hong Kong; China.
- ⁶⁵Department of Physics, National Tsing Hua University, Hsinchu; Taiwan.
- ⁶⁶IJCLab, Université Paris-Saclay, CNRS/IN2P3, 91405, Orsay; France.
- ⁶⁷Department of Physics, Indiana University, Bloomington IN; United States of America.
- ⁶⁸(^a)INFN Gruppo Collegato di Udine, Sezione di Trieste, Udine; (^b)ICTP, Trieste; (^c)Dipartimento Politecnico di Ingegneria e Architettura, Università di Udine, Udine; Italy.
- ⁶⁹(^a)INFN Sezione di Lecce; (^b)Dipartimento di Matematica e Fisica, Università del Salento, Lecce; Italy.
- ⁷⁰(^a)INFN Sezione di Milano; (^b)Dipartimento di Fisica, Università di Milano, Milano; Italy.
- ⁷¹(^a)INFN Sezione di Napoli; (^b)Dipartimento di Fisica, Università di Napoli, Napoli; Italy.
- ⁷²(^a)INFN Sezione di Pavia; (^b)Dipartimento di Fisica, Università di Pavia, Pavia; Italy.
- ⁷³(^a)INFN Sezione di Pisa; (^b)Dipartimento di Fisica E. Fermi, Università di Pisa, Pisa; Italy.
- ⁷⁴(^a)INFN Sezione di Roma; (^b)Dipartimento di Fisica, Sapienza Università di Roma, Roma; Italy.
- ⁷⁵(^a)INFN Sezione di Roma Tor Vergata; (^b)Dipartimento di Fisica, Università di Roma Tor Vergata, Roma; Italy.
- ⁷⁶(^a)INFN Sezione di Roma Tre; (^b)Dipartimento di Matematica e Fisica, Università Roma Tre, Roma; Italy.
- ⁷⁷(^a)INFN-TIFPA; (^b)Università degli Studi di Trento, Trento; Italy.
- ⁷⁸Universität Innsbruck, Department of Astro and Particle Physics, Innsbruck; Austria.
- ⁷⁹University of Iowa, Iowa City IA; United States of America.
- ⁸⁰Department of Physics and Astronomy, Iowa State University, Ames IA; United States of America.

- ⁸¹(^a)Departamento de Engenharia Elétrica, Universidade Federal de Juiz de Fora (UFJF), Juiz de Fora; (^b)Universidade Federal do Rio De Janeiro COPPE/EE/IF, Rio de Janeiro; (^c)Instituto de Física, Universidade de São Paulo, São Paulo; (^d)Rio de Janeiro State University, Rio de Janeiro; Brazil.
- ⁸²KEK, High Energy Accelerator Research Organization, Tsukuba; Japan.
- ⁸³Graduate School of Science, Kobe University, Kobe; Japan.
- ⁸⁴(^a)AGH University of Science and Technology, Faculty of Physics and Applied Computer Science, Krakow; (^b)Marian Smoluchowski Institute of Physics, Jagiellonian University, Krakow; Poland.
- ⁸⁵Institute of Nuclear Physics Polish Academy of Sciences, Krakow; Poland.
- ⁸⁶Faculty of Science, Kyoto University, Kyoto; Japan.
- ⁸⁷Kyoto University of Education, Kyoto; Japan.
- ⁸⁸Research Center for Advanced Particle Physics and Department of Physics, Kyushu University, Fukuoka ; Japan.
- ⁸⁹Instituto de Física La Plata, Universidad Nacional de La Plata and CONICET, La Plata; Argentina.
- ⁹⁰Physics Department, Lancaster University, Lancaster; United Kingdom.
- ⁹¹Oliver Lodge Laboratory, University of Liverpool, Liverpool; United Kingdom.
- ⁹²Department of Experimental Particle Physics, Jožef Stefan Institute and Department of Physics, University of Ljubljana, Ljubljana; Slovenia.
- ⁹³School of Physics and Astronomy, Queen Mary University of London, London; United Kingdom.
- ⁹⁴Department of Physics, Royal Holloway University of London, Egham; United Kingdom.
- ⁹⁵Department of Physics and Astronomy, University College London, London; United Kingdom.
- ⁹⁶Louisiana Tech University, Ruston LA; United States of America.
- ⁹⁷Fysiska institutionen, Lunds universitet, Lund; Sweden.
- ⁹⁸Departamento de Física Teórica C-15 and CIAFF, Universidad Autónoma de Madrid, Madrid; Spain.
- ⁹⁹Institut für Physik, Universität Mainz, Mainz; Germany.
- ¹⁰⁰School of Physics and Astronomy, University of Manchester, Manchester; United Kingdom.
- ¹⁰¹CPPM, Aix-Marseille Université, CNRS/IN2P3, Marseille; France.
- ¹⁰²Department of Physics, University of Massachusetts, Amherst MA; United States of America.
- ¹⁰³Department of Physics, McGill University, Montreal QC; Canada.
- ¹⁰⁴School of Physics, University of Melbourne, Victoria; Australia.
- ¹⁰⁵Department of Physics, University of Michigan, Ann Arbor MI; United States of America.
- ¹⁰⁶Department of Physics and Astronomy, Michigan State University, East Lansing MI; United States of America.
- ¹⁰⁷Group of Particle Physics, University of Montreal, Montreal QC; Canada.
- ¹⁰⁸Fakultät für Physik, Ludwig-Maximilians-Universität München, München; Germany.
- ¹⁰⁹Max-Planck-Institut für Physik (Werner-Heisenberg-Institut), München; Germany.
- ¹¹⁰Graduate School of Science and Kobayashi-Maskawa Institute, Nagoya University, Nagoya; Japan.
- ¹¹¹Department of Physics and Astronomy, University of New Mexico, Albuquerque NM; United States of America.
- ¹¹²Institute for Mathematics, Astrophysics and Particle Physics, Radboud University/Nikhef, Nijmegen; Netherlands.
- ¹¹³Nikhef National Institute for Subatomic Physics and University of Amsterdam, Amsterdam; Netherlands.
- ¹¹⁴Department of Physics, Northern Illinois University, DeKalb IL; United States of America.
- ¹¹⁵(^a)New York University Abu Dhabi, Abu Dhabi; (^b)University of Sharjah, Sharjah; United Arab Emirates.
- ¹¹⁶Department of Physics, New York University, New York NY; United States of America.
- ¹¹⁷Ochanomizu University, Otsuka, Bunkyo-ku, Tokyo; Japan.

- ¹¹⁸Ohio State University, Columbus OH; United States of America.
- ¹¹⁹Homer L. Dodge Department of Physics and Astronomy, University of Oklahoma, Norman OK; United States of America.
- ¹²⁰Department of Physics, Oklahoma State University, Stillwater OK; United States of America.
- ¹²¹Palacký University, Joint Laboratory of Optics, Olomouc; Czech Republic.
- ¹²²Institute for Fundamental Science, University of Oregon, Eugene, OR; United States of America.
- ¹²³Graduate School of Science, Osaka University, Osaka; Japan.
- ¹²⁴Department of Physics, University of Oslo, Oslo; Norway.
- ¹²⁵Department of Physics, Oxford University, Oxford; United Kingdom.
- ¹²⁶LPNHE, Sorbonne Université, Université Paris Cité, CNRS/IN2P3, Paris; France.
- ¹²⁷Department of Physics, University of Pennsylvania, Philadelphia PA; United States of America.
- ¹²⁸Department of Physics and Astronomy, University of Pittsburgh, Pittsburgh PA; United States of America.
- ¹²⁹(^a) Laboratório de Instrumentação e Física Experimental de Partículas - LIP, Lisboa; (^b) Departamento de Física, Faculdade de Ciências, Universidade de Lisboa, Lisboa; (^c) Departamento de Física, Universidade de Coimbra, Coimbra; (^d) Centro de Física Nuclear da Universidade de Lisboa, Lisboa; (^e) Departamento de Física, Universidade do Minho, Braga; (^f) Departamento de Física Teórica y del Cosmos, Universidad de Granada, Granada (Spain); (^g) Departamento de Física, Instituto Superior Técnico, Universidade de Lisboa, Lisboa; Portugal.
- ¹³⁰Institute of Physics of the Czech Academy of Sciences, Prague; Czech Republic.
- ¹³¹Czech Technical University in Prague, Prague; Czech Republic.
- ¹³²Charles University, Faculty of Mathematics and Physics, Prague; Czech Republic.
- ¹³³Particle Physics Department, Rutherford Appleton Laboratory, Didcot; United Kingdom.
- ¹³⁴IRFU, CEA, Université Paris-Saclay, Gif-sur-Yvette; France.
- ¹³⁵Santa Cruz Institute for Particle Physics, University of California Santa Cruz, Santa Cruz CA; United States of America.
- ¹³⁶(^a) Departamento de Física, Pontificia Universidad Católica de Chile, Santiago; (^b) Millennium Institute for Subatomic physics at high energy frontier (SAPHIR), Santiago; (^c) Instituto de Investigación Multidisciplinario en Ciencia y Tecnología, y Departamento de Física, Universidad de La Serena; (^d) Universidad Andres Bello, Department of Physics, Santiago; (^e) Instituto de Alta Investigación, Universidad de Tarapacá, Arica; (^f) Departamento de Física, Universidad Técnica Federico Santa María, Valparaíso; Chile.
- ¹³⁷Department of Physics, University of Washington, Seattle WA; United States of America.
- ¹³⁸Department of Physics and Astronomy, University of Sheffield, Sheffield; United Kingdom.
- ¹³⁹Department of Physics, Shinshu University, Nagano; Japan.
- ¹⁴⁰Department Physik, Universität Siegen, Siegen; Germany.
- ¹⁴¹Department of Physics, Simon Fraser University, Burnaby BC; Canada.
- ¹⁴²SLAC National Accelerator Laboratory, Stanford CA; United States of America.
- ¹⁴³Department of Physics, Royal Institute of Technology, Stockholm; Sweden.
- ¹⁴⁴Departments of Physics and Astronomy, Stony Brook University, Stony Brook NY; United States of America.
- ¹⁴⁵Department of Physics and Astronomy, University of Sussex, Brighton; United Kingdom.
- ¹⁴⁶School of Physics, University of Sydney, Sydney; Australia.
- ¹⁴⁷Institute of Physics, Academia Sinica, Taipei; Taiwan.
- ¹⁴⁸(^a) E. Andronikashvili Institute of Physics, Iv. Javakhishvili Tbilisi State University, Tbilisi; (^b) High Energy Physics Institute, Tbilisi State University, Tbilisi; (^c) University of Georgia, Tbilisi; Georgia.
- ¹⁴⁹Department of Physics, Technion, Israel Institute of Technology, Haifa; Israel.

- ¹⁵⁰Raymond and Beverly Sackler School of Physics and Astronomy, Tel Aviv University, Tel Aviv; Israel.
- ¹⁵¹Department of Physics, Aristotle University of Thessaloniki, Thessaloniki; Greece.
- ¹⁵²International Center for Elementary Particle Physics and Department of Physics, University of Tokyo, Tokyo; Japan.
- ¹⁵³Department of Physics, Tokyo Institute of Technology, Tokyo; Japan.
- ¹⁵⁴Department of Physics, University of Toronto, Toronto ON; Canada.
- ¹⁵⁵(^a) TRIUMF, Vancouver BC; (^b) Department of Physics and Astronomy, York University, Toronto ON; Canada.
- ¹⁵⁶Division of Physics and Tomonaga Center for the History of the Universe, Faculty of Pure and Applied Sciences, University of Tsukuba, Tsukuba; Japan.
- ¹⁵⁷Department of Physics and Astronomy, Tufts University, Medford MA; United States of America.
- ¹⁵⁸United Arab Emirates University, Al Ain; United Arab Emirates.
- ¹⁵⁹Department of Physics and Astronomy, University of California Irvine, Irvine CA; United States of America.
- ¹⁶⁰Department of Physics and Astronomy, University of Uppsala, Uppsala; Sweden.
- ¹⁶¹Department of Physics, University of Illinois, Urbana IL; United States of America.
- ¹⁶²Instituto de Física Corpuscular (IFIC), Centro Mixto Universidad de Valencia - CSIC, Valencia; Spain.
- ¹⁶³Department of Physics, University of British Columbia, Vancouver BC; Canada.
- ¹⁶⁴Department of Physics and Astronomy, University of Victoria, Victoria BC; Canada.
- ¹⁶⁵Fakultät für Physik und Astronomie, Julius-Maximilians-Universität Würzburg, Würzburg; Germany.
- ¹⁶⁶Department of Physics, University of Warwick, Coventry; United Kingdom.
- ¹⁶⁷Waseda University, Tokyo; Japan.
- ¹⁶⁸Department of Particle Physics and Astrophysics, Weizmann Institute of Science, Rehovot; Israel.
- ¹⁶⁹Department of Physics, University of Wisconsin, Madison WI; United States of America.
- ¹⁷⁰Fakultät für Mathematik und Naturwissenschaften, Fachgruppe Physik, Bergische Universität Wuppertal, Wuppertal; Germany.
- ¹⁷¹Department of Physics, Yale University, New Haven CT; United States of America.
- ^a Also Affiliated with an institute covered by a cooperation agreement with CERN.
- ^b Also at An-Najah National University, Nablus; Palestine.
- ^c Also at Borough of Manhattan Community College, City University of New York, New York NY; United States of America.
- ^d Also at Bruno Kessler Foundation, Trento; Italy.
- ^e Also at Center for High Energy Physics, Peking University; China.
- ^f Also at Centro Studi e Ricerche Enrico Fermi; Italy.
- ^g Also at CERN, Geneva; Switzerland.
- ^h Also at Département de Physique Nucléaire et Corpusculaire, Université de Genève, Genève; Switzerland.
- ⁱ Also at Departament de Física de la Universitat Autònoma de Barcelona, Barcelona; Spain.
- ^j Also at Department of Financial and Management Engineering, University of the Aegean, Chios; Greece.
- ^k Also at Department of Physics and Astronomy, Michigan State University, East Lansing MI; United States of America.
- ^l Also at Department of Physics and Astronomy, University of Louisville, Louisville, KY; United States of America.
- ^m Also at Department of Physics, Ben Gurion University of the Negev, Beer Sheva; Israel.
- ⁿ Also at Department of Physics, California State University, East Bay; United States of America.
- ^o Also at Department of Physics, California State University, Sacramento; United States of America.
- ^p Also at Department of Physics, King's College London, London; United Kingdom.

- ^q Also at Department of Physics, Stanford University, Stanford CA; United States of America.
- ^r Also at Department of Physics, University of Fribourg, Fribourg; Switzerland.
- ^s Also at Department of Physics, University of Thessaly; Greece.
- ^t Also at Department of Physics, Westmont College, Santa Barbara; United States of America.
- ^u Also at Hellenic Open University, Patras; Greece.
- ^v Also at Institutio Catalana de Recerca i Estudis Avancats, ICREA, Barcelona; Spain.
- ^w Also at Institut für Experimentalphysik, Universität Hamburg, Hamburg; Germany.
- ^x Also at Institute for Nuclear Research and Nuclear Energy (INRNE) of the Bulgarian Academy of Sciences, Sofia; Bulgaria.
- ^y Also at Institute of Particle Physics (IPP); Canada.
- ^z Also at Institute of Physics, Azerbaijan Academy of Sciences, Baku; Azerbaijan.
- ^{aa} Also at Institute of Theoretical Physics, Ilia State University, Tbilisi; Georgia.
- ^{ab} Also at L2IT, Université de Toulouse, CNRS/IN2P3, UPS, Toulouse; France.
- ^{ac} Also at Lawrence Livermore National Laboratory, Livermore; United States of America.
- ^{ad} Also at National Institute of Physics, University of the Philippines Diliman (Philippines); Philippines.
- ^{ae} Also at Technical University of Munich, Munich; Germany.
- ^{af} Also at The Collaborative Innovation Center of Quantum Matter (CICQM), Beijing; China.
- ^{ag} Also at TRIUMF, Vancouver BC; Canada.
- ^{ah} Also at Università di Napoli Parthenope, Napoli; Italy.
- ^{ai} Also at University of Chinese Academy of Sciences (UCAS), Beijing; China.
- ^{aj} Also at University of Colorado Boulder, Department of Physics, Colorado; United States of America.
- ^{ak} Also at Washington College, Maryland; United States of America.
- ^{al} Also at Yeditepe University, Physics Department, Istanbul; Türkiye.
- * Deceased